Development of Genetically Engineered Mouse Models of Brainstem Glioma: Therapeutic Efficacy of an Immune Mediated Gene Therapy Strategy

by

Flor M. Mendez

A dissertation submitted in partial fulfillment
of the requirements for the degree of
Doctor of Philosophy
(Cell and Developmental Biology)
in the University of Michigan
2020

Doctoral Committee:

Professor Roman Giger, Chair
Professor Maria G. Castro
Associate Professor, Maria E. Figueroa, University of Miami Health System
Associate Professor, Marina Pasca di Magliano

Flor M. Mendez

mendezf@umich.edu

ORCID iD: 0000-0002-9309-2500

Dedication

To my parents,
Jorge and Sofia Mendez,
To my siblings,
Jorge and Pablo
And to all of my friends,
Without whom none of my success would be possible

Acknowledgements

I am deeply grateful to my dissertation mentor, Dr. Maria G. Castro for her commitment to my graduate education. You always pushed me to think critically, and encouraged me to have the confidence to apply to fellowships and present my work at conferences. Thank you, for giving me the foundational tools to become an independent scientist. I am also thankful to Dr. Pedro Lowenstein, for his academic support and mentorship. Your thought provoking questions have broadened my scientific perspective. Thank you both for giving me the opportunity to be a part of your lab.

I am also thankful to all the members of the Castro-Lowenstein lab, past and present, for their support. To Felipe, thank you for serving as a second mentor who I could always go to for scientific or emotional support. You never failed to make me laugh even when times were hard. To Padma, thank you for your help with the many experiments we did together and the great contribution you made towards my project. To Stephen, thank you for collaborating with me and for always brightening my day. To Marta, thank you for teaching me everything I know about histology, and, also for making sure everything in the lab runs smoothly for all of us. To the many lab members, past and present, Alexandra, Carl, Neha, Nate, Robert, Vivek, Dan, Andrea, Patrick, Mahmoud, Maria Ventosa, Angela, Santiago, Belen, Fernando, Ayman, and Faisal, thank you for making every day enjoyable. To the past students that I had the opportunity to mentor Sheeba, Rocio, Ramya, Umayal, Ethan, and Jessica, thank you for contributing to the progress of my project.

I would also like to thank the members of my thesis committee- Roman Giger, Marina Pasca di Magliano, and Maria Figueroa for their guidance and feedback on my dissertation work. Thank you, also, to my undergraduate research mentor, Dr. Liz Bikram and to my Post-Baccalaureate Research and Education Program (PREP) mentor, Dr. Kate Barald, for encouraging me to pursue graduate training.

Finally, I would like to thank my family and friends for their love and support. Thank you for always being there for me. I could not have done this without you.

Table of Contents

List of Tables

List of Figures

Abstract

Diffuse intrinsic pontine glioma (DIPG) is an incurable pediatric brainstem tumor. Genomic studies of autopsy and biopsy tissue revealed the presence of recurrent mutations in activing A receptor, type 1 (ACVR1) and lysine to methionine mutations at position 27 (K27M) in the genes encoding histone H3 variants, H3.1 and H3.3. To study the role of the mutations on DIPG tumorigenesis we developed genetically engineered brainstem glioma models harboring recurrent DIPG mutations, ACVR1 G328V and histone H3.1 K27M. Histological analysis indicates tumors generated were diffuse and localized in the brainstem. Survival analysis demonstrated that ACVR1 G328V enhanced median survival, while the H3.1 K27M mutation did not significantly affect median survival independently of ACVR1 G328V. We also developed a transplantable model of DIPG by implanting mutant ACVR1 tumor neurospheres into the pons of immune competent mice. This enabled us to test the therapeutic efficacy and toxicity of immune stimulatory gene therapy using adenoviruses expressing thymidine kinase (TK) and fms-like tyrosine kinase 3 ligand (Flt3L). Our results show that adenoviral delivery of TK/Flt3L in mice bearing mutant ACVR1 brainstem glioma resulted in anti-tumor immunity, recruitment of anti-tumor specific T cells and increased median survival. Histopathological analysis shows that TK/Flt3L was well tolerated in the brainstem. The results from this thesis work provide support for continued clinical investigation into TK/Flt3L immune stimulatory gene therapy for DIP.

Chapter 1: Introduction[1]

Clinical aspects of DIPG

Diffuse Intrinsic Pontine Glioma (DIPG) is a highly aggressive pediatric brain cancer that is currently incurable. DIPG occurs in children of median age of 6-7 years and bears a bleak prognosis: a median survival of 11 months with only 10% of DIPG patients surviving two years from onset (1). A DIPG diagnosis results from the culmination of acute neuropathological symptoms including cranial nerve palsies, long-tract and cerebellar signs, in addition to the characteristic radiographic abnormality in the pons (1). The longstanding standard treatment for DIPG is focal radiation (2). Radiation provides mitigation of symptoms and slows down tumor growth in the majority of DIPG patients (3,4). Unfortunately, the efficacy of radiotherapy is limited and provides only transient symptomatic relief and meager benefits to DIPG patient survival (4-7). Numerous clinical trials have evaluated other treatments (alone and in combination with radiation) such as cytotoxic chemotherapy, small molecule inhibitors, and immunotherapies. However, none of these therapies have demonstrated a significant improvement in patient survival without imposing substantial adverse side effects (7).

The location of DIPG tumors poses a challenge for diagnosis and treatment. DIPG tumors infiltrate the pons, a region of the brainstem that regulates basic functions like breathing, blood

[1] Portions of this chapter have been published in: Mendez, F.M., Nunez, F.J., Garcia-Fabiani, M.B., Haase S., Carney, S., Gauss, J.C., Becher, O.J., Lowenstein, P.R., and Castro, M.G. Epigenetic reprogramming and chromatin accessibility in pediatric diffuse intrinsic pontine gliomas: a neural developmental disease, *Neuro-Oncology*, 2019, noz218.

pressure, and heart rate. The crucial functions of the pons and the inability to differentiate tumor cells from normal tissue in the operating room makes surgical resection impossible. Even a biopsy of the tumor was felt to be unnecessary given that the results would not change clinical management. Contemporary practice still relies on the characteristic MRI abnormality of these tumors to confirm a DIPG diagnosis: a T2 hyperintense signal abnormality occupying at least 50% of the pons (8). This general practice will likely continue until molecular and pathological evaluation of DIPG tumors is able to meaningfully impact the standard of care. Nevertheless, biopsy remains a significant aspect of DIPG management, as the scarcity of DIPG samples poses challenges to the characterization and development of novel therapeutic agents for this disease. Progress has been made recently with numerous studies reporting on the safety and low morbidity of computer-aided stereotactic biopsies since their development in 1978 (9-12). There is also evidence suggesting that liquid biopsies, utilizing cerebral spinal fluid or plasma, represent a promising future strategy to diagnose and monitor DIPG via the distinct markers present on the circulating tumor DNA (13). While the dire need to improve DIPG treatment remains, the increase in biopsy has facilitated significant advances in determining the hallmark genetic characteristics of DIPG—namely the 2012 discovery of H3K27M mutations in approximately 85% of DIPG tumors (14,15). Biopsies are now being increasingly performed at academic medical centers in order to designate patients into genetically stratified clinical trials, with the hope that such targeted treatments will provide improvements in DIPG treatment(16).

Pathological evaluation of DIPG describes a diffuse tumor of the pons, often infiltrating the of medulla and midbrain, with otherwise typical characteristics of histopathological heterogenous glial neoplasms (17). Historically, high-grade glioma was defined by the World Health Organization (WHO) based on histopathological characteristics such as the presence of

microvascular proliferation or necrosis. However, the most recent WHO classification of central nervous system tumors, published in 2016, began incorporating molecular testing as part of its diagnostic criteria. This led the WHO to define a new neoplastic entity establishing midline gliomas (e.g., brainstem, thalamic, spinal cord) harboring H3K27M mutations and diffuse growth as "diffuse midline gliomas, H3K27M-mutant" (18). This term includes 80% of DIPGs harboring H3K27M mutations (14,15,19). Herein, we refer to mutations of lysine 27 to methionine as H3K27M, due to the nomenclature used in the original reports. However, based on standard mutation nomenclature it is lysine 28 that is mutated to methionine (20).

Normal postnatal development of the human and murine pons

Our understanding of DIPG may be enhanced by studying the postnatal development of the human pons. A morphometric analysis of the human pons 0-18 years of age found that there is a rapid, sixfold increase in the volume of the pons from birth to age five, followed by slower but continued growth throughout childhood (21). MRI and histological analysis of myelin basic protein indicate that this expansion of the pons is likely due to an increase of myelination in the basis pontis (21). Ki67 staining also revealed that the number of proliferative cells began to decline rapidly from 0-7 months followed by a further decline by age 3, and only a small population persisted throughout childhood (21). Two populations of vimentin/nestin-expressing cells were also identified — a dorsal group near the ventricular surface that persists throughout childhood, and a parenchymal population that declines by 7 months (21). Monje et al., utilized 24 normal postmortem brainstem samples and analyzed neural precursor cells in the midbrain, pons, and medulla. They identified a nestin positive population in the ventral pons that peaks first during infancy, and then peaks for a second time at age 6 (22). The results from these

studies indicate that the human pons is undergoing continuous growth during childhood. It is noteworthy that two independent studies one using pons volume as a metric and the other using density of nestin-positive cells as a metric, suggest that there is a peak growth at approximately 5 or 6 years of age, which correlates with age of incidence of DIPG. A murine study also observed a fivefold increase in the basis pontis postnatally, while the tegmentum grew fourfold (23). However, this rapid growth is not due to myelination as in the human pons, but is reportedly due to proliferation (23). The pons is the most proliferative brainstem region in comparison to the midbrain or medulla (23). A parenchymal progenitor population of sex-determining region Y-box 2 (Sox2+), oligodendrocyte transcription factor 2 (Olig2+) was identified as the main proliferative progenitor population, and Lindquist et al., also found that the majority of adult pons oligodendrocytes were found to be derived from postnatal Sox2+ progenitors (23). Overall, the murine pons growth postnatally resembles human pons growth. Lineage tracing studies using markers of progenitor cell populations could help increase our understanding of the cell of origin of DIPG.

Cell of origin in DIPG

If DIPG originates from a postnatal cell then the cell of origin in DIPG may be the proliferative Ki67+/Olig2+ proliferative population identified by Tate. et al., in the postnatal pons, or the nestin+ population identified by Monje and colleagues (21,22). The hypothesis that DIPG arises from a postnatal precursor cell is supported by the findings of Funato et al., demonstrating that the H3.3 K27M mutation, together with platelet derived growth factor receptor A (PDGFRA) activation and p53 loss, was sufficient to induce neoplastic

transformation in human embryonic stem cells (ESCs) and that expression of H3.3 K27M led to a resetting of neural precursors to a more primitive stem cell state (24).

However, it is also possible that the cell of origin is an embryonic precursor cell. Pathania et al., performed in utero electroporation to over express H3.3 K27M in neural progenitor cells in the lower rhombic lip of the developing hindbrain where some pontine nuclei are derived. They found that in combination with Trp53 loss it was sufficient to induce both focal and diffuse tumors, but expression of H3.3 K27M postnatally did not yield the same results (25). Sun et al., also demonstrated that the H3.3 K27M mutation was sufficient to immortalize human fetal hindbrain-derived neural progenitor cells, but not cortex derived progenitor cells (26). This finding suggested that only human fetal hindbrain-derived neural progenitor cells could become oncogenic with the introduction of the highly prevalent H3.3 K27M mutation.

In support of a developmental origin, whether postnatal or prenatal, single cell RNA sequencing of six H3 K27M mutated glioma patients identified that they have a developmental hierarchy, with some tumor cells having transcriptional profiles that were associated with either astrocytic differentiation, oligodendrocytic differentiation, and oligodendrocytic progenitor-like programs (27) .This study also revealed that the largest fraction of stem-like cells in DIPGs were oligodendrocyte progenitor-like cells (OPCs), supporting the hypothesis of a precursor OPC cell of origin for DIPG (27).

Genetic mutations in DIPG

The developmental regulator activin A receptor type 1 (ACVR1) is a frequently mutated gene in DIPG present in approximately 24% of patients(28). There are six somatic mutations occurring in either the glycine serine rich domain or the kinase domain (**Figure 1.1)** (29-32). The

most frequent mutation is the G328V mutation, which we model in Chapter 2. ACVR1 mutations are typically observed in younger DIPG patients(29-32). ACVR1 has been shown to be

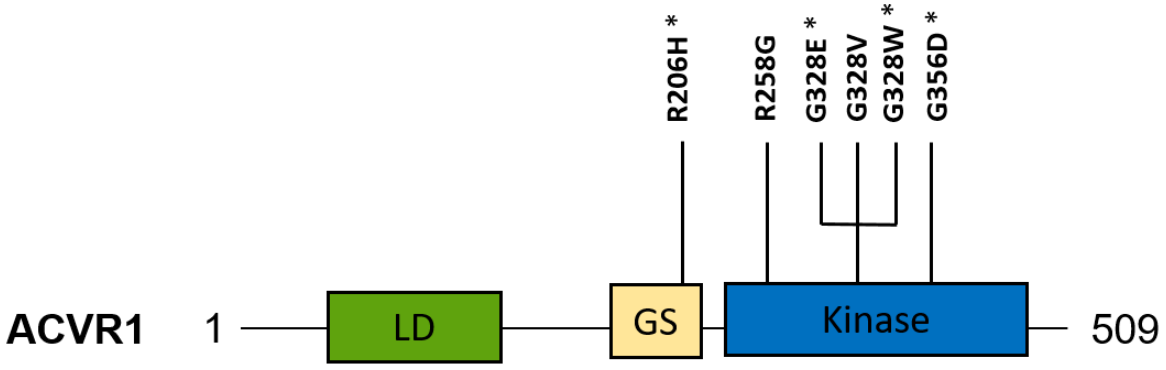

Figure 1.1 ACVR1 mutations in DIPG

A schematic of ACVR1 domain organization showing the position of mutations that have been described in DIPG. Mutations labeled with an asterisk have also been described to occur in patients with FOP. The ligand binding (LD), glycine serine rich (GS), and kinase domain are labelled.

necessary to establish proper patterning in late gastrulation during embryogenesis for normal craniofacial and cardiac development (33-35). The receptor is part of the transforming growth factor beta (TGF-β) family. Normally, upon bone morphogenetic protein (BMP) ligand binding, type 2 BMP receptor kinase phosphorylates ACVR1, a type 1 BMP receptor. This initiates a downstream signaling cascade through phosphorylation of the Smad transcription factors (**Figure 1.2**)(36). However, ACVR1 mutations result in ligand independent activation of the Smad1/5/8 signaling pathway(29-32,37).

Canonically, ACVR1 phosphorylates Smad1/5/8 (38). ACVR1 is also mutated in the congenital disorder fibrodysplasia ossificans progressive (FOP) (39). Interestingly, cells expressing mutated ACVR1 respond to activin ligands to which wild-type ACVR1 does not normally respond (40,41). In models of FOP, activin-ACVR1 signaling was sufficient to induce heterotypic ossification (40,41). DIPG cells harboring mutated ACVR1 have also been shown to

exhibit an aberrant response to activin A (42). Activin receptor signaling regulates

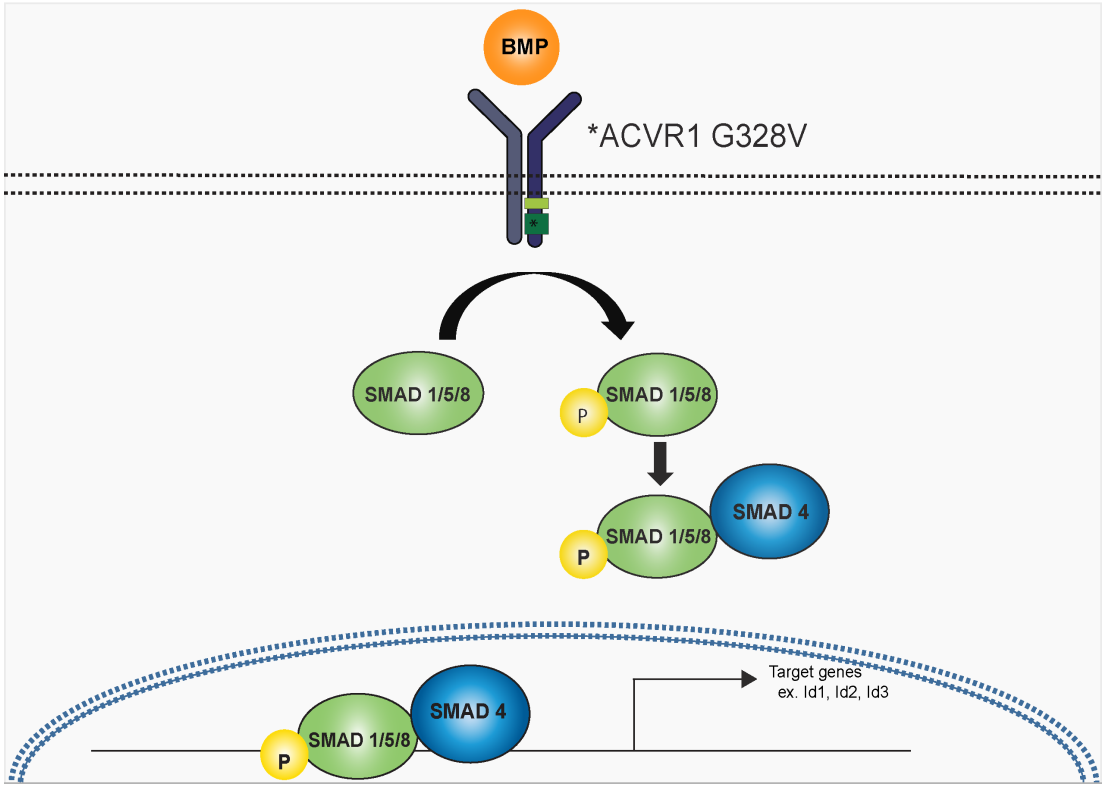

Figure 1.2 ACVR1 signaling pathway

A cartoon of the ACVR1 signaling pathway. ACVR1 is a type I BMP receptor which forms a heteromeric complex with type II BMP receptors upon BMP ligand binding. Activated ACVR1 then phosphorylates the Smad1/5/8 transcription factors. Phosphorylated Smad1/5/8 transcription factors are then able to bind to Smad 4 and translocate into the nucleus to regulate transcription. An asterisk represents the ACVR1 G328V mutation which results in auto-activation of this pathway independent of BMP ligand binding.

oligodendrocyte lineage cell responses during white matter development and after injury(43).

During development, BMPs are tightly regulated temporally and spatially by other signaling pathways (36). Postnatally, BMPs promote astrogliogenesis while inhibiting both neurogenesis and oligodendrogliogenesis (36). Although a lot is known about BMP signaling in the brain, the role of BMP signaling or ACVR1 has not been studied in the early postnatal pons. Identifying the implications of ACVR1 or other BMP interacting/inhibitory pathways on neural

precursor or proliferative populations could provide new directions for development of therapies. In addition to activating ACVR1 mutations, there have also been amplifications in inhibitor of DNA binding protein 2 (ID2), ID3, mutations in BMP3, BMPK, and others in approximately 19% of DIPG, underscoring the importance of the BMP pathway in DIPG (44). Hoeman et al., found that in vitro expression of ACVR1 R206H upregulated mesenchymal markers and activated signaling of signal transducer and activator of transcription 3 (Stat3) (45). Using a replication-competent avian sarcoma-leukosis virus long terminal repeat splice acceptor (RCAS) mouse model with PDGFA, the authors also found that ACVR1 R206H accelerated gliomagenesis and cooperates with H3.1 K27M to accelerate tumor growth and malignancy (30). In vivo inhibition of ACVR1 with the LDN212854 inhibitor also significantly increased median survival in the RCAS model described above (45). In addition, treatment with ACVR1 inhibitors, LDN-139189 and LDN-214117, prolonged survival in orthotropic patient-derived xenograft models of ACVR1 R206H (42). Thus, ACVR1 may be an important therapeutic target for the treatment of DIPG.

TP53, the gene encoding the tumor suppressor p53, is mutated in 42% of DIPG tumors. Survival and apoptosis in the developing and adult nervous systems are regulated by p53 (29,46). In the brain, p53 is preferentially expressed in progenitor cells, and in vitro experiments using neurospheres (NS) from p53 null mice suggested that TP53 regulates cell cycle progression and apoptosis (47,48). An increased proliferation rate in neural stem cells could make them susceptible to acquiring additional mutations that lead to malignancy.

Protein phosphatase, Mg2+/Mn2+-dependent 1D (PPMI1D), mutated in 23% of DIPG cases, is expressed in the fetal mouse brain and germline mutations of *PPM1D* lead to an intellectual disability syndrome, suggesting a role in neurodevelopment (31). PPM1D

dephosphorylates the DNA damage response proteins p53, checkpoint kinase 2, ataxia telangiectasia mutated, and, gamma-H2A histone family member X to enable re-entry into the cell cycle following cellular stress (49). PPMI1D plays a critical role in central nervous system homeostasis by regulating G2/M cell cycle progression in adult neural progenitor cells through inhibition of p53 activity (50). Thus, PPM1D and p53 together modulate the balance between self-renewal of neural progenitor cells while minimizing genotoxic stress. In DIPG, truncating mutations of PPM1D that stabilize the protein are mutually exclusive with TP53 mutations (31,51).

DIPGs are also characterized by amplifications of genes that regulate the G1-S cell cycle progression, particularly cyclin D family members CCND1, CCND2, CCND3 and cyclin dependent kinase inhibitors CDK4 and CDK6 (31,52,53). Cyclins and cyclin dependent kinases form a complex that phosphorylates retinoblastoma protein, allowing for cell cycle progression (54). The regulation of the cell cycle progression and length is important for neurogenesis. In vitro, neural precursor cells with dominant negative forms of CDK2, CDK4, and CDK6 undergo cell cycle arrest (55). The overexpression of cyclin D and CDK4 in neural progenitors of developing brain shortened G1 length and inhibited neurogenesis demonstrating that a lengthening of G1 regulates the switch from proliferation to neurogenesis (56). Uncontrolled proliferation is a characteristic of many cancers, and there are currently four clinical trials testing the efficacy of CDK4/6 inhibitors that were initially developed for other cancers in DIPG (NCT02255461, NCT03387020, NCT03355794, NCT02644460). The results of these clinical trials will shed light on the effectiveness of CDK4/6 inhibitors as a single therapeutic agent in DIPG.

The most frequent mutation in DIPG is a K27M mutation that occurs on genes encoding histone H3 variants H3.3 and H3.1/2 (14,15,19). Histones are proteins that package DNA into compact units called nucleosomes, an octamer comprised of four core histones (H2A, H2B, H3, and H4) and approximately 147 base pairs of DNA (57). Nucleosome cores are connected by a strand of linker DNA that is stabilized by the recognition and binding of histone H1 (57). Histone H3 is post-translationally modified (methylation, acetylation, ubiquitiniation, sumoylation, etc.) on the N-terminal tail to regulate transcription, DNA replication and repair. H3.1 and H3.2 are canonical histones encoded by multiple genes which are "replication-coupled," meaning that they are synthesized and deposited on DNA during S-phase (**Table 1.1**) (57). The histone variant H3.3 is a non-canonical histone (**Table 1.1**). Non-canonical histones, in contrast, are usually encoded by one or two genes, and are expressed throughout the cell cycle

(57).

Table 1 Summary of human histone H3 variants

Histone	Gene	Deposition	Oncohistone in DIPG
H3.1	*HIST1H3A*	Canonical	
	HIST1H3B		H3.1K27M
	HIST1H3C		H3.1K27M
	HIST1H3D		
	HIST1H3E		
	HIST1H3F		
	HIST1H3G		
	HIST1H3H		
	HIST1H3I		
	HIST1H3J		
H3.2	*HIST2H3A*	Canonical	
	HIST2H3B		
	HIST2H3C		H3.2K27M
	HIST2H3D		
H3.3	*H3F3A*	Non-canonical	H3.3K27M
	H3F3B		
	H3F3C		

Table 1-1: Summary of histone H3 variants

Table listing genes encoding for canonical and non-canonical histone H3 variants. Despite many genes encoding for canonical histone H3 variants H3.1 and H3.2 only the *HIST1H3B*, *HIST1H3C,* and *HIST2H3C* genes have been observed to be mutated in DIPG. Three genes encode for the H3.3 variant, but only the *H3F3FA* gene is mutated in DIPG.

Histone variants have distinct functions—for example H3.3. is typically deposited on transcriptionally active genes and generally harbors post-translational modifications associated with activation. Meanwhile H3.1 and H3.2 are associated with inactivation modifications (58). An analysis of histone H3 gene expression in silico during human brain development found that genes encoding the H3.3 variant, including H3F3A, were present at all developmental stages; however, their expression did gradually decrease across developmental stages (59). In contrast, the genes encoding the H3.1 variant, including HIST1H3B are silenced at early developmental stages (59). One important caveat that the authors noted was that H3.1 transcripts lack

polyadenylation and thus are potentially underrepresented in poly(A)-derived cDNA libraries and RNA-seq data sets used in the study (59).

Polycomb Repressive Complex 2 (PRC2), is a Polycomb group (PcG) protein, which is composed of three core subunits enhancer of zeste homolog 1 (EZH1) or EZH2, embryonic ectoderm development (EED), and suppressor of zeste 12 homolog (SUZ12)—that mediates the repression of developmental genes (60). EZH1 and EZH2 contain a conserved catalytic Su(var)3-9/enhancer-of-zeste/trithorax (SET) domain found in many lysine methyl transferases, which catalyzes the di-, and tri-methylation of histone 3 lysine 27 (H3K27me2/3) (61). H3K27me3 is a repressive mark that is associated with inactive gene promoters (60). The trithorax group of proteins, on the other hand, are antagonistic regulators of PcG proteins and include the SET1 family (SET1A, SET1B, MLL1, MLL2, MLL3, and MLL4 in humans), which catalyze methylation of histone 3 lysine 4 (62). Tri-methylation of histone 3 lysine 4 (H3K4me3) is associated with active chromatin (62). In DIPG cells, the genomic distribution of H3K4me3 methylation is largely unaltered compared with neural stem cells (63).

H3K27M functions as a dominant negative mutation that dramatically reduces global levels of H3K27me3 in DIPG cells and tissue even though H3K27M protein makes up only a small percentage of total H3 (3-17% in DIPG cells as measured by mass spectrometry)(63-65). Several hypotheses have been suggested to explain the mechanism of global reduction of H3K27me3 by the H3K27M mutation. Lewis et al., observed that synthetic H3K27M peptides interact with the EZH2 active site (64). In support of this, co-immunoprecipitation by experiments of wild-type or H3.3 K27M containing mono-nucleosomes revealed enrichment of EZH2 and SUZ12 proteins in mutated nucleosomes (65). Bender et al., also demonstrated that the H3.3 K27M mutation decreased EZH2 methyltranferase enzymatic activity (65).

Additionally, a biochemical study demonstrated that EZH2 recognizes the histone H3 tail (66). The authors also showed that inhibition of EZH2 catalytic activity by H3K27M could be alleviated through enhanced acetylation of surrounding chromatin regions (66). Consistent with this, a crystal structure of the human PRC2 complex with the H3K27M peptide demonstrated that the mutant peptide binds to the active site of the SET domain. Furthermore, the binding of EED to H3K27me3, present as a result of an existing repressive mark, leads to the stabilization of the SET domain. This enhances the binding of PRC2 with the H3K27M peptide (67). The resulting theories suggest that H3K27M binds to the EZH2 component of the PRC2 complex, to inactivate or sequester the complex, thus preventing it from carrying it out di- and tri-methylation on wild-type nucleosomes (**Figure 1.3 A**).

However, Piunti, A. et al., reported that EZH2 and SUZ12 are largely excluded from chromatin containing H3.3 K27M. Instead mutant K27M proteins are found in regions that contain H3K27 acetylation, which many groups had reported to be increased in H3.3 K27M mutant cells (64,68,69). Subsequently, they found that PRC2 activity is required for DIPG cell

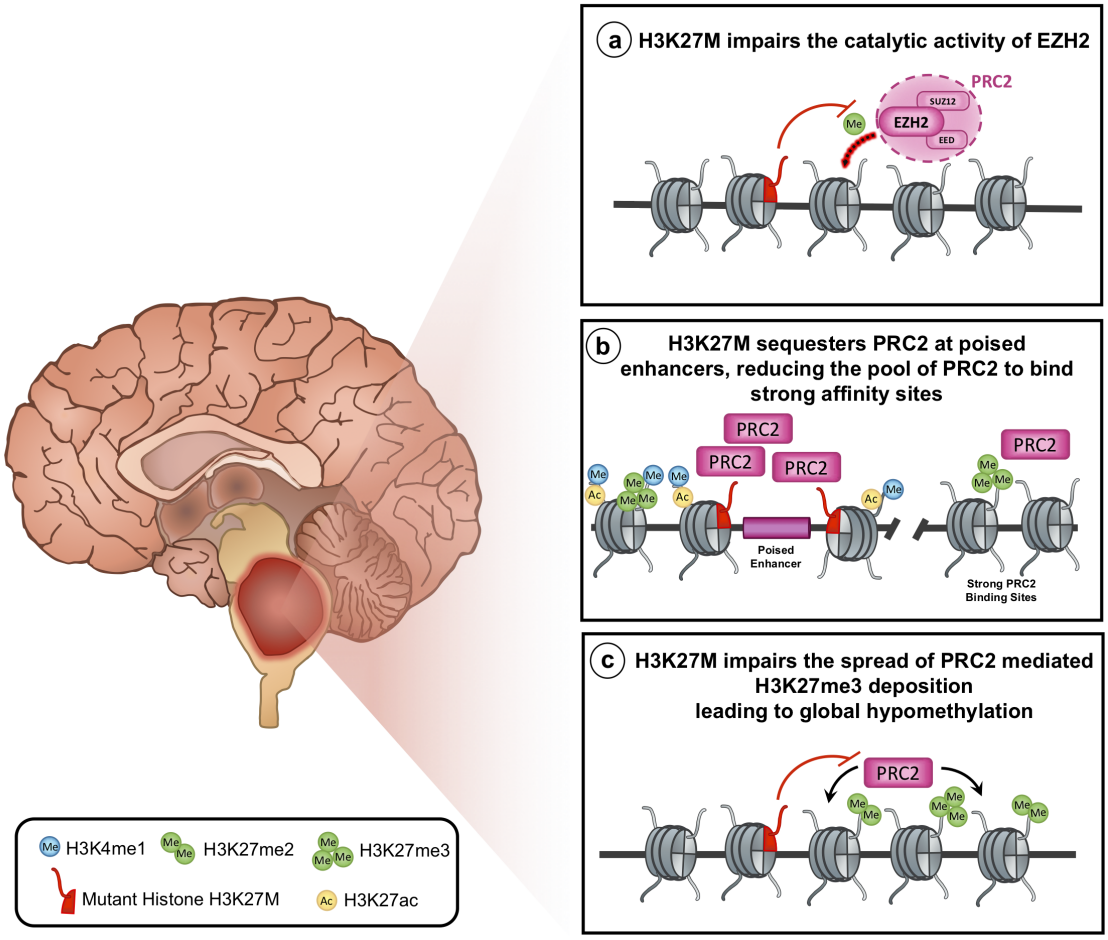

Figure 1.3 Mechanisms by which H3K27M leads to defective PRC2 activity and global hypomethylation.

(A) H3K27M mutatant histone inhibits (shown by curved bracket) the catalytic activity of EZH2 to deposit the H3K27me3 mark (shown by red arrow). (B) PRC2 is sequestered at poised enhancers b binding to H3K27M, which restrains the available PRC2 pool from binding to its strong affinity sites. (C) H3K27M interferes (shown by curved bracket) with the spread of the H3K27me3 mark by PRC2 (shown by black arrows) leading to global hypomethylation and transcriptional de-repression.

maintenance and growth through potentially dependent or independent repression of p16, a

[2] This figure was originally published in: Mendez, F.M., Nunez, F.J., Garcia-Fabiani, M.B., Haase S., Carney, S., Gauss, J.C., Becher, O.J., Lowenstein, P.R., and Castro, M.G. Epigenetic reprogramming and chromatin accessibility in pediatric diffuse intrinsic pontine gliomas: a neural developmental disease, *Neuro-Oncology*, 2019, noz218.

PRC2 target gene (68). Indeed, others have observed locus specific enrichment of H3K27me3 in H3K27M expressing cells, and hypothesize that H3K27M promotes tumorigenesis through repression of tumor suppressors (63). In support of this, using a genetic mouse model, Cordero et al., found that the H3.3 K27M mutation in the context of PDGF signaling promoted gliomagenesis through repression of the p16 tumor suppressor (70). Additionally, a mouse model generated by neonatal induction of H3.3 K27M, PDGFRA, and Trp53 demonstrated that H3.3 K27M accelerated tumor development, and that genes enriched in H3.3 K27M tumors were associated with bivalently regulated neural developmental genes (71). Silveira et al., observed that knockdown of H3F3A, the gene encoding the H3K27M mutation, restored H3K27me3 levels (72). The restoration of this repressive mark resulted in a promoter shift from active to bivalent state in 32-48% of genes upregulated by K27M(72). Similarly, a study using embryonic stem cells expressing the H3.3 K27me3 mutation found that EZH2 (a component of PRC2) is sequestered to poised enhancers, which was unique to H3K27M-expressing cells compared with wild-type H3.3 ESCs. The authors propose that the limited availability of PRC2 to bind its strong affinity sites across the genome leads to global hypomethylation (**Figure 1.3 B**). The authors also found that H3K27M is enriched at highly transcribed genes and is low within regions that are enriched in H3K27me3 peaks, thereby allowing for H3K27me3 silencing at those sites. Recently, Harutyunyan et al., have reported that the global deposition of H3K27me2/3 is reduced in H3.3 K27M cells and that removal of H3K27M could rescue this effect (73). These findings suggest that neither the recruitment of PRC2 nor its ability to deposit H3K27me3 in the local proximity of unmethylated cytosine-phosphate-guanine (CpG) islands is affected by H3K27M. Instead the ability of PRC2 to facilitate the spread of the H3K27me3 mark is inhibited by H3K27M, represented by the reduced distribution of H3K27me3 at these sites (**Figure 1.3 C**)

(73). Interestingly, posterior fossa type A ependymomas with high expression of enhancer of zeste homolog inhibitory protein (EXHIP) are also characterized by global loss of H3K27me3 and retention of this mark at CpG islands (74-76). Several groups have recently reported that a conserved sequence in EZHIP functions as an endogenous H3K27M analog that inhibits PRC2 activity (76-78). Jain et al, propose a model where EZHIP blocks H3K27me3 spreading by inhibiting allosterically-activated PRC2 (76). Thus, the K27M mutation and EZHIP appear to deregulate PRC2 activity by similar mechanisms. In chapter 2, I describe the development of a mouse model with the ACVR1 G328V and H3.1 K27 mutations that enabled us to study the function of these mutations in DIPG tumorigenesis.

Immunotherapy

The dismal prognosis of DIPG requires the development of novel treatment approaches. Immunotherapy, an approach that uses the body's immune system to fight cancer has grown immensely. Several immunotherapies have been approved by the Food and Drug Administration (FDA) including a dendritic cell vaccine for prostate cancer, and pembrolizumab, a monoclonal antibody for the PD-1 receptor, an immune checkpoint protein, which received approval for the treatment of unresectable or metastatic solid tumors with high microsatellite instability or mismatch repair deficiency(79-81). These successes in solid tumors have yielded much interest in the use of immunotherapies for the treatment of brain tumors.

Nevertheless, there are several features of high-grade gliomas that need to considered for the successful implementation of immunotherapeutic strategies. For example, some of the most promising immunotherapies are immune checkpoint blockade drugs. Immune checkpoint blockade drugs are based on the use of monoclonal antibodies that block inhibitory signals of T

cell activation (82). However, the efficacy of immune checkpoint inhibitors is thought to correlate with mutational burden, and both adult glioblastoma and DIPG tumors have a low mutational burden (83,84). Despite the proposed correlation, there are some patients with low tumor burden that benefit from immune checkpoint blockade drug, and there are currently a number of ongoing clinical trials testing the safety and efficacy of these drugs in DIPG (85-88). Another feature of gliomas is high tumor heterogeneity which is a problem for single targeted immunotherapies such as peptide vaccines targeting specific tumor antigens, since high heterogeneity can lead to antigen escape (89,90).

The unique environment of the brain also poses a challenge. The brain has a functional lymphatic system, and there is evidence of immunosurveillance within the brain and T cell entry(91,92). However, in comparison to peripheral organs, the brain has few resident professional antigen presenting cells (APCs) (93). The presentation of antigen to T cells by APCs is essential for the activation of the adaptive immune response (94). Perhaps not surprisingly, glioblastomas have few infiltrating immune cells (95). The glioma microenvironment also has high levels of immunosuppressive cytokines such as TGF-β and IL-10 (96,97). At late stages of glioma, TGF-β promotes the expansion of regulatory T cells (96,97). Meanwhile, IL-10 has been shown to inhibit the activation and effector function of T cells, monocytes, and macrophages (97,98). In addition, IL-10 also downregulates MHC class II expression on monocytes, and inhibits anti-tumor immune responses by inhibiting production of interferon-gamma (IFN-γ) and tumor necrosis factor-alpha (TNF-α) by immune cells (97,99). Gliomas also promote the expansion of an immunosuppressive network of immune cells such as myeloid-derived suppressor cells (MDSCs), tumor associated macrophages/microglia (TAMs),

and regulatory T cells (Tregs) which further prevent gliomas from initiating an effective antitumor immune response (96).

DIPG tumor microenvironment

The DIPG microenvironment has not been as extensively studied as that of adult gliomas has. One recent study compared the tumor immune microenvironment of DIPG with adult glioblastoma tumors found that DIPG tumors had less infiltrating T cells (100). Using tissue microarrays a second study found that, compared to control adjacent brain tissue, DIPG samples did not have extensive TAMs, nor increased T cell infiltration (101). In addition, macrophages from DIPG tumors expressed fewer inflammatory factors compared to macrophages from adult glioblastoma tumors, including lower levels of IL6, IL1A, IL1B, CCL3, CCL4, among other inflammatory factors (100). DIPG tumor cells also secreted fewer cytokines and chemokines compared to GBM tumor cells (100,101). Overall, initial studies of the DIPG tumor immune microenvironment suggest that DIPG tumors are unable to initiate effective anti-tumor immune responses. In addition, it appears that DIPGs do not have the immunosuppressive factors that characterize adult gliomas, therefore immunotherapies that improve the recruitment of cytotoxic lymphocytes may be especially effective since they may not need to overcome an immunosuppressive tumor microenvironment (101).

Immune stimulatory gene therapy

Our laboratory has successfully employed a strategy based on increasing dendritic cell infiltration into the tumor microenvironment (102-107). Dendritic cells are the most efficient

antigen presenting cells (102,108). They take up antigens, process them and load them onto major histocompatibility complex (MHC) class I and II molecules. Dendritic cells then migrate to the draining lymph nodes and present antigens to T cells, initiating antigen-specific immune responses (94). Our strategy to enhance anti-tumor immune responses relies on the adenoviral delivery of two genes, a conditionally cytotoxic gene, thymidine kinase, and Flt3L. Flt3L, is a growth factor that induces dendritic cell differentiation, proliferation, and activation (102,109). TK phosphorylates the prodrug ganciclovir (GCV) to GCV-monophosphate. Cellular kinases convert it into GCV triphosphate which inhibits DNA polymerase causing DNA chain termination (110,111). Several phase I clinical trials have demonstrated that adenoviral administration of thymidine kinase is safe, although higher doses do cause neurotoxicity(112-115). A phase III randomized control clinical trial in Europe demonstrated that adenoviral delivery of TK followed by intervenes GCV was safe and prolonged time to death, however it did not improve overall survival (116).

Thus, our laboratory has used a combination therapy of adenoviral delivery of Ad-TK and Ad-Flt3L (**Figure 1.4**). This strategy relies on Ad-TK/GCV to induce tumor cell death while the delivery of Ad-Flt3L results in the recruitment of dendritic cells into the tumor microenvironment (106,117). Cell death results in the release of tumor antigens and damage associated molecular pattern molecules which trigger an immune response against self-antigens (111). Indeed, we previously demonstrated that dying tumor cells release high-mobility group box 1 (HMGB1), into the tumor microenvironment, an endogenous toll-like receptor 2 (TLR2) ligand (106,107). Toll-like receptors (TLRs), are pattern recognition receptors that recognize patterns expressed by pathogens and DAMPs and stimulate dendritic cell activation(118).

HMGB1 activated dendritic cells then travel to the draining lymph nodes where they prime T cells to elicit an antigen specific cytotoxic immune response (106,107).

Our laboratory has demonstrated that the combination of Ad-TK/Ad-Flt3L results in tumor regression, long term survival, and immunological memory in mouse and rat models of adult glioblastoma (103,104,119). This combination therapy is currently being investigated in a Phase 1 clinical trial at the University of Michigan [NCT01811992] (120). We hypothesize that this therapy will also be effective for the treatment of DIPG, a tumor characterized by low immune cell infiltration. However, DIPGs are biologically very different tumors from adult gliomas. In chapter 3 of this thesis, I present evidence suggesting that this therapy is safe and effective in mouse model of brainstem glioma harboring the ACVR1 DIPG mutation.

Summary

DIPG is a rare pediatric brainstem tumor for which there is no treatment. Alterations in developmental and epigenetic mechanisms drive disease progression in DIPG. It is likely that DIPGs arise from an NPC that accumulates characteristic mutations. It is thought that the histone H3K27M mutation serves as the initial event, making the transformed cells susceptible to acquiring TP53, ACVR1, and additional mutations. The goal of this thesis was to generate immune competent, genetically engineered mouse models of brainstem glioma to investigate the role of relevant DIPG mutations, and test the safety and effectiveness of immune stimulatory gene therapy in this biologically unique pediatric glioma.

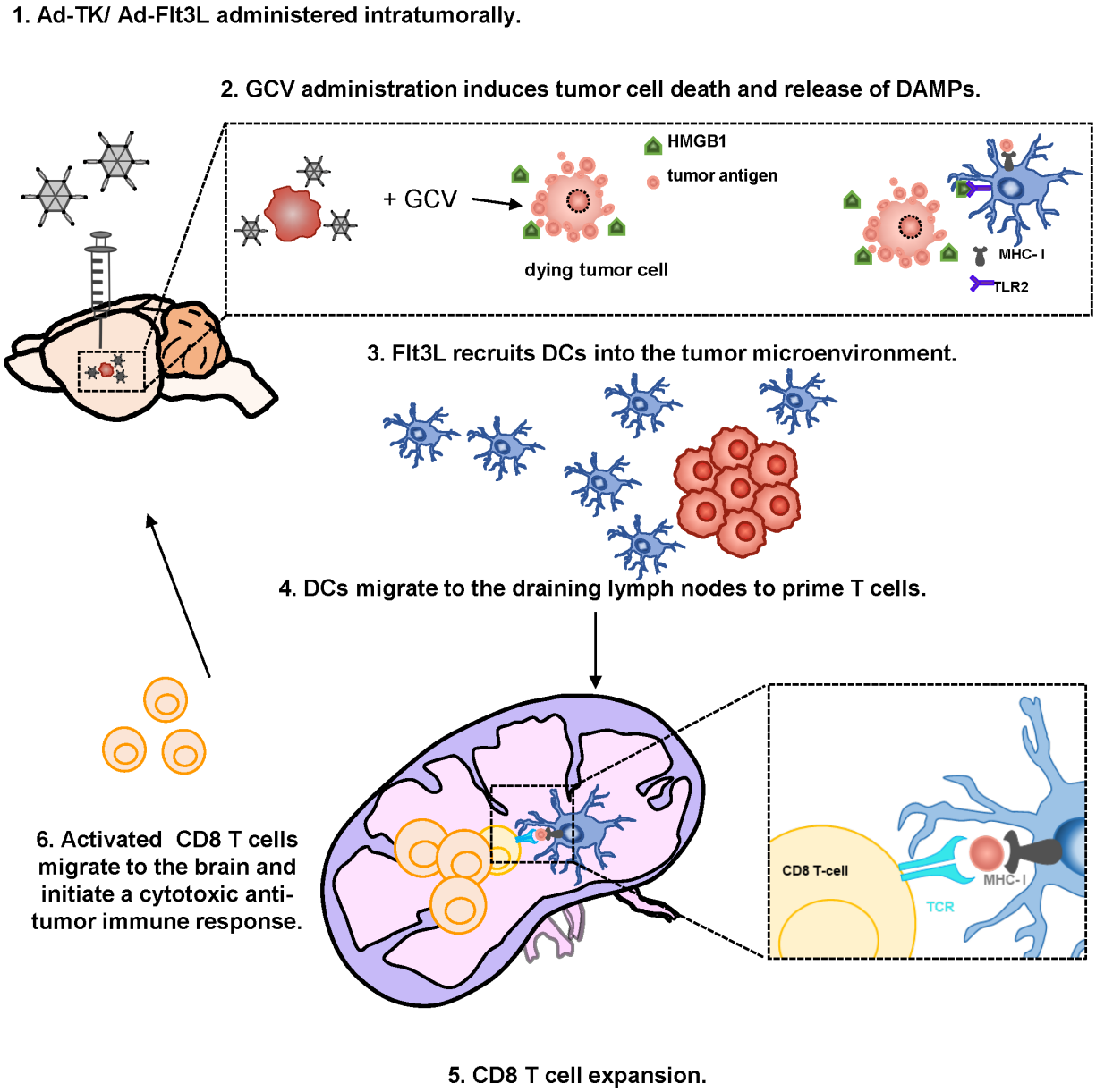

Figure 1.4 Diagram of adenoviral mediated TK/Flt3L gene therapy[3]

A combination of Ad-Tk/Flt3L is administered intratumorally. The prodrug, GCV, is administered via intraperitoneal injection. TK converts GCV into a toxic metabolite resulting in tumor cell death and release of damage associated molecules, such as HMGB1 and tumor antigens. Flt3L recruits dendritic cells into the tumor microenvironment where they take up tumor antigens released by dying tumor cells and present them to T cells via MHC complexes.

[3] Image modified from David B. Altshuler, Padma Kadiyala, Felipe J. Nuñez, Fernando M. Nuñez, Stephen Carney, Mahmoud S. Alghamri, Maria B. Garcia-Fabiani, Antonela S. Asad, Alejandro J. Nicola Candia, Marianela Candolfi, Joerg Lahann, James J. Moon, Anna Schwendeman, Pedro R. Lowenstein & Maria G. Castro. Prospects of biological and synthetic pharmacotherapies for glioblastoma, Expert Opinion on Biological Therapy. 2020.

HMGB1 is a TLR2 ligand that induces the activation of dendritic cells. Activated dendritic cells migrate to the draining lymph nodes where they present tumor antigens to naïve T cells, resulting in the expansion of tumor specific CD8 T cells which migrate to the brain and initiate a cytotoxic antitumor immune response.

References

1. Hoffman LM, Veldhuijzen van Zanten SEM, Colditz N, Baugh J, Chaney B, Hoffmann M*, et al.* Clinical, Radiologic, Pathologic, and Molecular Characteristics of Long-Term Survivors of Diffuse Intrinsic Pontine Glioma (DIPG): A Collaborative Report From the International and European Society for Pediatric Oncology DIPG Registries. J Clin Oncol **2018**;36(19):1963-72 doi 10.1200/JCO.2017.75.9308.
2. Donaldson SS, Laningham F, Fisher PG. Advances toward an understanding of brainstem gliomas. J Clin Oncol **2006**;24(8):1266-72 doi 10.1200/JCO.2005.04.6599.
3. Langmoen IA, Lundar T, Storm-Mathisen I, Lie SO, Hovind KH. Management of pediatric pontine gliomas. Childs Nerv Syst **1991**;7(1):13-5.
4. Hargrave D, Bartels U, Bouffet E. Diffuse brainstem glioma in children: critical review of clinical trials. Lancet Oncol **2006**;7(3):241-8 doi 10.1016/S1470-2045(06)70615-5.
5. Gallitto M, Lazarev S, Wasserman I, Stafford JM, Wolden SL, Terezakis SA*, et al.* Role of Radiation Therapy in the Management of Diffuse Intrinsic Pontine Glioma: A Systematic Review. Adv Radiat Oncol **2019**;4(3):520-31 doi 10.1016/j.adro.2019.03.009.
6. Robison NJ, Kieran MW. Diffuse intrinsic pontine glioma: a reassessment. J Neurooncol **2014**;119(1):7-15 doi 10.1007/s11060-014-1448-8.
7. Vanan MI, Eisenstat DD. DIPG in Children - What Can We Learn from the Past? Front Oncol **2015**;5:237 doi 10.3389/fonc.2015.00237.
8. Schroeder KM, Hoeman CM, Becher OJ. Children are not just little adults: recent advances in understanding of diffuse intrinsic pontine glioma biology. Pediatr Res **2014**;75(1-2):205-9 doi 10.1038/pr.2013.194.
9. Gleason CA, Wise BL, Feinstein B. Stereotactic localization (with computerized tomographic scanning), biopsy, and radiofrequency treatment of deep brain lesions. Neurosurgery **1978**;2(3):217-22 doi 10.1227/00006123-197805000-00006.
10. Roujeau T, Machado G, Garnett MR, Miquel C, Puget S, Geoerger B*, et al.* Stereotactic biopsy of diffuse pontine lesions in children. J Neurosurg **2007**;107(1 Suppl):1-4 doi 10.3171/PED-07/07/001.
11. Gupta N, Goumnerova LC, Manley P, Chi SN, Neuberg D, Puligandla M*, et al.* Prospective feasibility and safety assessment of surgical biopsy for patients with newly diagnosed diffuse intrinsic pontine glioma. Neuro Oncol **2018**;20(11):1547-55 doi 10.1093/neuonc/noy070.
12. Puget S, Beccaria K, Blauwblomme T, Roujeau T, James S, Grill J*, et al.* Biopsy in a series of 130 pediatric diffuse intrinsic Pontine gliomas. Childs Nerv Syst **2015**;31(10):1773-80 doi 10.1007/s00381-015-2832-1.
13. Lu VM, Power EA, Zhang L, Daniels DJ. Liquid biopsy for diffuse intrinsic pontine glioma: an update. J Neurosurg Pediatr **2019**:1-8 doi 10.3171/2019.6.PEDS19259.

14. Schwartzentruber J, Korshunov A, Liu XY, Jones DT, Pfaff E, Jacob K*, et al.* Driver mutations in histone H3.3 and chromatin remodelling genes in paediatric glioblastoma. Nature **2012**;482(7384):226-31 doi 10.1038/nature10833.
15. Wu G, Broniscer A, McEachron TA, Lu C, Paugh BS, Becksfort J*, et al.* Somatic histone H3 alterations in pediatric diffuse intrinsic pontine gliomas and non-brainstem glioblastomas. Nat Genet **2012**;44(3):251-3 doi 10.1038/ng.1102.
16. Kieran MW, Goumnerova LC, Prados M, Gupta N. Biopsy for diffuse intrinsic pontine glioma: a reappraisal. J Neurosurg Pediatr **2016**;18(3):390-1 doi 10.3171/2015.6.PEDS15374.
17. Buczkowicz P, Bartels U, Bouffet E, Becher O, Hawkins C. Histopathological spectrum of paediatric diffuse intrinsic pontine glioma: diagnostic and therapeutic implications. Acta Neuropathol **2014**;128(4):573-81 doi 10.1007/s00401-014-1319-6.
18. Louis DN, Perry A, Reifenberger G, von Deimling A, Figarella-Branger D, Cavenee WK*, et al.* The 2016 World Health Organization Classification of Tumors of the Central Nervous System: a summary. Acta Neuropathol **2016**;131(6):803-20 doi 10.1007/s00401-016-1545-1.
19. Khuong-Quang DA, Buczkowicz P, Rakopoulos P, Liu XY, Fontebasso AM, Bouffet E*, et al.* K27M mutation in histone H3.3 defines clinically and biologically distinct subgroups of pediatric diffuse intrinsic pontine gliomas. Acta Neuropathol **2012**;124(3):439-47 doi 10.1007/s00401-012-0998-0.
20. Leske H, Rushing E, Budka H, Niehusmann P, Pahnke J, Panagopoulos I. K27/G34 versus K28/G35 in histone H3-mutant gliomas: A note of caution. Acta Neuropathol **2018**;136(1):175-6 doi 10.1007/s00401-018-1867-2.
21. Tate MC, Lindquist RA, Nguyen T, Sanai N, Barkovich AJ, Huang EJ*, et al.* Postnatal growth of the human pons: a morphometric and immunohistochemical analysis. J Comp Neurol **2015**;523(3):449-62 doi 10.1002/cne.23690.
22. Monje M, Mitra SS, Freret ME, Raveh TB, Kim J, Masek M*, et al.* Hedgehog-responsive candidate cell of origin for diffuse intrinsic pontine glioma. Proc Natl Acad Sci U S A **2011**;108(11):4453-8 doi 10.1073/pnas.1101657108.
23. Lindquist RA, Guinto CD, Rodas-Rodriguez JL, Fuentealba LC, Tate MC, Rowitch DH*, et al.* Identification of proliferative progenitors associated with prominent postnatal growth of the pons. Nat Commun **2016**;7:11628 doi 10.1038/ncomms11628.
24. Funato K, Major T, Lewis PW, Allis CD, Tabar V. Use of human embryonic stem cells to model pediatric gliomas with H3.3K27M histone mutation. Science **2014**;346(6216):1529-33 doi 10.1126/science.1253799.
25. Pathania M, De Jay N, Maestro N, Harutyunyan AS, Nitarska J, Pahlavan P*, et al.* H3.3(K27M) Cooperates with Trp53 Loss and PDGFRA Gain in Mouse Embryonic Neural Progenitor Cells to Induce Invasive High-Grade Gliomas. Cancer Cell **2017**;32(5):684-700 e9 doi 10.1016/j.ccell.2017.09.014.
26. Sun Y, Xu C, Pan C, Chen X, Geng Y, Wu Y*, et al.* Diffuse Intrinsic Pontine Gliomas Exhibit Cell Biological and Molecular Signatures of Fetal Hindbrain-Derived Neural Progenitor Cells. Neurosci Bull **2019**;35(2):216-24 doi 10.1007/s12264-018-00329-6.
27. Filbin MG, Tirosh I, Hovestadt V, Shaw ML, Escalante LE, Mathewson ND*, et al.* Developmental and oncogenic programs in H3K27M gliomas dissected by single-cell RNA-seq. Science **2018**;360(6386):331-5 doi 10.1126/science.aao4750.

28. Taylor KR, Vinci M, Bullock AN, Jones C. ACVR1 mutations in DIPG: lessons learned from FOP. Cancer Res **2014**;74(17):4565-70 doi 10.1158/0008-5472.CAN-14-1298.
29. Taylor KR, Mackay A, Truffaux N, Butterfield Y, Morozova O, Philippe C*, et al.* Recurrent activating ACVR1 mutations in diffuse intrinsic pontine glioma. Nat Genet **2014**;46(5):457-61 doi 10.1038/ng.2925.
30. Buczkowicz P, Hoeman C, Rakopoulos P, Pajovic S, Letourneau L, Dzamba M*, et al.* Genomic analysis of diffuse intrinsic pontine gliomas identifies three molecular subgroups and recurrent activating ACVR1 mutations. Nat Genet **2014**;46(5):451-6 doi 10.1038/ng.2936.
31. Wu G, Diaz AK, Paugh BS, Rankin SL, Ju B, Li Y*, et al.* The genomic landscape of diffuse intrinsic pontine glioma and pediatric non-brainstem high-grade glioma. Nat Genet **2014**;46(5):444-50 doi 10.1038/ng.2938.
32. Fontebasso AM, Papillon-Cavanagh S, Schwartzentruber J, Nikbakht H, Gerges N, Fiset PO*, et al.* Recurrent somatic mutations in ACVR1 in pediatric midline high-grade astrocytoma. Nat Genet **2014**;46(5):462-6 doi 10.1038/ng.2950.
33. Komatsu Y, Scott G, Nagy A, Kaartinen V, Mishina Y. BMP type I receptor ALK2 is essential for proper patterning at late gastrulation during mouse embryogenesis. Dev Dyn **2007**;236(2):512-7 doi 10.1002/dvdy.21021.
34. Dudas M, Sridurongrit S, Nagy A, Okazaki K, Kaartinen V. Craniofacial defects in mice lacking BMP type I receptor Alk2 in neural crest cells. Mech Dev **2004**;121(2):173-82 doi 10.1016/j.mod.2003.12.003.
35. Kaartinen V, Dudas M, Nagy A, Sridurongrit S, Lu MM, Epstein JA. Cardiac outflow tract defects in mice lacking ALK2 in neural crest cells. Development **2004**;131(14):3481-90 doi 10.1242/dev.01214.
36. Bond AM, Bhalala OG, Kessler JA. The dynamic role of bone morphogenetic proteins in neural stem cell fate and maturation. Dev Neurobiol **2012**;72(7):1068-84 doi 10.1002/dneu.22022.
37. Shen Q, Little SC, Xu M, Haupt J, Ast C, Katagiri T*, et al.* The fibrodysplasia ossificans progressiva R206H ACVR1 mutation activates BMP-independent chondrogenesis and zebrafish embryo ventralization. J Clin Invest **2009**;119(11):3462-72 doi 10.1172/JCI37412.
38. Miyazono K, Kamiya Y, Morikawa M. Bone morphogenetic protein receptors and signal transduction. J Biochem **2010**;147(1):35-51 doi 10.1093/jb/mvp148.
39. Shore EM, Xu M, Feldman GJ, Fenstermacher DA, Cho TJ, Choi IH*, et al.* A recurrent mutation in the BMP type I receptor ACVR1 causes inherited and sporadic fibrodysplasia ossificans progressiva. Nat Genet **2006**;38(5):525-7 doi 10.1038/ng1783.
40. Hino K, Ikeya M, Horigome K, Matsumoto Y, Ebise H, Nishio M*, et al.* Neofunction of ACVR1 in fibrodysplasia ossificans progressiva. Proc Natl Acad Sci U S A **2015**;112(50):15438-43 doi 10.1073/pnas.1510540112.
41. Hatsell SJ, Idone V, Wolken DM, Huang L, Kim HJ, Wang L*, et al.* ACVR1R206H receptor mutation causes fibrodysplasia ossificans progressiva by imparting responsiveness to activin A. Sci Transl Med **2015**;7(303):303ra137 doi 10.1126/scitranslmed.aac4358.
42. Carvalho D, Taylor KR, Olaciregui NG, Molinari V, Clarke M, Mackay A*, et al.* ALK2 inhibitors display beneficial effects in preclinical models of ACVR1 mutant diffuse intrinsic pontine glioma. Commun Biol **2019**;2:156 doi 10.1038/s42003-019-0420-8.

43. Dillenburg A, Ireland G, Holloway RK, Davies CL, Evans FL, Swire M*, et al.* Activin receptors regulate the oligodendrocyte lineage in health and disease. Acta Neuropathol **2018**;135(6):887-906 doi 10.1007/s00401-018-1813-3.
44. Mackay A, Burford A, Carvalho D, Izquierdo E, Fazal-Salom J, Taylor KR*, et al.* Integrated Molecular Meta-Analysis of 1,000 Pediatric High-Grade and Diffuse Intrinsic Pontine Glioma. Cancer Cell **2017**;32(4):520-37 e5 doi 10.1016/j.ccell.2017.08.017.
45. Hoeman CM, Cordero FJ, Hu G, Misuraca K, Romero MM, Cardona HJ*, et al.* ACVR1 R206H cooperates with H3.1K27M in promoting diffuse intrinsic pontine glioma pathogenesis. Nature Communications **2019**;10(1) doi 10.1038/s41467-019-08823-9.
46. Hede SM, Nazarenko I, Nister M, Lindstrom MS. Novel Perspectives on p53 Function in Neural Stem Cells and Brain Tumors. J Oncol **2011**;2011:852970 doi 10.1155/2011/852970.
47. Meletis K, Wirta V, Hede SM, Nister M, Lundeberg J, Frisen J. p53 suppresses the self-renewal of adult neural stem cells. Development **2006**;133(2):363-9 doi 10.1242/dev.02208.
48. Jansen S, Geuer S, Pfundt R, Brough R, Ghongane P, Herkert JC*, et al.* De Novo Truncating Mutations in the Last and Penultimate Exons of PPM1D Cause an Intellectual Disability Syndrome. Am J Hum Genet **2017**;100(4):650-8 doi 10.1016/j.ajhg.2017.02.005.
49. Lu X, Nannenga B, Donehower LA. PPM1D dephosphorylates Chk1 and p53 and abrogates cell cycle checkpoints. Genes Dev **2005**;19(10):1162-74 doi 10.1101/gad.1291305.
50. Zhu YH, Zhang CW, Lu L, Demidov ON, Sun L, Yang L*, et al.* Wip1 regulates the generation of new neural cells in the adult olfactory bulb through p53-dependent cell cycle control. Stem Cells **2009**;27(6):1433-42 doi 10.1002/stem.65.
51. Akamandisa MP, Nie K, Nahta R, Hambardzumyan D, Castellino RC. Inhibition of mutant PPM1D enhances DNA damage response and growth suppressive effects of ionizing radiation in diffuse intrinsic pontine glioma. Neuro Oncol **2019**;21(6):786-99 doi 10.1093/neuonc/noz053.
52. Paugh BS, Broniscer A, Qu C, Miller CP, Zhang J, Tatevossian RG*, et al.* Genome-wide analyses identify recurrent amplifications of receptor tyrosine kinases and cell-cycle regulatory genes in diffuse intrinsic pontine glioma. J Clin Oncol **2011**;29(30):3999-4006 doi 10.1200/JCO.2011.35.5677.
53. Zarghooni M, Bartels U, Lee E, Buczkowicz P, Morrison A, Huang A*, et al.* Whole-genome profiling of pediatric diffuse intrinsic pontine gliomas highlights platelet-derived growth factor receptor alpha and poly (ADP-ribose) polymerase as potential therapeutic targets. J Clin Oncol **2010**;28(8):1337-44 doi 10.1200/JCO.2009.25.5463.
54. Giacinti C, Giordano A. RB and cell cycle progression. Oncogene **2006**;25(38):5220-7 doi 10.1038/sj.onc.1209615.
55. Ferguson KL, Callaghan SM, O'Hare MJ, Park DS, Slack RS. The Rb-CDK4/6 signaling pathway is critical in neural precursor cell cycle regulation. J Biol Chem **2000**;275(43):33593-600 doi 10.1074/jbc.M004879200.
56. Lange C, Huttner WB, Calegari F. Cdk4/cyclinD1 overexpression in neural stem cells shortens G1, delays neurogenesis, and promotes the generation and expansion of basal progenitors. Cell Stem Cell **2009**;5(3):320-31 doi 10.1016/j.stem.2009.05.026.

57. Buschbeck M, Hake SB. Variants of core histones and their roles in cell fate decisions, development and cancer. Nat Rev Mol Cell Biol **2017**;18(5):299-314 doi 10.1038/nrm.2016.166.
58. Maehara K, Harada A, Sato Y, Matsumoto M, Nakayama KI, Kimura H*, et al.* Tissue-specific expression of histone H3 variants diversified after species separation. Epigenetics Chromatin **2015**;8:35 doi 10.1186/s13072-015-0027-3.
59. Ren M, van Nocker S. In silico analysis of histone H3 gene expression during human brain development. Int J Dev Biol **2016**;60(4-6):167-73 doi 10.1387/ijdb.150334sv.
60. Corley M, Kroll KL. The roles and regulation of Polycomb complexes in neural development. Cell Tissue Res **2015**;359(1):65-85 doi 10.1007/s00441-014-2011-9.
61. Cao R, Wang L, Wang H, Xia L, Erdjument-Bromage H, Tempst P*, et al.* Role of histone H3 lysine 27 methylation in Polycomb-group silencing. Science **2002**;298(5595):1039-43 doi 10.1126/science.1076997.
62. Schuettengruber B, Martinez AM, Iovino N, Cavalli G. Trithorax group proteins: switching genes on and keeping them active. Nat Rev Mol Cell Biol **2011**;12(12):799-814 doi 10.1038/nrm3230.
63. Chan KM, Fang D, Gan H, Hashizume R, Yu C, Schroeder M*, et al.* The histone H3.3K27M mutation in pediatric glioma reprograms H3K27 methylation and gene expression. Genes Dev **2013**;27(9):985-90 doi 10.1101/gad.217778.113.
64. Lewis PW, Muller MM, Koletsky MS, Cordero F, Lin S, Banaszynski LA*, et al.* Inhibition of PRC2 activity by a gain-of-function H3 mutation found in pediatric glioblastoma. Science **2013**;340(6134):857-61 doi 10.1126/science.1232245.
65. Bender S, Tang Y, Lindroth AM, Hovestadt V, Jones DT, Kool M*, et al.* Reduced H3K27me3 and DNA hypomethylation are major drivers of gene expression in K27M mutant pediatric high-grade gliomas. Cancer Cell **2013**;24(5):660-72 doi 10.1016/j.ccr.2013.10.006.
66. Brown ZZ, Muller MM, Jain SU, Allis CD, Lewis PW, Muir TW. Strategy for "detoxification" of a cancer-derived histone mutant based on mapping its interaction with the methyltransferase PRC2. J Am Chem Soc **2014**;136(39):13498-501 doi 10.1021/ja5060934.
67. Justin N, Zhang Y, Tarricone C, Martin SR, Chen S, Underwood E*, et al.* Structural basis of oncogenic histone H3K27M inhibition of human polycomb repressive complex 2. Nature Communications **2016**;7(1) doi 10.1038/ncomms11316.
68. Piunti A, Hashizume R, Morgan MA, Bartom ET, Horbinski CM, Marshall SA*, et al.* Therapeutic targeting of polycomb and BET bromodomain proteins in diffuse intrinsic pontine gliomas. Nat Med **2017**;23(4):493-500 doi 10.1038/nm.4296.
69. Herz HM, Morgan M, Gao X, Jackson J, Rickels R, Swanson SK*, et al.* Histone H3 lysine-to-methionine mutants as a paradigm to study chromatin signaling. Science **2014**;345(6200):1065-70 doi 10.1126/science.1255104.
70. Cordero FJ, Huang Z, Grenier C, He X, Hu G, McLendon RE*, et al.* Histone H3.3K27M Represses p16 to Accelerate Gliomagenesis in a Murine Model of DIPG. Mol Cancer Res **2017**;15(9):1243-54 doi 10.1158/1541-7786.MCR-16-0389.
71. Larson JD, Kasper LH, Paugh BS, Jin H, Wu G, Kwon CH*, et al.* Histone H3.3 K27M Accelerates Spontaneous Brainstem Glioma and Drives Restricted Changes in Bivalent Gene Expression. Cancer Cell **2019**;35(1):140-55 e7 doi 10.1016/j.ccell.2018.11.015.

72. Silveira AB, Kasper LH, Fan Y, Jin H, Wu G, Shaw TI, *et al.* H3.3 K27M depletion increases differentiation and extends latency of diffuse intrinsic pontine glioma growth in vivo. Acta Neuropathol **2019**;137(4):637-55 doi 10.1007/s00401-019-01975-4.
73. Harutyunyan AS, Krug B, Chen H, Papillon-Cavanagh S, Zeinieh M, De Jay N, *et al.* H3K27M induces defective chromatin spread of PRC2-mediated repressive H3K27me2/me3 and is essential for glioma tumorigenesis. Nat Commun **2019**;10(1):1262 doi 10.1038/s41467-019-09140-x.
74. Bayliss J, Mukherjee P, Lu C, Jain SU, Chung C, Martinez D, *et al.* Lowered H3K27me3 and DNA hypomethylation define poorly prognostic pediatric posterior fossa ependymomas. Sci Transl Med **2016**;8(366):366ra161 doi 10.1126/scitranslmed.aah6904.
75. Pajtler KW, Wen J, Sill M, Lin T, Orisme W, Tang B, *et al.* Molecular heterogeneity and CXorf67 alterations in posterior fossa group A (PFA) ependymomas. Acta Neuropathol **2018**;136(2):211-26 doi 10.1007/s00401-018-1877-0.
76. Jain SU, Do TJ, Lund PJ, Rashoff AQ, Diehl KL, Cieslik M, *et al.* PFA ependymoma-associated protein EZHIP inhibits PRC2 activity through a H3 K27M-like mechanism. Nat Commun **2019**;10(1):2146 doi 10.1038/s41467-019-09981-6.
77. Hubner JM, Muller T, Papageorgiou DN, Mauermann M, Krijgsveld J, Russell RB, *et al.* EZHIP / CXorf67 mimics K27M mutated oncohistones and functions as an intrinsic inhibitor of PRC2 function in aggressive posterior fossa ependymoma. Neuro Oncol **2019** doi 10.1093/neuonc/noz058.
78. Piunti A, Smith ER, Morgan MAJ, Ugarenko M, Khaltyan N, Helmin KA, *et al.* CATACOMB: An endogenous inducible gene that antagonizes H3K27 methylation activity of Polycomb repressive complex 2 via an H3K27M-like mechanism. Sci Adv **2019**;5(7):eaax2887 doi 10.1126/sciadv.aax2887.
79. Kantoff PW, Higano CS, Shore ND, Berger ER, Small EJ, Penson DF, *et al.* Sipuleucel-T immunotherapy for castration-resistant prostate cancer. N Engl J Med **2010**;363(5):411-22 doi 10.1056/NEJMoa1001294.
80. Le DT, Durham JN, Smith KN, Wang H, Bartlett BR, Aulakh LK, *et al.* Mismatch repair deficiency predicts response of solid tumors to PD-1 blockade. Science **2017**;357(6349):409-13 doi 10.1126/science.aan6733.
81. Marcus L, Lemery SJ, Keegan P, Pazdur R. FDA Approval Summary: Pembrolizumab for the Treatment of Microsatellite Instability-High Solid Tumors. Clin Cancer Res **2019**;25(13):3753-8 doi 10.1158/1078-0432.CCR-18-4070.
82. Wei SC, Duffy CR, Allison JP. Fundamental Mechanisms of Immune Checkpoint Blockade Therapy. Cancer Discov **2018**;8(9):1069-86 doi 10.1158/2159-8290.CD-18-0367.
83. Hodges TR, Ott M, Xiu J, Gatalica Z, Swensen J, Zhou S, *et al.* Mutational burden, immune checkpoint expression, and mismatch repair in glioma: implications for immune checkpoint immunotherapy. Neuro Oncol **2017**;19(8):1047-57 doi 10.1093/neuonc/nox026.
84. Fecci PE, Sampson JH. The current state of immunotherapy for gliomas: an eye toward the future. J Neurosurg **2019**;131(3):657-66 doi 10.3171/2019.5.JNS181762.
85. Ansell SM, Lesokhin AM, Borrello I, Halwani A, Scott EC, Gutierrez M, *et al.* PD-1 blockade with nivolumab in relapsed or refractory Hodgkin's lymphoma. N Engl J Med **2015**;372(4):311-9 doi 10.1056/NEJMoa1411087.

86. Henon C, Blay JY, Massard C, Mir O, Bahleda R, Dumont S*, et al.* Long lasting major response to pembrolizumab in a thoracic malignant rhabdoid-like SMARCA4-deficient tumor. Ann Oncol **2019**;30(8):1401-3 doi 10.1093/annonc/mdz160.
87. Aspeslagh S, Chabanon RM, Champiat S, Postel-Vinay S. Understanding genetic determinants of resistance to immune checkpoint blockers. Semin Cancer Biol **2019** doi 10.1016/j.semcancer.2019.12.020.
88. Foster JB, Madsen PJ, Hegde M, Ahmed N, Cole KA, Maris JM*, et al.* Immunotherapy for pediatric brain tumors: past and present. Neuro Oncol **2019**;21(10):1226-38 doi 10.1093/neuonc/noz077.
89. Patel AP, Tirosh I, Trombetta JJ, Shalek AK, Gillespie SM, Wakimoto H*, et al.* Single-cell RNA-seq highlights intratumoral heterogeneity in primary glioblastoma. Science **2014**;344(6190):1396-401 doi 10.1126/science.1254257.
90. Sampson JH, Heimberger AB, Archer GE, Aldape KD, Friedman AH, Friedman HS*, et al.* Immunologic escape after prolonged progression-free survival with epidermal growth factor receptor variant III peptide vaccination in patients with newly diagnosed glioblastoma. J Clin Oncol **2010**;28(31):4722-9 doi 10.1200/JCO.2010.28.6963.
91. Sampson JH, Gunn MD, Fecci PE, Ashley DM. Brain immunology and immunotherapy in brain tumours. Nat Rev Cancer **2020**;20(1):12-25 doi 10.1038/s41568-019-0224-7.
92. Owens T, Bechmann I, Engelhardt B. Perivascular spaces and the two steps to neuroinflammation. J Neuropathol Exp Neurol **2008**;67(12):1113-21 doi 10.1097/NEN.0b013e31818f9ca8.
93. Perry VH. A revised view of the central nervous system microenvironment and major histocompatibility complex class II antigen presentation. J Neuroimmunol **1998**;90(2):113-21 doi 10.1016/s0165-5728(98)00145-3.
94. Guermonprez P, Valladeau J, Zitvogel L, Thery C, Amigorena S. Antigen presentation and T cell stimulation by dendritic cells. Annu Rev Immunol **2002**;20:621-67 doi 10.1146/annurev.immunol.20.100301.064828.
95. Orrego E, Castaneda CA, Castillo M, Bernabe LA, Casavilca S, Chakravarti A*, et al.* Distribution of tumor-infiltrating immune cells in glioblastoma. CNS Oncol **2018**;7(4):CNS21 doi 10.2217/cns-2017-0037.
96. Kamran N, Alghamri MS, Nunez FJ, Shah D, Asad AS, Candolfi M*, et al.* Current state and future prospects of immunotherapy for glioma. Immunotherapy **2018**;10(4):317-39 doi 10.2217/imt-2017-0122.
97. Perng P, Lim M. Immunosuppressive Mechanisms of Malignant Gliomas: Parallels at Non-CNS Sites. Front Oncol **2015**;5:153 doi 10.3389/fonc.2015.00153.
98. Moore KW, de Waal Malefyt R, Coffman RL, O'Garra A. Interleukin-10 and the interleukin-10 receptor. Annu Rev Immunol **2001**;19:683-765 doi 10.1146/annurev.immunol.19.1.683.
99. Hishii M, Nitta T, Ishida H, Ebato M, Kurosu A, Yagita H*, et al.* Human glioma-derived interleukin-10 inhibits antitumor immune responses in vitro. Neurosurgery **1995**;37(6):1160-6; discussion 6-7 doi 10.1227/00006123-199512000-00016.
100. Lin GL, Nagaraja S, Filbin MG, Suva ML, Vogel H, Monje M. Non-inflammatory tumor microenvironment of diffuse intrinsic pontine glioma. Acta Neuropathol Commun **2018**;6(1):51 doi 10.1186/s40478-018-0553-x.
101. Lieberman NAP, DeGolier K, Kovar HM, Davis A, Hoglund V, Stevens J*, et al.* Characterization of the immune microenvironment of diffuse intrinsic pontine glioma:

implications for development of immunotherapy. Neuro Oncol **2019**;21(1):83-94 doi 10.1093/neuonc/noy145.
102. Curtin JF, King GD, Candolfi M, Greeno RB, Kroeger KM, Lowenstein PR*, et al.* Combining cytotoxic and immune-mediated gene therapy to treat brain tumors. Curr Top Med Chem **2005**;5(12):1151-70 doi 10.2174/156802605774370856.
103. Ali S, King GD, Curtin JF, Candolfi M, Xiong W, Liu C*, et al.* Combined immunostimulation and conditional cytotoxic gene therapy provide long-term survival in a large glioma model. Cancer Res **2005**;65(16):7194-204 doi 10.1158/0008-5472.CAN-04-3434.
104. King GD, Muhammad AK, Curtin JF, Barcia C, Puntel M, Liu C*, et al.* Flt3L and TK gene therapy eradicate multifocal glioma in a syngeneic glioblastoma model. Neuro Oncol **2008**;10(1):19-31 doi 10.1215/15228517-2007-045.
105. Ghulam Muhammad AK, Candolfi M, King GD, Yagiz K, Foulad D, Mineharu Y*, et al.* Antiglioma immunological memory in response to conditional cytotoxic/immune-stimulatory gene therapy: humoral and cellular immunity lead to tumor regression. Clin Cancer Res **2009**;15(19):6113-27 doi 10.1158/1078-0432.CCR-09-1087.
106. Curtin JF, Liu N, Candolfi M, Xiong W, Assi H, Yagiz K*, et al.* HMGB1 mediates endogenous TLR2 activation and brain tumor regression. PLoS Med **2009**;6(1):e10 doi 10.1371/journal.pmed.1000010.
107. Candolfi M, Yagiz K, Foulad D, Alzadeh GE, Tesarfreund M, Muhammad AK*, et al.* Release of HMGB1 in response to proapoptotic glioma killing strategies: efficacy and neurotoxicity. Clin Cancer Res **2009**;15(13):4401-14 doi 10.1158/1078-0432.CCR-09-0155.
108. Guery JC, Adorini L. Dendritic cells are the most efficient in presenting endogenous naturally processed self-epitopes to class II-restricted T cells. J Immunol **1995**;154(2):536-44.
109. Maraskovsky E, Brasel K, Teepe M, Roux ER, Lyman SD, Shortman K*, et al.* Dramatic increase in the numbers of functionally mature dendritic cells in Flt3 ligand-treated mice: multiple dendritic cell subpopulations identified. J Exp Med **1996**;184(5):1953-62 doi 10.1084/jem.184.5.1953.
110. Moolten FL. Tumor chemosensitivity conferred by inserted herpes thymidine kinase genes: paradigm for a prospective cancer control strategy. Cancer Res **1986**;46(10):5276-81.
111. Castro MG, Candolfi M, Wilson TJ, Calinescu A, Paran C, Kamran N*, et al.* Adenoviral vector-mediated gene therapy for gliomas: coming of age. Expert Opin Biol Ther **2014**;14(9):1241-57 doi 10.1517/14712598.2014.915307.
112. Sandmair AM, Loimas S, Puranen P, Immonen A, Kossila M, Puranen M*, et al.* Thymidine kinase gene therapy for human malignant glioma, using replication-deficient retroviruses or adenoviruses. Hum Gene Ther **2000**;11(16):2197-205 doi 10.1089/104303400750035726.
113. Trask TW, Trask RP, Aguilar-Cordova E, Shine HD, Wyde PR, Goodman JC*, et al.* Phase I study of adenoviral delivery of the HSV-tk gene and ganciclovir administration in patients with current malignant brain tumors. Mol Ther **2000**;1(2):195-203 doi 10.1006/mthe.2000.0030.

114. Smitt PS, Driesse M, Wolbers J, Kros M, Avezaat C. Treatment of relapsed malignant glioma with an adenoviral vector containing the herpes simplex thymidine kinase gene followed by ganciclovir. Mol Ther **2003**;7(6):851-8 doi 10.1016/s1525-0016(03)00100-x.
115. Germano IM, Fable J, Gultekin SH, Silvers A. Adenovirus/herpes simplex-thymidine kinase/ganciclovir complex: preliminary results of a phase I trial in patients with recurrent malignant gliomas. J Neurooncol **2003**;65(3):279-89 doi 10.1023/b:neon.0000003657.95085.56.
116. Westphal M, Yla-Herttuala S, Martin J, Warnke P, Menei P, Eckland D*, et al.* Adenovirus-mediated gene therapy with sitimagene ceradenovec followed by intravenous ganciclovir for patients with operable high-grade glioma (ASPECT): a randomised, open-label, phase 3 trial. Lancet Oncol **2013**;14(9):823-33 doi 10.1016/S1470-2045(13)70274-2.
117. Curtin JF, King GD, Barcia C, Liu C, Hubert FX, Guillonneau C*, et al.* Fms-like tyrosine kinase 3 ligand recruits plasmacytoid dendritic cells to the brain. J Immunol **2006**;176(6):3566-77 doi 10.4049/jimmunol.176.6.3566.
118. Kaisho T, Akira S. Regulation of dendritic cell function through Toll-like receptors. Curr Mol Med **2003**;3(4):373-85 doi 10.2174/1566524033479726.
119. King GD, Muhammad AK, Larocque D, Kelson KR, Xiong W, Liu C*, et al.* Combined Flt3L/TK gene therapy induces immunological surveillance which mediates an immune response against a surrogate brain tumor neoantigen. Mol Ther **2011**;19(10):1793-801 doi 10.1038/mt.2011.77.
120. Lowenstein PR, Orringer DA, Sagher O, Heth J, Hervey-Jumper SL, Mammoser AG*, et al.* First-in-human phase I trial of the combination of two adenoviral vectors expressing HSV1-TK and FLT3L for the treatment of newly diagnosed resectable malignant glioma: Initial results from the therapeutic reprogramming of the brain immune system. **2019**;37(15_suppl):2019- doi 10.1200/JCO.2019.37.15_suppl.2019.

Chapter 2 : Generation of Mouse Models of Brainstem Glioma[4]

Abstract

Diffuse intrinsic pontine glioma (DIPG) is a brain tumor most commonly diagnosed in children of median age 6-7 and the prognosis is very poor. Information from genomic studies of autopsy and biopsy tissue has revealed the presence of recurrent activating mutations in ACVR1 and dominant negative K27M mutations in the genes encoding histone H3 variants, H3.3 and H3.1. We developed genetically engineered immunocompetent mouse models to assess the role of ACVR1 G328V and the commonly co-expressed H3.1 K27M on DIPG pathogenesis using the Sleeping Beauty (SB) transposase system to target neural stem cells in the subventricular zone. We observed that ACVR1 G328V enhanced median survival, while the H3.1 K27M mutation did not significantly affect median survival on its own. Histological analysis of ACVR1 G328V mutant tumors displayed increased downstream signaling of bone morphogenetic pathway (BMP) as demonstrated by increased phospho-smad1/5 levels. We also demonstrated that the H3.1 K27M mutant tumors had decreased H3K27me3 levels. Additionally, transcriptome analysis of mutant ACVR1 neurospheres (NS) identified an increase in the transforming growth factor beta (TGF-β) signaling pathway and the regulation of cell differentiation. These data indicate that we are able to use the SB transposase system to develop *in vivo* and *in vitro* models

[4] Portions of this chapter have been submitted for publication in Clinical Cancer Research in collaboration with the following co-authors: Padma Kadiyala, Felipe J. Nunez, Stephen Carney, Fernando Nunez, Jessica C. Gauss, Ramya Ravindran, Sheeba Pawar, Marta Edwards, Pedro R. Lowenstein, and Maria G. Castro.

of relevant DIPG mutations. We also demonstrate that tumors can be induced in the brainstem and that we can generate transplantable models which allow for rapid testing of novel therapeutics.

Introduction

Diffuse Intrinsic pontine glioma (DIPG) is a highly aggressive pediatric brainstem tumor for which there is no current treatment. Consequently, the percent of children who survive for longer than two years is less than ten percent. The most frequent DIPG mutations affect the N-terminal tail of histone H3.3 and histone H3.1 and result in the change of a lysine to methionine at residue 27 (1-3). It has been reported that the K27M mutation inhibits Enhancer Of Zeste 2 (EZH2) histone methyltransferase activity causing a global hypomethylation of H3K27 (4). Post-translational modifications regulate chromatin structure and transcription and are particularly important during normal development, stem cell maintenance and differentiation(5,6) . Thus, a mutation that affects histone modifications may have a profound impact on gene expression with oncogenic consequences.

Recently it was described that the next most frequently mutated gene in DIPG is ACVR1 (mutated in 24% of DIPG cases) (7-10). ACVR1 encodes a type 1 BMP receptor and the six mutations reported are believed to result in constitutive BMP pathway activation (7-10). BMPs play important roles in the development of neural stem cells (11). Spatial temporal regulation of the BMPs enables them to fulfill their multiple roles. During neurogenesis BMPs initially promote neural lineage commitment and inhibit oligodendrocyte commitment, while during gliogenesis BMPs promote astrocyte lineage commitment (11). Additionally, in adulthood BMP signaling is important for the maintenance and differentiation of neural stem cells in the

subventricular zone and subgranular zone (11). Interestingly, the mutations found in DIPG overlap with germline mutations in ACVR1 that cause the musculoskeletal disorder fibrodysplasia ossificans progressiva (FOP) and some patients with this disorder have been reported to have atypical neurological symptoms and white matter lesions (12).

Mouse models are crucial to elucidate the mechanisms by which ACVR1 G328V and H3.1 K27M contribute to DIPG pathogenesis in order to develop targeted therapies against these mutations. We used the sleeping beauty (SB) transposase system to develop mouse models of DIPG. SB is a transposase that is able to recognize inverted repeats/direct repeats (IR/DR) sites on DNA transposons and carry out a cut and paste reaction to integrate transposon DNA into a host genome(13). The SB system can be utilized to generate endogenous tumors that resemble gliomas through delivery of DNA transposons that encode oncogenes and tumor suppressors (14-18). We utilized the SB transposase system to introduce plasmids encoding the activating ACVR1 mutation and H3.1 K27M mutation in the context of upregulated NRAS and p53 knockdown into neural stem cells in the subventricular zone. In our mouse model ACVR1 G328V was associated with increased median survival while the H3.1 K27M mutation did not alter median survival independently of ACVR1. Transcriptome analysis of ACVR1 mutant NS identified an increase in the TGF-β signaling pathway and signaling pathways regulating the pluripotency of stem cells. We also show that the SB system can be utilized to deliver plasmid DNA into the fourth ventricle of postnatal day 1 mice to generate brainstem gliomas. Additionally, we demonstrate that tumor neurospheres derived from the SB generated tumors can be implanted into the pons of adult mice to rapidly develop immune competent transplantable mouse models of DIPG.

Methods

Experimental model:

All animal studies were conducted according to guidelines approved by the Institutional Animal Care and Use Committee at the University of Michigan. Animals were housed in an AAALAC accredited animal facility and had constant access to food and water; they were monitored daily for tumor burden. Males and females were used. The strain of mice utilized in the study was C57BL/6 (Jackson Laboratory, 000664). A murine model of glioma was generated by employing the SB transposon system to integrate plasmid DNA into the genome of postnatal day 1 (P1) mouse pups. The plasmids utilized were as follows: (i) SB Transposase and luciferase (pT2C-LucPGK-SB100X, henceforth referred to as SB/Luc) (ii) a short-hairpin against p53 (pT2-shp53-GFP4, henceforth referred to as shp53) or shp53-NO-GFP (iii) a constitutively active mutant of NRAS (pT2CAG-NRASV12, henceforth referred to as NRAS) with or without (4) mutant ACVR1 G328V (pkt-ACVR1-G328V-IRES-Katushka; henceforth referred to as mACVR1) (1-3). To create the mACVR1 plasmid we cloned pCMV5-ALK2-WT into pKT2-IRES-Katushka by blunt cloning. Then, we used the QuikChange II Site-Directed Mutagenesis Kit (Agilent, 200523) to introduce (c.983G>T, p.Gly328Val) mutation into pKT2-ALK2-WT-IRES-Katushka, to generate pKT2-ACVR1-G328V-IRES-Katushka (Addgene plasmid #77437). The resultant mACVR1 plasmid was confirmed by Sanger sequencing. SB/Luc, shp53 and NRAS plasmids were the generous gift of Dr. John Ohlfest (University of Minnesota, now deceased). The pCMV5-ALK2-WT plasmid was a generous gift from Jeff Wrana (Addgene plasmid #11741). All experiments were performed using post-natal day 1 (P1) or P2 wild-type C57BL/6 mice. The plasmid combinations injected were as follows: (1) (i) shp53 and NRAS (henceforth referred to as wt-ACVR1), (ii) shp53, NRAS, and ACVR1m. Mice were injected according to a previously

described protocol (2). Briefly, plasmids were mixed in mass ratios of 1:2:2:2:2 (20 µg plasmid in a total of 40 µL plasmid mixture) with in vivo-jetPEI® (Polyplus Transfection, 201-50G) (2.8 µL per 40 µL plasmid mixture) and dextrose (5% total) and maintained at room temperature for at least 20 minutes prior to injection. Anesthesia was performed by placing the pup on ice for 2 minutes and then on a neonatal stereotaxic stage cooled to 2-8°C to maintain anesthesia. The lateral ventricle (1.5 mm AP, 0.7 mm lateral, and 1.5 mm deep from the λ-suture) or fourth ventricle (3 mm posterior to the λ-suture and 3 mm deep) were targeted (4). Plasmid uptake and tumor development and progression was monitored as previously described (2,3). Animals were monitored daily for signs of morbidity (ataxia, impaired mobility, hunched posture, seizures, or scruffy fur). Symptomatic mice were transcardially perfused using Tyrode's solution and fixed with 4% paraformaldehyde (PFA) (2,3,5).

Immunohistochemistry (IHC) of paraffin embedded brains:

Immunhistochemistry staining was performed as previously described (2,3). Briefly, after perfusion, mouse brains were harvested and post-fixed in 4% PFA then paraffin embedded. Tissue was sectioned using a rotary microtome. Heat mediated antigen retrieval was performed using either 1X Rodent Decloaker (Biocare Medical, RD 913) or citrate buffer (10 mM citric acid, 0.05% non-ionic detergent, pH 6) at 125°C for 30 seconds and at 90°C for 10s followed by quenching of endogenous peroxides using 0.3 % H2O2 for 30 minutes, and permeabilization with 0.025% Triton in TBS. Sections were blocked with 10% horse serum, 0.1% BSA in TBS) for 30 minutes and then incubated overnight at 4°C with primary antibody diluted in 0.1% BSA in TBS. For 3,3′-Diaminobenzidine (DAB) staining the VECTASTAIN ABC HRP Kit (Vector Laboratories, PK-4000) was used. The Alexa Flour 488 Tyramide SuperBoost Kit (Thermo Fisher Scientific, NC1136352) was used for the phospho Smad1/Smad5/Smad8 (Ser463/465)

(MilliporeSigma, AB3848-I) antibody. Bright-field images were obtained using Olympus MA BX53 microscope. Flourescent images were obtained using confocal microscopy (Carl Zeiss: MIC-System). A list of all antibodies can be found on Appendix Table A1.

Primary (NS):

Mouse (NS) were generated from tumors that were developed using the SB system by injection of the following plasmid combinations (1) (i) shp53 and NRAS, or (ii) shp53, NRAS, and ACVR1m into the lateral ventricle (1.5 mm AP, 0.7 mm lateral, and 1.5 mm deep from the λ-suture) following previously described protocols (2,3,5,6). When animals became symptomatic they were anesthetized then transcardially perfused with Tyrode's solution. The brains were harvested and tumors were identified by fluorescence expression. The tumor was then extracted and placed in 300 µL of media in an Eppendorf tube. Then, the tumor was mechanically dissociated using a sterile plastic pestle that fit the walls of the Eppendorf tube. This was followed by incubation with 1 mL of a cell dissociation buffer (Accutase, 423201), then filtered through a 70 µm strainer and maintained in neural stem-cell media [DMEM/F12 with L-Glutamine (Gibco, 11320-033), B-27 supplement (Gibco, 12587- 010), N-2 supplement (Gibco, 17502-048), Penicillin-Streptomycin (Corning, Cellgro, 30-001-CI), and Normocin (InvivoGen, ant-nr-1)] at 37 °C, 5% CO2. hFGF and hEGF (Shenendoah Biotech,100-26, 100-146) were supplemented twice weekly at 1 µL (20 ng/µL each stock, 1000x stock) per 1 mL media. Primary mutant ACVR1 glioma NS were transduced with pLVX-OVA to generate mACVR1-OVA NS and selected with 5 ug/mL puromycin (Sigma, P8833). pLVX-OVA was generated by cloning cytoplasmic ovalbumin from pCI-neo-cOVA (Addgene plasmid #25097) into pLVX-mCherry-c1 (Takarabio, 632561) by Nde1 and EcoR1 directed cloning.

Western blot:

NS were harvested and re-suspended in RIPA buffer (MilliporeSigma, R0278) with 1X of Halt™ Protease and Phosphatase Inhibitor Cocktail, EDTA-free (100X) (Thermo Scientific, 78441). The Pierce™ BCA Protein Assay Kit (Thermo Scientific, 23227) was used to measure protein concentration. 20 µg of protein extract were run on a 4-12% SDS-PAGE PAGE gel (Thermo Fisher Scientific, NuPAGE®, NP0322BOX) and transferred to nitrocellulose membranes (Bio-Rad, 1620112). The membrane was probed with 1:500 of anti-phospho Smad1/Smad5/Smad8 (Ser463/465) (MilliporeSigma, AB3848-I); 1:500 of anti-Smad1 antibody (Abcam, ab63356); 1:500 of anti-Id1 (Biocheck, BCH-1/37-2); and 1:10,000 of β-actin antibody (MilliporeSigma, A1978). The secondary antibodies used were: 1:4000 of goat anti-rabbit (Dako, Agilent Technologies, P0448) and 1:20,000 of rabbit anti-mouse (Dako, Agilent Technologies, P0260). SuperSignal West Femto (Thermo Fisher Scientific, 34095) was used to for detection.

In vitro experiments with ACVR1 inhibitor:

LDN-214117 is a specific ACVR1 inhibitor (7). To determine an effective concentration to inhibit ACVR1 signaling in our mouse NS we plated wild type or mutant ACVR1 cells in a T-25 flak containing growth media supplemented with varying concentrations of LDN-214117 (0.03 uM, 0.1 uM, 0.3 uM, 1 uM); Selleck Chemicals, S7147) or equivalent DMSO control. NS were incubated with inhibitor for 90 minutes and then cells were collected to assess phosphorylation of Smad1/5 and Id2 by western blot.

Immunocytochemistry:

SU-DIPG-VI and SU-DIPG-XX1 were obtained from Dr. Michelle Monje at Stanford University (Stanford, Ca) in accordance with an institutionally approved protocol at each institution. Cells were cultured in DMEM with 10% FBS. 1 X 105 cells per well were plated on glass slides coated with 2% gelatin. Cells were fixed with 4% PFA and permeabilized with PBS 1X plus

0.3% Tween. ICC was performed with 1:100 Id1 (Biocheck, BCH-1/195-14), pERK1/2 (Cell Signaling, 4370), pMEK1/2 (Santa Cruz, sc-7995-R), and 1:1000 goat anti-rabbit antibody, Alexa Flour 488 (Invitrogen, A -11034).

RNA-seq analysis:

RNA-seq analysis was performed in collaboration with the Bioinformatics Core at the University of Michigan. Read files from the University of Michigan Sequencing Core's storage were downloaded and concatenated into a single fastq file for each sample. The quality of the raw reads data for each sample was assessed using FastQC [1] (version v0.11.3) to identify features of the data that may indicate quality problems (e.g. low quality scores, over-represented sequences, inappropriate GC content). The Tuxedo Suite software package was used for alignment, differential expression analysis, and post-analysis diagnostics. Briefly, we aligned reads to the reference genome including both mRNAs and lncRNAs (UCSC mm10) using TopHat (version 2.0.13) and Bowtie2 (version 2.2.1.). The default parameter settings for alignment were used, with the exception of: "--b2-very-sensitive" telling the software to spend extra time searching for valid alignments. We used FastQC for a second round of quality control (post-alignment), to ensure that only highquality data would be input to expression quantitation and differential expression analysis. We performed two different analysis techniques to specify differential expression: Tuxedo and DESeq2, using UCSC mm10.fa as the reference genome sequence. The volcano plot was produced using an R base script and encompasses all genes identified by our RNA-seq analysis. In order to identify significantly differentially expressed genes, we set a log2 fold change cut-off of 0.585 and –log10(FDR) greater than 1.3, where circles represent individual genes and colors as indicated (red-upregulated, green-downregulated) shown in Figure 3A. The data was analyzed using Advaita Bio's iPathwayGuide

(https://www.advaitabio.com/ipathwayguide). This software analysis tool implements the 'Impact Analysis' approach that takes into consideration the direction and type of all signals on a pathway, the position, role and type of every gene, etc., as described in (8-11). Gene Ontology (GO) enrichment analysis was performed using iPathwayGuide (http://www.advaitabio.com/ipathwayguide), displaying up- and down-regulated genes associated with the same GO and was shown in Figure 3C. GO Biological Processes, selected for relevance to phenotype, were plotted in a horizontal bar graph using graphpad shown in Figure 3B. All 100 differentially expressed genes between wt-ACVR1 and mutant-ACVR1 NS were converted to excel with their corresponding gene names in uppercase in first column and log2-fold change values in second column to create the rank file. This rank file is used as an input for gene set enrichment analysis (GSEA) pre-ranking on program downloaded from Broad Institute (http://software.broadinstitute.org/gsea/index.jsp). In addition, Broad Institute provides a gene set containing all GOs (c5.all.v7.0.symbols.gmt), which is also required to perform the pre-ranking using 2000 permutations and gene set size range of 0 to 200. The enrichment map is generated using the Cytoscape platform and requires the rank and gmt files along with the positive/negative GSEA report files. Each node represents an individual GO, the size is reflective of the number of genes within that set, and the red color signifies positively regulated pathways. We set a pvalue cut off of 0.001 and FDR of 0.5. The stringency of our FDR was lowered due to encompass the underlying biological pathways differentially regulated by ACVR1 are shown in yellow in Figure 3D. The enrichment score plots for Regulation of BMP signaling Pathway and Regulation of Cell Differentiation are shown in Figure 3E and 3F respectively, which are images provided in the GSEA Pre-ranking report.

Statistical analysis

All data were analyzed using GraphPad Prism version 8. Animals studies were performed with at least 3 animals per group. The statistical test used is indicated in each figure. A $p \leq 0.05$ was considered significant.

Results

Mouse model of glioma expressing DIPG mutations induced by transforming neural progenitor cells using the SB transposase system

To assess the impact of DIPG mutations in glioma pathogenesis we generated a genetically engineered mouse model of DIPG using the SB transposase system (14,15). We induced tumors by activation of the receptor tyrosine kinase (RTK)-RAS- phosphatidylinositol 3-kinase (PI3K) pathway, which is upregulated in a large percentage of DIPGs, and through inactivation of *TP53,* also commonly mutated in DIPG (19-21). This was achieved through the delivery of the following plasmids: *NRASV12*, a short hair pin targeting tumor *protein p53* (*TP53)* (shP53), and SB transposase/firefly luciferase, with or without *ACVR1*^{G328V} or H3.1 K27M (**Fig. 2.1 A**) into the lateral ventricle of neonatal mice to target neural progenitor cells in the subventricular zone (**Fig. 2.1 B**). The four experimental groups were: (1) control (wt-ACVR1 and wt- H3.1) [*NRASV12* and shp53)], (2) mutant ACVR1 (mACVR1) [*NRASV12*, shp53, *ACVR1*^{G328V}] (3) mutant H3.1 (H3.1 K27M) [*NRASV12*, shp53, *HIST1H3B*^{K27M}], and *(4)* mutant ACVR1/H3.1 K27M) (*NRASV12*, shp53, *ACVR1*^{G328V}, *HIST1H3B*^{K27M}*)*. The median survival (MS) of animals in the control group was 80 days post injection (dpi) (**Fig. 2.1 C**). mACVR1 tumors (MS=119 dpi) had enhanced survival compared to control group [Mantel-Cox test; p = 0.0029] (**Fig. 2.1C**). H3.1 K27M did not have an effect on survival compared to the control group [Mantel-Cox test; p = not significant (ns)] (**Fig 2.1C**). Surprisingly, tumors harboring

NRAS/shp53/ACVR1 G328V/H3.1 K27M had increased survival compared to both the control group ($p<0.0001$) and the mACVR1 group [Mantel-Cox test; $p=0.0371$] (**Fig. 2.1C**). Tumors induced with ACVR1 G328V had increased immunostaining of phopho-Smad1/5, a transducer of BMP signaling as compared to the NRAS/shP53 control (**Fig. 2.2A**). Furthermore, tumors induced with a plasmid combination including H3.1 K27M have decreased immunostaining of H3K27me3 as compared to the NRAS/shP53 control consistent with the global H3K27me3 loss observed in patients with H3K27M mutations (**Fig. 2.2B**).

Characterization of mutant ACVR1 NS

To assess the role of ACVR1 G328V we generated *in vitro* cultures from the mACVR1 tumors. This was done by harvesting the brain once animals became symptomatic, excising the tumor which was identified by a Katushka fluorescent reporter, and dissociating the tumor to generate a single cell suspension. In culture the cells form 3D structures which we refer to as tumor NS (**Fig. 2.3A**). We characterized the in vitro tumor NS expressing mACVR1 and observed that they exhibited elevated levels of phospho-smad1/5 (**Fig. 2.3B**) and elevated levels of Id1 (**Fig. 2.3B**). To test the effect of a specific inhibitor of ACVR1, LDN-214117, on phospho-Smad1/5 signaling we treated mACVR1 NS with increasing concentrations of LDN-214117. We observed decreased levels of phospho-Smad1/5 and Id2, while the levels of total Smad1 remain unchanged (**Fig. 2.3C**). These results indicate that ACVR1 G328V activates the BMP signaling pathway in mACVR1 NS.

To identify genes regulated by mACVR1 we performed RNAseq analysis on mACVR1 and wt-ACVR1 NS and identified genes that were differentially regulated (1.5-fold; FDR-corrected $P < 0.05$) (**Figure 2.4A**). The top three pathways that were impacted by ACVR1 G328V were focal adhesion (FDR corrected, $p=0.004$), the TGF-beta signaling pathway (FDR corrected,

p=0.004), and signaling pathways regulating pluripotency of stem cells (FDR corrected, p=0.009) (**Figure 2.4B**). Over expressed genes within the TGF-Beta pathway included ACVR1, and inhibitor of DNA binding genes Id1, Id2, and Id3 (**Figure 2.4B**). Gene set enrichment analysis (GSEA) suggests an enrichment in the response to BMP and the regulation of cell differentiation (**Fig. 2.4C-E**).

Since one of the top signaling pathways involved the regulation of pluripotency in stem cells, we evaluated whether mACVR1 tumors express CD133, CD44, and Aldh1, stem cell markers. Intracranial wt-ACVR1 or mACVR1 tumors were established in the pons of adult mice using SB derived NS. The results demonstrate that mACVR1 tumors have increased expression of the cancer stem cell markers CD133 (p=0.0002) and CD44 (p=0.0112) (**Fig. 2.5A**). However, we did not observe differences in the expression of another cancer stem cell marker, i.e., Aldehyde dehydrogenase 1 family, member A1 (Aldh1) (**Fig. 2.5A**). We next investigated the tumor initiating potential of wt-ACVR1 and mACVR1 NS *in vivo*. With wt-ACVR1 NS, the minimum number of cells required to generate brainstem gliomas with 100% penetrance was 1,000 cells, whereas, with mACVR1 NS it was possible to generate brainstem gliomas with 100% penetrance using 500 cells (**Fig. 2.5B**). These results indicate that mACVR1 NS have a greater tumor initiating potential.

Generation of gliomas in the brainstem using SB system

To test if we could generate gliomas in a more physiologically relevant location we injected the SB plasmids into the fourth ventricle of postnatal day 1 mice which is near the pons (**Fig. 2.6A**). The median survival (MS) of mice in the mACVR1 group was 127 dpi while the median survival for the wt-ACVR1 group was MS=85 dpi (**Fig. 2.6B**). All tumors, regardless of ACVR1 mutation status, displayed high cellularity, nuclear atypia, invasive features, and grew in

the brainstem (**Fig. 2.6C**). Tumors expressed markers of glial cells including oligodendrocyte transcription factor 2 (Olig2) (**Fig. 2.6D)**, glial fibrillary acidic protein (GFAP) (**Fig. 2.6E**), and the neural stem cell marker, Sox2 (**Fig. 2.6F**). Both the wt-ACVR1 group and mACVR1 tumors were positive for phosphorylated extracellular signal-regulated kinase (pERK) 1/2 (**Fig. 2.6G**). Additionally, we confirmed that tumors expressing mACVR1 exhibited activated Smad1/5/8 transcription factors (**Fig. 2.6H**). This correlated with increased levels of the downstream canonical target gene, inhibitor of DNA binding 1 (Id1) (**Fig. 2.6I**). Since the SB tumors were generated from tumors induced by activation of the RTK-RAS-PI3K signaling pathway we checked if this pathway was activated in DIPG cultures. Indeed, we found that SU-DIPG VI (wt-ACVR1) and SU-DIPG XX1 (mACVR1) cultures were positive for phosphorylated ERK1/2 (**Fig. 2.7A**). We also observed that mACVR1 DIPG cells had increased levels of ID1 compared to WT ACVR1 DIPG cultures (**Fig. 2.7B).**

Transplantable mouse model of brainstem glioma for pre-clinical testing

To develop a model that can be utilized for rapid pre-clinical testing of DIPG therapies, we implanted mACVR1 NS into the pons of immune competent adult C57BL/6 mice (**Fig. 2.8A**). The median survival of mice bearing mACVR1 brainstem gliomas was 19 dpi (**Fig. 2.8B**), giving us an adequate therapeutic window. Mice bearing mACVR1 brainstem gliomas are positive for Ki67 (proliferating cells), GFAP (astrocyte marker), Vimentin (astrocytes and ependymal cells), Iba1 (microglia), but negative for MBP (a marker of mature oligodendrocytes) (**Fig. 2.8C**). The tumors are also positive for pERK1/2 and pMEK1/2 demonstrating activation of the RTK-RAS-PI3K signaling pathway (**Fig. 2.8C**). We also observed expression of Id1 a downstream target gene of BMP-Smad1/5 signaling (**Fig. 2.8C**). Therefore, tumors derived by intracranial

implantation of mACVR1 tumor NS maintain key features of the spontaneous tumors derived using the SB system and are amenable to pre-clinical therapeutic implementation.

Discussion

The development of molecularly and histologically accurate animal models is critical for the identification and testing of novel therapeutic targets. When we initiated our study there were no available models studying the biology of a subgroup of DIPG patients co-expressing ACVR1 and H3.1 K27M mutations. Therefore, we utilized the SB transposase system to generate endogenous mouse models of ACVR1 G328V and H3.1 K27M DIPG. The SB system efficiently and reproducibly integrates plasmid DNA into the neural progenitor cells' host chromosomal DNA of neonatal mice, allowing for the functional assessment of the role of candidate DIPG genes in promoting tumor progression (14,15,17,18). Additionally, tumors arise in an immune competent mouse. Although, H3.1 K27M and ACVR1 mutations are hypothesized to be potential tumorigenic drivers in DIPG, we were not able to generate tumors with mACVR1 alone, H3.1-K27M alone, or a combination of mACVR1, H3.1-K27M, and activated PIK3CA. This is consistent with reports that mutations of ACVR1 were not sufficient to make Tp53 null mouse astrocytes tumorigenic, and that PDGF signaling was required to generate tumors with H3.3 K27M and Tp53 loss (10,22). For this reason, it was necessary to utilize additional tumorigenic drivers. We used NRAS, in combination with p53 knockdown, because it has been shown to be able to generate mouse models of glioblastoma that have histologically relevant features by activation of the RTK/RAS pathway, which is altered in 61.7% of DIPG cases (15,17-19). We developed gliomas in the cerebral hemispheres by injecting plasmids encoding NRASV12D, shp53, ACVR1 G328V and/ or H3.1 K27M into the lateral ventricles. Tumors

harboring the ACVR1 G328V mutation exhibited elevated phospho-Smad1/5 levels. We also observed that mutant H3.1 K27M tumors had decreased levels of H3k27me3, a phenotype of K27M mutations. Thus, our SB generated tumors exhibited the well documented phenotypes of the ACVR1 and H3.1 K27M mutations.

Since DIPG tumors originate in the pons, it was important for us to be able to test if we could develop gliomas in the pons. To do this, we injected plasmids encoding NRASV12D, shp53, and ACVR1 G328V into the fourth ventricle and showed that it was possible to induce tumors in the brainstem. Both the lateral ventricle and brainstem models of ACVR1 G328V exhibited a significantly increased median survival compared with wt-ACVR1 tumors. This is in contrast with results from Hoeman C.M. and colleagues in which the authors found that in an RCAS model of DIPG, driven by p53 loss and PDDGF-A, ACVR1 R206H accelerated tumor growth, in the presence or absence of H3.1 K27M (23). One potential reason for the difference in survival observed between our models may lie in the specific amino acid substitution that was modelled. We used the ACVR1 G328V mutation since this mutation was reported to be the most common of the six recurrent ACVR1 mutations. Recently it was reported that only amino acid substitutions of ACVR1 at the G328 residue confer a significant increase in survival (24). Thus, our SB model of ACVR1 G328V is consistent with what is seen in patients with mutations of glycine at position 328.

Transcriptional profiling of neurospheres expressing mACVR1 versus wt-ACVR1 confirmed upregulation of the TGF-beta pathway in mACVR1 NS, and identify pathways regulating the pluripotency of stem cells to be increased by the ACVR1 mutation. Additionally, we observed that mACVR1 NS have increased levels of stemness markers CD133 and CD44 after re-implantation and greater tumor initiation potential when compared to wt-ACVR1 NS.

Taken together, our data suggests mACVR1 regulates stemness and tumor initiation potential. Interestingly, clonal evolution analysis of a DIPG tumor found that the ACVR1 mutation was present along with the H3.1 K27M mutation in all tumor clones, in contrast to secondary mutations found only in some subclones, implicating mACVR1in DIPG tumor initiation (25). In addition, Hoeman C.M. and colleagues observed that ACVR1 R206H contributed to increased tumor incidence using the RCAS model driven by p53 loss and PDDGF-A, supporting our results that ACVR1 plays a role in tumor initiation (23).

The SB model also enabled us to generate an intracranial model of brainstem glioma through implantation of tumor NS into the pons of adult C57BL/6 mice. This implantation model has an intact immune system, and short latency enabling it to be used for pre-clinical testing of immune-mediated strategies for DIPG. We implanted tumors with mACVR1 NS, however, it would be possible to generate tumor NS expressing other DIPG mutations in order to test the effect of specific DIPG mutations on the efficacy of a pre-clinical therapy.

In conclusion, we demonstrate the amenability of the SB transposase to be used to develop genetically and histologically accurate models of DIPG. We generated models of ACVR1 G328V and H3.1 K27M, two genes mutated in DIPG. Uncovering the role of these mutations on DIPG tumorigenesis and disease progression could provide novel mechanistic insights useful to develop novel therapeutic targets for this incurable and deadly pediatric brainstem tumor.

Figures

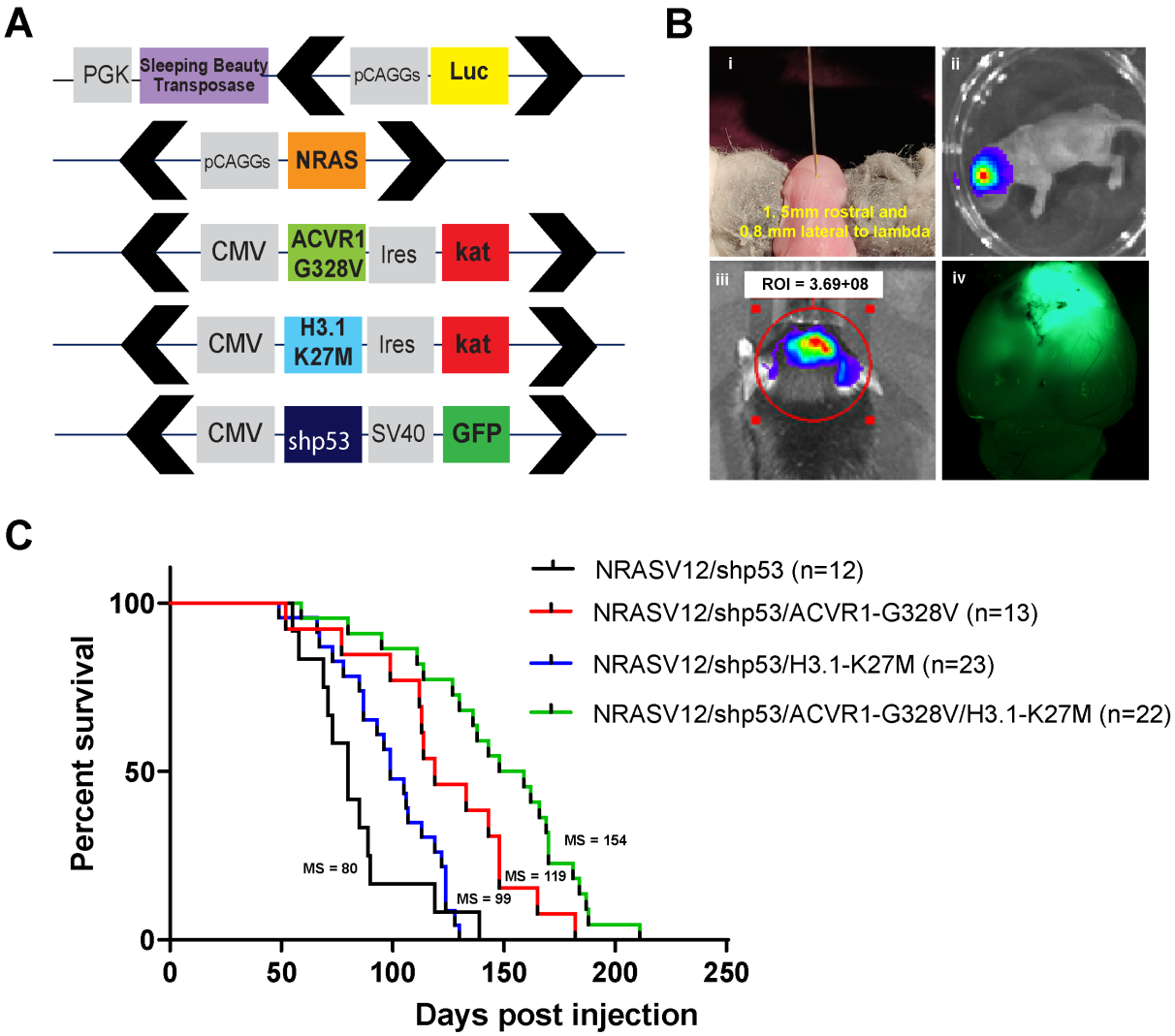

Figure 2.1 DIPG mouse models induced in the lateral ventricle

(**A**) Schematic representation of SB transposase and transposon plasmids used to develop gliomas with DIPG mutations in the lateral ventricle. Black arrows indicate position of inverted repeat and direct repeat (IR/DR) sequences which flank specific DNA sequences. (**B**) (i) neonatal mouse on stereotaxic frame. Lateral ventricle coordinates: 1.5 mm ventral and 0.8 mm lateral to the lambda, (ii) bioluminescence imaging at 1-day post injection (dpi) confirming the efficiency of the in vivo transfection. (iii) bioluminescence imaging at endpoint stage showing a large tumor (iv) fluorescence image of a GFP fluorescent tumor. (**C**) Kaplan-Meier survival curves for mice bearing lateral ventricle gliomas induced with NRASV12/shp53 (n = 12), NRASV12/shp53/ ACVR1G328V (n = 13), NRASV12/shp53/ H3.1 K27M (n = 23), NRASV12/shp53/ ACVR1G328V/ H3.1 K27M (n = 22). MS = median survival.

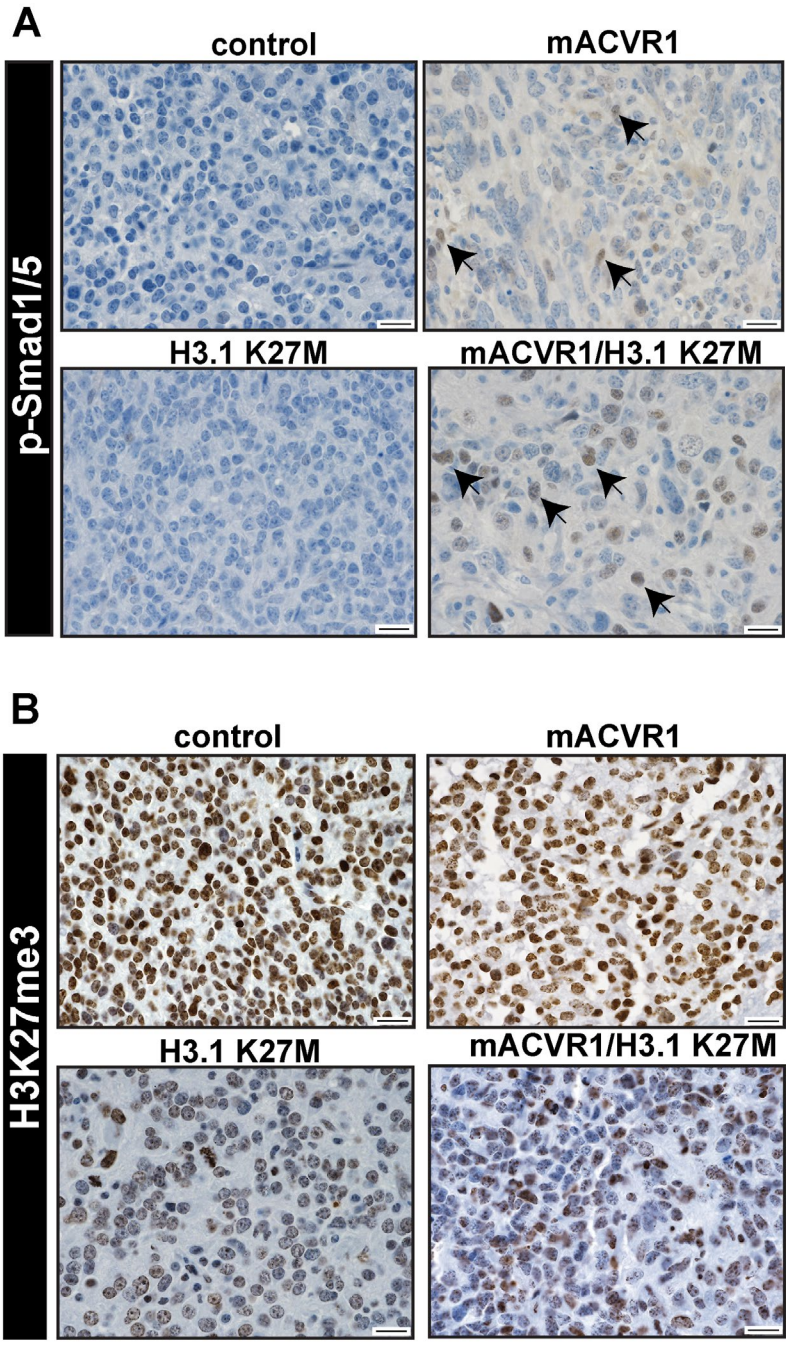

Figure 2.2 Characterization of DIPG gliomas induced in the lateral ventricle

(**A**) IHC staining for phospho-Smad1/5 (p-Smad1/5) protein in paraffin embedded SB brainstem tumor sections of the (1) control group, (2) mACVR1, (3)H3.1 K27M) and (4) mACVR1/ H3.1 K27M. Scale bar is 20 µm. Arrows represent positive staining. (**B**) IHC staining for H3K27me3 protein in paraffin embedded SB brainstem tumor sections of the (1) control group, (2) mACVR1, (3)H3.1 K27M) and (4) mACVR1/ H3.1 K27M. Scale bar is 20 µm. Tumors harboring the H3.1 K27M have decreased positive staining for H3K27me3 compared to the control group or the mACVR1 group.

[5]

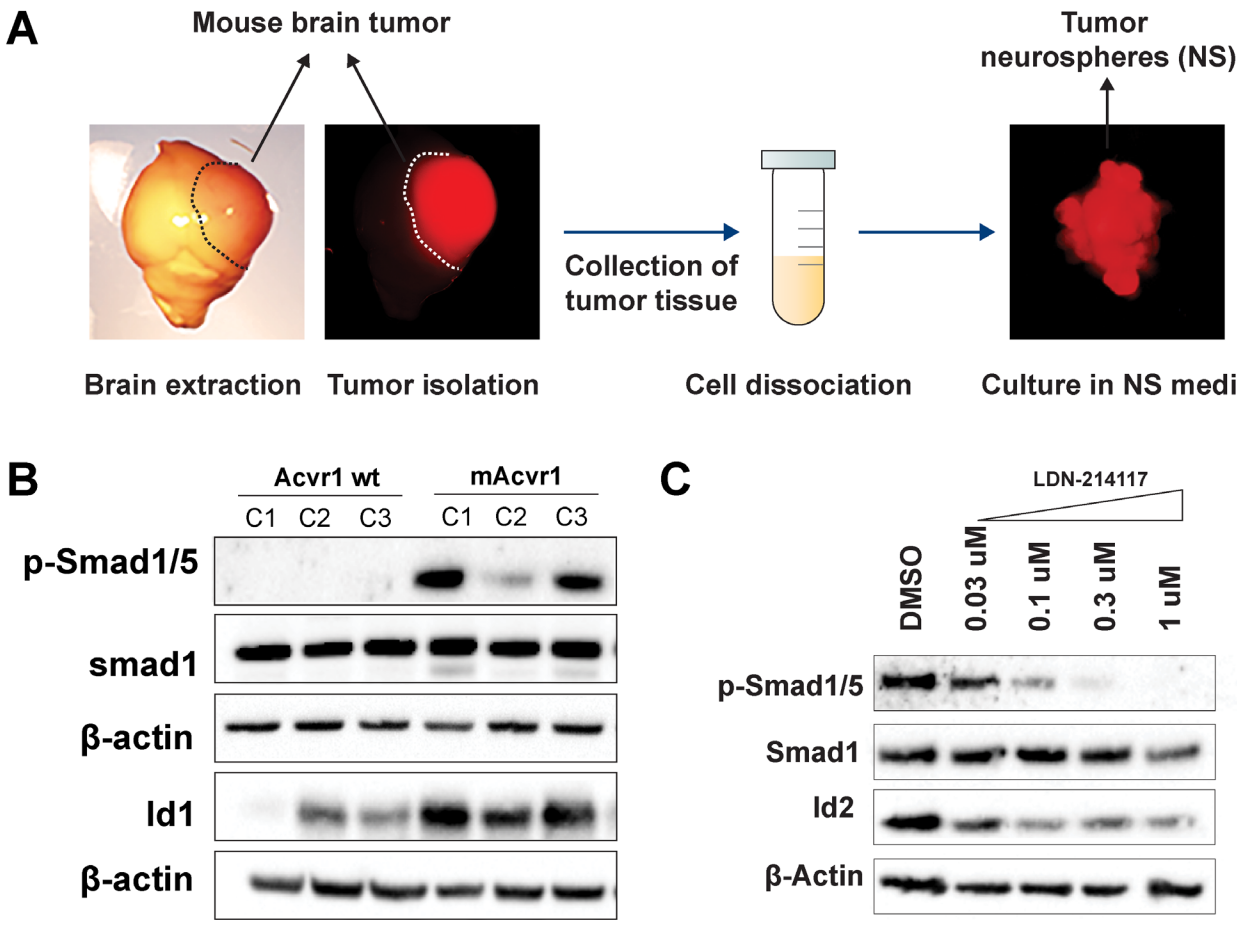

Figure 2.3 ACVR1 G328V activates the phosphor-Smad1/5 signaling pathway

(**A**) A bright field and fluorescent image of a brain harvested from a mouse that reached the end point stage. The tumor area is delineated by the dotted line and is positive for the fluorescent reporter, Katushka. The tumor is then isolated and the tumor tissue is dissociated and cultured *in vitro* where tumor NS form. (**B**) WB assay was performed on three different clones of wt-ACVR1 and mACVR1 NS to assess the protein level of phopho-Smad1/5, Smad1, and Id1, a downstream Smad1/5 regulated gene. ß-actin: loading control. C1, C2, C3 represent the clones of NS used. (**C**) WB assay was performed on mACVR1 NS treated with LDN-214117 (0.03-1uM) and blotted for Smad1/5, Smad1, and Id2; ß-actin: loading control.

[5] The schematic from Figure 2.3A has been previously published in: Mendez, F.M., Nunez, F.J., Zorilla-Veloz R.I., Lowenstein, P.R., and Castro, M.G. Native Chromatin Immunoprecipitation Using Murine Brain Tumor Neurospheres, Journal of Visual Experiments, 2018; Jan 29;(131).

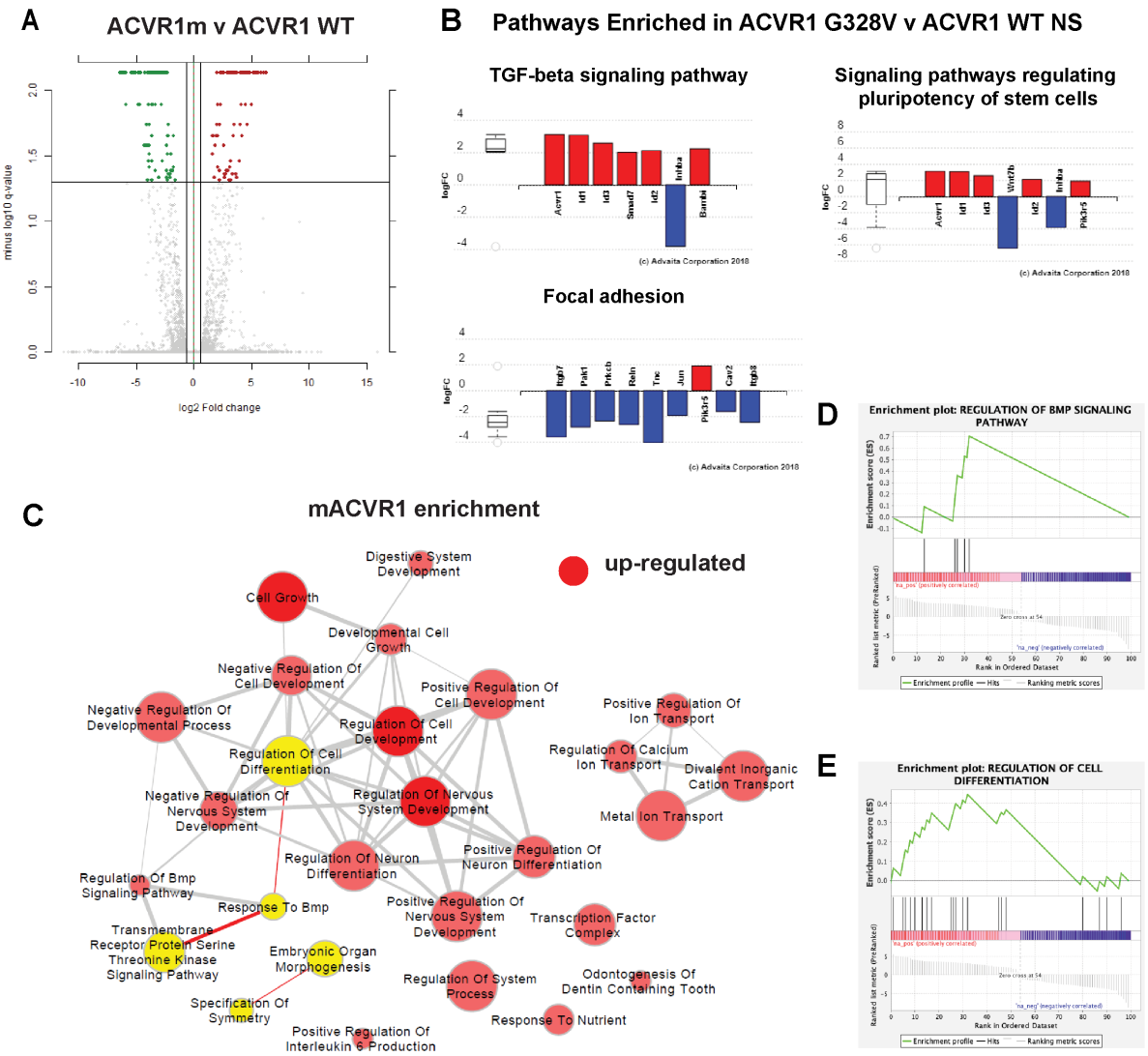

Figure 2.4 ACVR1G328V upregulates genes involved in the TGF-ß /Smad signaling and pathways related to stem cell maintenance and focal adhesion

(**A**) Differential gene expression in mACVR1 tumors analyzed by RNA-seq. Volcano plot comparing differentially expressed genes in mACVR1 versus wt-ACVR1 mouse NS. The log 10 (FDR corrected p-values); q-values were plotted against the log 2 (Fold Change: FC) in gene expression. Genes upregulated by ≥ 1.3 fold and with a FDR corrected p-value < 0.05 are depicted as red dots; genes that were downregulated by ≥1.3 fold and with a FDR corrected p-value < 0.05 are depicted as green dots. (**B**) Differentially expressed pathway genes associated with mACVR1 in mACVR1 versus wt-ACVR1 mouse NS. Plot of the log (FC) of genes with an FDR corrected p-value < 0.05. (**C**) Pathway enrichment maps of DE genes in mACVR1 versus wt-ACVR1 NS. Clusters of nodes depicted in red illustrate differentially upregulated pathways resulting from GSEA (P < 0.05; FDR < 0.5). The yellow highlighted nodes indicate up-regulated GO terms containing ACVR1. (**D**) GSEA enrichment plot of regulation of BMP signaling pathway genes identified by RNA-Seq analysis in mACVR1 versus wt-ACVR1 mouse NS. (**E**) GSEA enrichment plot of regulation of cell differentiation genes identified by RNA-Seq analysis in mACVR1 versus wt-ACVR1 mouse NS.

Figure 4

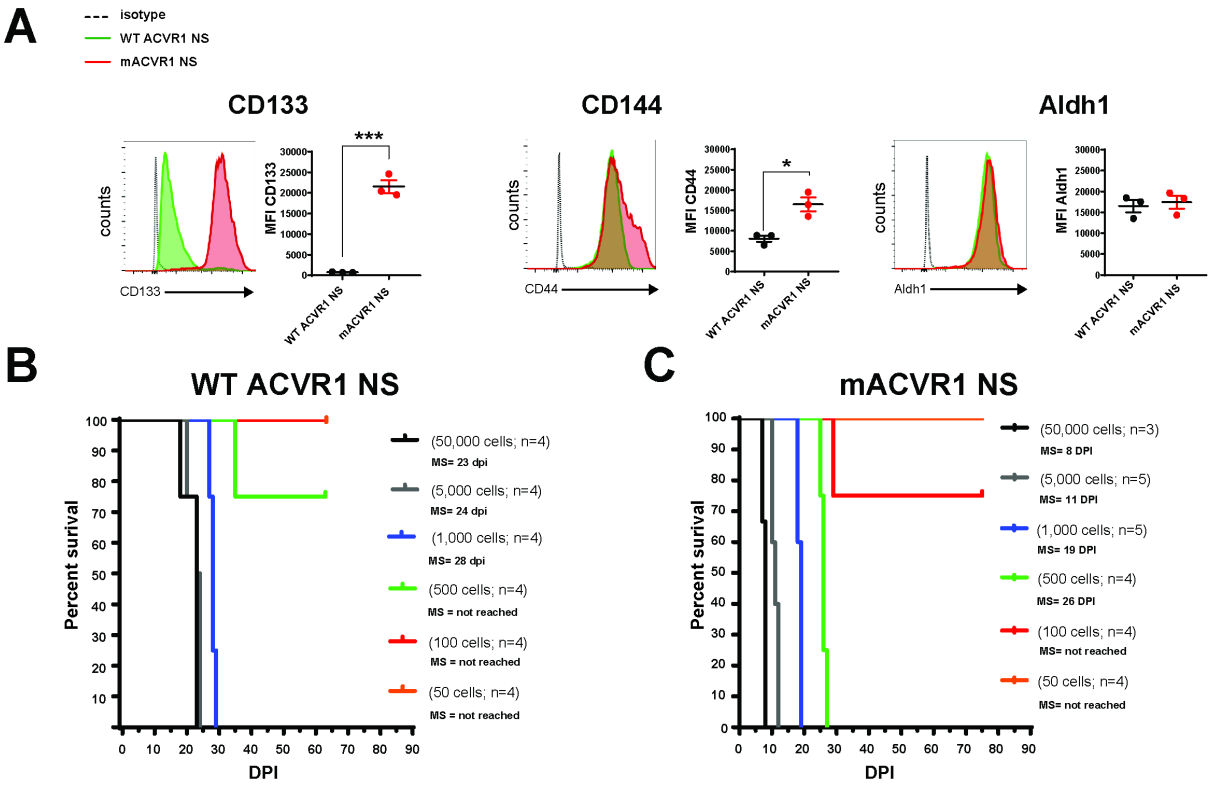

Figure 2.5 Increased expression of stem cell markers and greater tumor initiation potential in mACVR1 NS compared to WT ACVR1 NS

(A) Levels of CD133, CD44, and Aldh1 in the tumor microenvironment of mice bearing wt-ACVR1 or mACVR1 was assessed when animals displayed signs of tumor burden. Representative histograms display each marker's expression (green = wt-ACVR1, red = mACVR1). MFI = mean fluorescence intensity; * $p < 0.05$; *** $p < 0.001$; unpaired t test. Bars represent mean ± standard error of the mean (SEM) (n = 3 biological replicates). (B-C) In vivo tumor initiation capacity. Kaplan-Meier survival curves for mice intracranially implanted with different numbers of wt-ACVR1 (B) or mACVR1 NS (C) as indicated in the plot. MS: median survival.

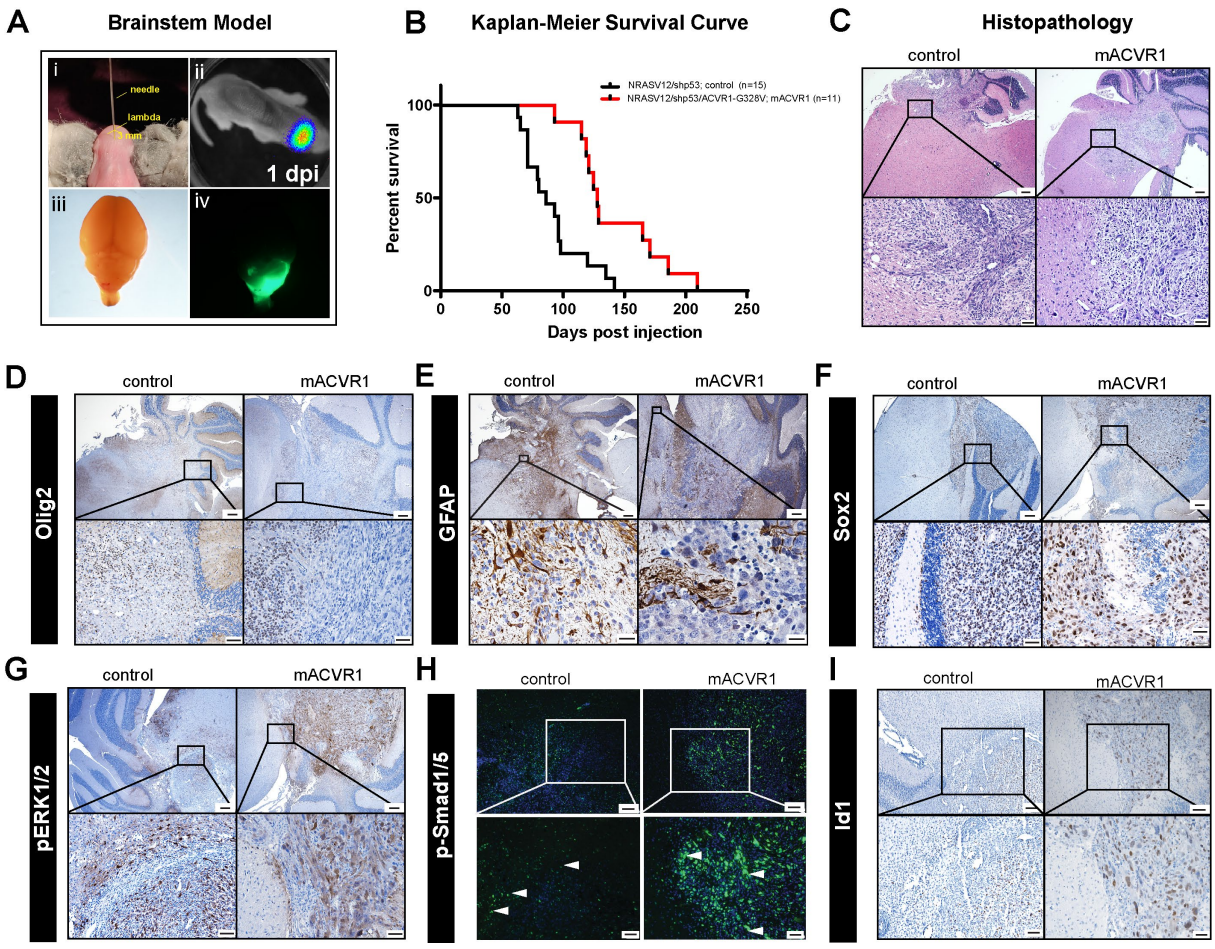

Figure 2.6 Generation of mouse brainstem glioma model using the SB transposase system.

(**A**)Schematic representation of brainstem glioma model. (i) One day old pups were injected in the fourth ventricle (3 mm posterior to the λ-suture and 3 mm deep) with plasmid cocktail. (ii) Bioluminescence imaging at 1-day post injection (dpi) confirming the efficiency of the in vivo transfection. (iii) Brightfield image of brainstem tumor (iv) Fluorescence image of brainstem tumor with GFP reporter protein. (**B**). Kaplan-Meier survival curve for genetically engineered mice bearing brainstem gliomas induced with NRASV12/shp53;[control] (n = 15), NRASV12/shp53/ ACVR1G328V (n = 11), (**C**) Hematoxylin and eosin stained paraffin embedded SB brainstem tumor sections (control and mACVR1). Scale bar in the upper panel images is 200 µm. Scale bar in the bottom panel images is 20 µm. (**D-I**) Immunohistochemistry (IHC) staining for: (**D**) Olig2, an oligodendrocyte marker (scale bar in the upper panel image is 200 µm, scale bar for the bottom panel images is 50 µm) (**E**) GFAP, an astrocyte marker (scale bar in the upper panel image is 200 µm, scale bar for the bottom panel images is 20 µm) (**F**) Sox2, a transcription factor that plays an important role in the maintenance of neural stem cells (scale bar in the upper panel image is 200 µm, scale bar for the bottom panel images is 50 µm) (**G**) phosphorylated ERK-1/2 protein (pERK1/2) (scale bar in the upper panel image is 200 µm, scale bar for the bottom panel images is 50 µm).

(**H**) phospho-Smad1/5 (scale bar in the upper panel image is 100 μm, scale bar for the bottom panel images is 50 μm, white arrows indicate positive expression) (**I**) Id1 (scale bar in the upper panel image is 100 μm, scale bar for the bottom panel images is 50 μm).

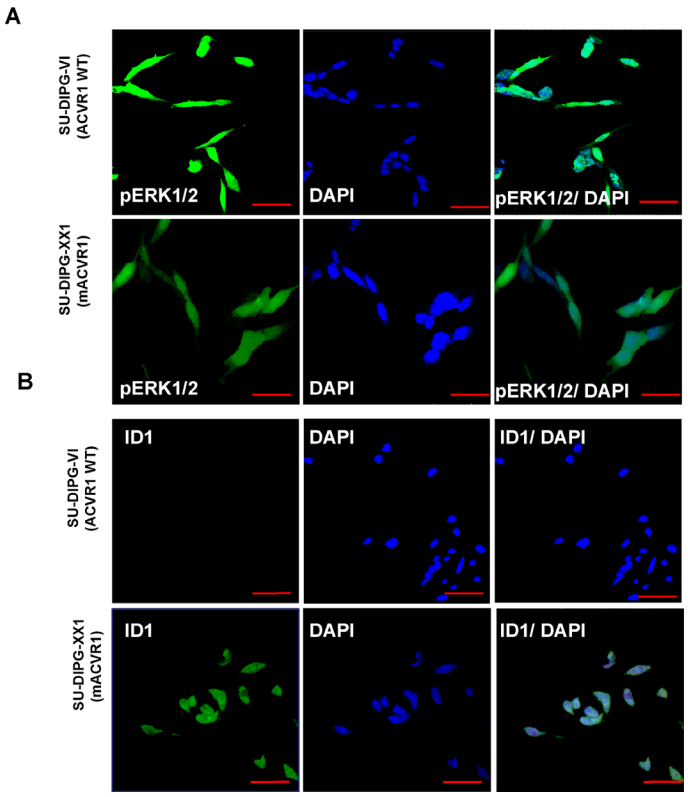

Figure 2.7 DIPG cells express pERK1/2 and ID1

Immunocytochemistry (ICC) staining for (**A**) pERK1/2 and (**B**) ID1 on human DIPG cells: SU-DIPG VI (wt-ACVR1) and SU DIPG XX1 (mACVR1). Scale bar = 50 µm.

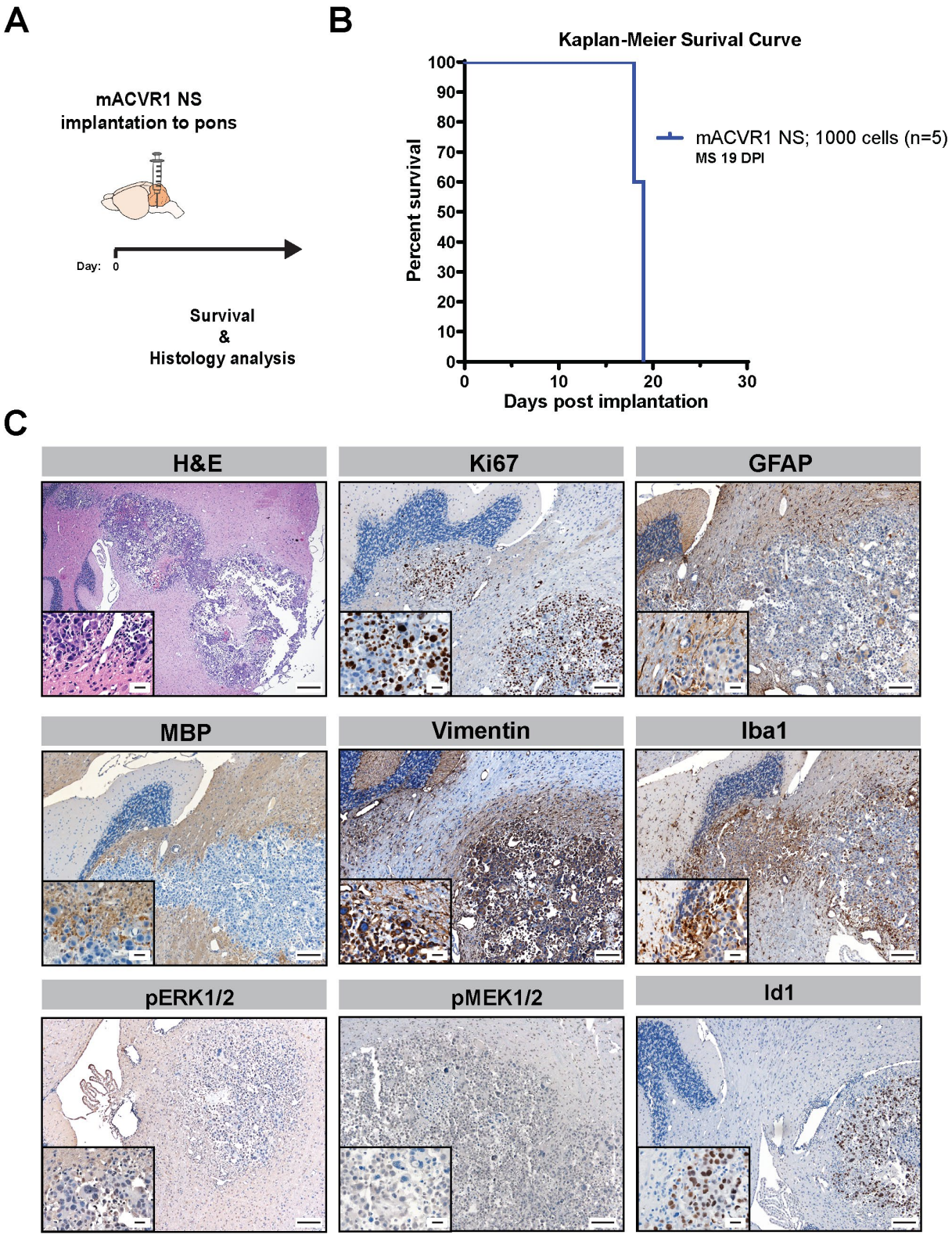
A
mACVR1 NS
implantation to pons
Day: 0
Survival
&
Histology analysis
B
Kaplan-Meier Surival Curve
Percent survival
100
90
80
70
60
50
40
30
20
10
0
0
10
20
30
Days post implantation
mACVR1 NS; 1000 cells (n=5)
MS 19 DPI
C
H&E
Ki67
GFAP
MBP
Vimentin
Iba1
pERK1/2
pMEK1/2
Id1

Figure 2.8 Transplantable model of DIPG

(**A**) Schematic of experimental design showing assessment of survival and histology in mice bearing mACVR1 brainstem gliomas. (**B**) Kaplan-Meier survival curve of mice bearing mACVR1 intracranial gliomas. MS = median survival. (**C**)Paraffin embedded mACVR1 tumor sections were stained with Hematoxylin and Eosin (H&E), Ki67 (proliferating cells), GFAP (astrocytes), MBP (myelin sheaths and oligodendrocytes), Vimentin (ependymal cells and astrocytes), Iba1 (microglia), pERK1/2, pMEK1/2, or Id1. Scale bar = 200 μm for the H&E. Scale bar = 100 μm for the immunostains. Scale bar for all magnified insets = 20 μm.

References

1. Schwartzentruber J, Korshunov A, Liu XY, Jones DT, Pfaff E, Jacob K*, et al.* Driver mutations in histone H3.3 and chromatin remodelling genes in paediatric glioblastoma. Nature **2012**;482(7384):226-31 doi 10.1038/nature10833.
2. Khuong-Quang DA, Buczkowicz P, Rakopoulos P, Liu XY, Fontebasso AM, Bouffet E*, et al.* K27M mutation in histone H3.3 defines clinically and biologically distinct subgroups of pediatric diffuse intrinsic pontine gliomas. Acta Neuropathol **2012**;124(3):439-47 doi 10.1007/s00401-012-0998-0.
3. Wu G, Broniscer A, McEachron TA, Lu C, Paugh BS, Becksfort J*, et al.* Somatic histone H3 alterations in pediatric diffuse intrinsic pontine gliomas and non-brainstem glioblastomas. Nat Genet **2012**;44(3):251-3 doi 10.1038/ng.1102.
4. Lewis PW, Muller MM, Koletsky MS, Cordero F, Lin S, Banaszynski LA*, et al.* Inhibition of PRC2 activity by a gain-of-function H3 mutation found in pediatric glioblastoma. Science **2013**;340(6134):857-61 doi 10.1126/science.1232245.
5. Bannister AJ, Kouzarides T. Regulation of chromatin by histone modifications. Cell Res **2011**;21(3):381-95 doi 10.1038/cr.2011.22.
6. Wang YC, Peterson SE, Loring JF. Protein post-translational modifications and regulation of pluripotency in human stem cells. Cell Res **2014**;24(2):143-60 doi 10.1038/cr.2013.151.
7. Buczkowicz P, Hoeman C, Rakopoulos P, Pajovic S, Letourneau L, Dzamba M*, et al.* Genomic analysis of diffuse intrinsic pontine gliomas identifies three molecular subgroups and recurrent activating ACVR1 mutations. Nat Genet **2014**;46(5):451-6 doi 10.1038/ng.2936.
8. Taylor KR, Vinci M, Bullock AN, Jones C. ACVR1 mutations in DIPG: lessons learned from FOP. Cancer Res **2014**;74(17):4565-70 doi 10.1158/0008-5472.CAN-14-1298.
9. Fontebasso AM, Papillon-Cavanagh S, Schwartzentruber J, Nikbakht H, Gerges N, Fiset PO*, et al.* Recurrent somatic mutations in ACVR1 in pediatric midline high-grade astrocytoma. Nat Genet **2014**;46(5):462-6 doi 10.1038/ng.2950.
10. Wu G, Diaz AK, Paugh BS, Rankin SL, Ju B, Li Y*, et al.* The genomic landscape of diffuse intrinsic pontine glioma and pediatric non-brainstem high-grade glioma. Nat Genet **2014**;46(5):444-50 doi 10.1038/ng.2938.
11. Bond AM, Bhalala OG, Kessler JA. The dynamic role of bone morphogenetic proteins in neural stem cell fate and maturation. Dev Neurobiol **2012**;72(7):1068-84 doi 10.1002/dneu.22022.
12. Kan L, Kitterman JA, Procissi D, Chakkalakal S, Peng CY, McGuire TL*, et al.* CNS demyelination in fibrodysplasia ossificans progressiva. J Neurol **2012**;259(12):2644-55 doi 10.1007/s00415-012-6563-x.
13. Izsvak Z, Ivics Z. Sleeping beauty transposition: biology and applications for molecular therapy. Mol Ther **2004**;9(2):147-56 doi 10.1016/j.ymthe.2003.11.009.
14. Wiesner SM, Decker SA, Larson JD, Ericson K, Forster C, Gallardo JL*, et al.* De novo induction of genetically engineered brain tumors in mice using plasmid DNA. Cancer Res **2009**;69(2):431-9 doi 10.1158/0008-5472.CAN-08-1800.
15. Calinescu AA, Nunez FJ, Koschmann C, Kolb BL, Lowenstein PR, Castro MG. Transposon mediated integration of plasmid DNA into the subventricular zone of

neonatal mice to generate novel models of glioblastoma. J Vis Exp **2015**(96) doi 10.3791/52443.
16. Calinescu AA, Yadav VN, Carballo E, Kadiyala P, Tran D, Zamler DB*, et al.* Survival and Proliferation of Neural Progenitor-Derived Glioblastomas Under Hypoxic Stress is Controlled by a CXCL12/CXCR4 Autocrine-Positive Feedback Mechanism. Clin Cancer Res **2017**;23(5):1250-62 doi 10.1158/1078-0432.CCR-15-2888.
17. Koschmann C, Calinescu AA, Nunez FJ, Mackay A, Fazal-Salom J, Thomas D*, et al.* ATRX loss promotes tumor growth and impairs nonhomologous end joining DNA repair in glioma. Sci Transl Med **2016**;8(328):328ra28 doi 10.1126/scitranslmed.aac8228.
18. Nunez FJ, Mendez FM, Kadiyala P, Alghamri MS, Savelieff MG, Garcia-Fabiani MB*, et al.* IDH1-R132H acts as a tumor suppressor in glioma via epigenetic up-regulation of the DNA damage response. Sci Transl Med **2019**;11(479) doi 10.1126/scitranslmed.aaq1427.
19. Mackay A, Burford A, Carvalho D, Izquierdo E, Fazal-Salom J, Taylor KR*, et al.* Integrated Molecular Meta-Analysis of 1,000 Pediatric High-Grade and Diffuse Intrinsic Pontine Glioma. Cancer Cell **2017**;32(4):520-37 e5 doi 10.1016/j.ccell.2017.08.017.
20. Paugh BS, Qu C, Jones C, Liu Z, Adamowicz-Brice M, Zhang J*, et al.* Integrated molecular genetic profiling of pediatric high-grade gliomas reveals key differences with the adult disease. J Clin Oncol **2010**;28(18):3061-8 doi 10.1200/JCO.2009.26.7252.
21. Panditharatna E, Kilburn LB, Aboian MS, Kambhampati M, Gordish-Dressman H, Magge SN*, et al.* Clinically Relevant and Minimally Invasive Tumor Surveillance of Pediatric Diffuse Midline Gliomas Using Patient-Derived Liquid Biopsy. Clin Cancer Res **2018**;24(23):5850-9 doi 10.1158/1078-0432.CCR-18-1345.
22. Allis CD, Jenuwein T. The molecular hallmarks of epigenetic control. Nat Rev Genet **2016**;17(8):487-500 doi 10.1038/nrg.2016.59.
23. Hoeman CM, Cordero FJ, Hu G, Misuraca K, Romero MM, Cardona HJ*, et al.* ACVR1 R206H cooperates with H3.1K27M in promoting diffuse intrinsic pontine glioma pathogenesis. Nature Communications **2019**;10(1) doi 10.1038/s41467-019-08823-9.
24. Carvalho D, Taylor KR, Olaciregui NG, Molinari V, Clarke M, Mackay A*, et al.* ALK2 inhibitors display beneficial effects in preclinical models of ACVR1 mutant diffuse intrinsic pontine glioma. Commun Biol **2019**;2:156 doi 10.1038/s42003-019-0420-8.
25. Nikbakht H, Panditharatna E, Mikael LG, Li R, Gayden T, Osmond M*, et al.* Spatial and temporal homogeneity of driver mutations in diffuse intrinsic pontine glioma. Nature Communications **2016**;7:11185 doi 10.1038/ncomms11185.

Chapter 3 : Efficacy of Immune Stimulatory Gene Therapy in Mouse Models of Brainstem Glioma[6]

Abstract

Diffuse intrinsic pontine glioma (DIPG) bears a dismal prognosis. Mutant ACVR1 (mACVR1) neurospheres (NS) were implanted into the pons of immune competent mice to test the therapeutic efficacy and toxicity of immune stimulatory gene therapy using adenoviruses expressing thymidine kinase (TK) and fms-like tyrosine kinase 3 ligand (Flt3L). mACVR1 NS expressing the surrogate tumor antigen ovalbumin were generated to investigate if TK/Flt3L treatment induces the recruitment of tumor-antigen specific T cells to the tumor microenvironment (TME). Adenoviral delivery of TK/Flt3L in mice bearing brainstem gliomas resulted in anti-tumor immunity, recruitment of anti-tumor specific T cells to the TME and increased median survival. This study provides insights into the phenotype and function of the tumor immune microenvironment in a mouse model of brainstem glioma harboring mACVR1. Immune stimulatory gene therapy targeting the hosts' anti-tumor immune response inhibits tumor progression and increases median survival of mice bearing mACVR1 tumors.

[6] Portions of this chapter have been submitted for publication in Clinical Cancer Research in collaboration with the following co-authors: Padma Kadiyala, Felipe J. Nunez, Stephen Carney, Fernando Nunez, Jessica C. Gauss, Ramya Ravindran, Sheeba Pawar, Marta Edwards, Pedro R. Lowenstein, and Maria G. Castro.

Introduction

Brain and central nervous system tumors are the leading cause of cancer death in children(1). Diffuse intrinsic pontine glioma (DIPG) occurs mainly in children, and accounts for 10-20% of pediatric brain tumors (2). DIPG originates in the pons and is highly invasive making surgical removal impossible. The median survival is 8-11 months, and has not improved in more than 40 years (3). Radiation can temporarily provide symptom relief and extend survival by a few months it can cause detrimental effects on developing brain (4,5). Thus, there is a critical need to identify an effective therapy for DIPG.

It would be advantageous to harness the power of the immune system to elicit effective anti-tumor immunity in DIPG patients. Immune mediated treatment modalities have yielded promising clinical benefits in melanoma, non-small-cell lung cancer, renal cell cancer, and prostate cancer (6-9). We have also previously shown the efficacy of an immune stimulatory gene therapy approach in several rat and mouse models of adult glioblastoma (10,11). This approach has recently completed its Phase I Clinical Trial accrual for the treatment of adult patients with newly diagnosed glioblastoma multiforme (World Health Organization (WHO) grade IV (NCT01811992)). This immune-mediated gene therapy approach is based on adenoviral delivery of herpes simplex virus type 1-thymidine kinase (TK) and Fms-like tyrosine kinase 3 ligand (Flt3L). Upon administration of the prodrug, ganciclovir, proliferating tumor cells expressing TK undergo immunogenic cell death (10,11). Dying tumor cells, release damage-associated molecular patterns (DAMPs), such as high-mobility group B1 protein (HMGB1), calreticulin, and adenosine triphosphate (ATP) (10,12). Meanwhile, Flt3L elicits the recruitment of dendritic cells to the tumor microenvironment (10). HMGB1 released by dying tumor cells activates dendritic cells through Toll-like receptor 2 (TLR2) mediated signaling (10).

Activated dendritic cells pick up the tumor antigens and traffic to the draining lymph nodes, where they generate a specific anti-tumor cytotoxic T-cell response (10,13). Herein, we aimed to test the efficacy of this immune stimulatory approach in an immunocompetent mouse model of mutant ACVR1 brainstem glioma.

Treatment with TK/Flt3L immune stimulatory gene therapy significantly improved median survival compared to standard of care. The TK/Flt3L gene therapy induced a strong anti-tumor cytotoxic immune response demonstrated by an increase in the frequency of tumor antigen-specific CD8 T cells in mice treated with TK/Flt3L therapy when compared to saline controls. Our results suggest that immune-mediated gene therapy could be a promising therapeutic approach for DIPG.

Methods

Implantable syngeneic murine brainstem glioma models:

Female C57BL/6 mice between 6-8 weeks were used for all implantation experiments. Intracranial tumors were generated by stereotaxic injection of 1000 ACVR1m tumor NS into the pons using a 5 µl Hamilton syringe with a removable 33-gauge needle with the following coordinates: (0.8mm posterior; 1.00mm lateral to the λ-suture and 5mm deep). Animals were anesthetized, then the skin over the incision site was cut and retracted, and a burr hole was drilled into one side of the skull using a 0.45 mm drill bit corresponding to the pons coordinates. Tumor NS were delivered in a 2 µl volume after holding the needle in place for 2 minutes. Each injection was performed over the course of 7 minutes; the needle was left in place for an additional minute before being slowly withdrawn from the brain.

Intratumoral injection of adenoviral vectors and radiation treatment:

We used first generation Ad.hCMV.hsFLT3L (Ad-Flt3L) + Ad.hCMV.TK (Ad-TK)(10,13). Five days post tumor implantation (dpi) mice were assigned to four treatment groups: (i) control group: empty Ad(Ad0)/saline); Ad0 was delivered intratumorally (i.t) and saline intraperitoneally (i.p.), (ii) gene therapy: Ad-TK(1×10^8 plaque-forming units (pfu)/Ad-Flt3L(2×10^8 pfu of Ad-TK) /GCV; Ad-TK/Ad-Flt3Ldelivered i.t., ganciclovir (GCV) (Biotang; RG001-1g) was administered i.p. at 25 mg/kg/daily for 10d, starting 1d post-gene therapy, (iii) Standard of care (IR): Ad0/saline+IR; an overall dose of 20 Gy IR was administered (2 Gy/d for 10d), and (iv) Gene therapy + standard of care: Ad-TK/Ad-Flt3L/GCV+IR. Intratumoral injections of adenoviral vectors was delivered in μL volume in three locations to depths of 4.4, 4.5, and 4.6 mm, at the coordinates detailed above. Sample size was n = 5 for each treatment group. For the functional analysis of T cells in the tumor microenvironment (TME), 8 days post tumor implantation mice were assigned to either the control group or the gene therapy group detailed above. Sample size was n = 3; where per sample it was necessary to pool tumor tissue from three mice for the control and five mice for the gene therapy group due to the size of the tumor.

Flow cytometry:

For flow cytometry experiments were performed using protocols described before (10,11,13). Flow data were acquired on a FACSAria flow cytometer (BD Biosciences) and analyzed using Flow Jo version 10 (Treestar). Prior to staining cells with antibodies, live/dead staining was carried out using fixable viability dye (eBioscience). Then, cells were resuspended in PBS containing 2% fetal bovine serum (FBS) (flow buffer) and non-specific antibody binding was blocked with CD16/CD32 (Biolegend, 101335). All stains were carried out for 30 minutes at 4°C

with 3X flow buffer washes between live/dead staining, blocking, surface staining, cell fixation, intracellular staining and data acquisition. The fixation/ permeabilization staining kit (BD Biosciences, 554714) was used for all intracellular stains. Antibody information is included in supplementary table 1. For T cell functional analysis within the TME, the cells from the tumor mass were stained with anti-mouse CD45, CD3, CD8, and SIINFEKL-H2Kb-tetramer-PE. For IFNγ stains, single cell suspensions generated from the tumor mass were stimulated with 25 ug/mL of mACVR1-OVA lysate for 24 hours in 10% FCS-containing media followed by 6 h incubation with Brefeldin and monensin. Cells were stained with CD3 and CD8 antibodies, followed by intracellular staining for IFNγ. To assess tumor cell stemness tumor cell suspensions generated from wt-ACVR1 and mACVR1 implanted tumors were stained for CD133, CD44, and Aldh1.

Assessment of damage associated molecule release:

To assess for release of damage associated molecules after treatment with either radiation (3G) or Ad-TK (500 MOI)/GCV (25μM), 10,000 mACVR1 NS were plated on 6-well plates. The next day they were treated with Ad-TK (500 MOI) and/or radiation (3G). Following a 48 hour incubation they were treated with GCV (25 μM). The following day they were stained with calreticulin or high mobility group box 1 (HMGB1) antibodies following flow cytometry protocols described above. To assess ATP release, we used the ATP determination kit following manufacturer's instructions (Invitrogen, A22066) to measure ATP levels in media after 48 hours of treatment. Media was used to generate the ATP standard curve.

T cell Proliferation analysis:

Splenocytes from 21 dpi mACVR1-OVA brainstem glioma-bearing mice treated with saline or gene therapy, as detailed above, were labeled with Carboxyfluorescein succinimidyl ester

(CFSE) per manufacturer's instructions and cultured with 100 nM SIINFEKL peptide (Anaspec, 60193-1; dissolved in H20 and stored in -80 °C) for 4 days. As a positive control we used splenocytes from Rag2 knockout/transgenic OT-I T cell receptor mice (Taconic, 2334) stimulated with SIINFEKL. As a negative control we used unstimulated splenocytes. Cells were then stained with CD3 and CD8, and T cell proliferation was assessed based on CFSE dye dilution.

Cytotoxic T cell assay:

Splenocytes from saline or gene therapy treated mice were incubated with mACVR1-OVA NS for 24 hours at the indicated ratios (1:1, 10:1, 20:1). Lysis of tumor cells was assessed by using Annexin-V. (14,15).

Complete blood count (CBC) and serum chemistry:

Collected blood was transferred to EDTA tubes for CBC (RAM Scientific, 077058) or in serum separation tubes (Sarstedt, 41.1378.005). CBC and serum chemistry was performed by the In-Vivo Animal Core (IVAC) at the University of Michigan.

Neuropathological analysis:

To assess the safety of vector delivery into the brainstem, non-tumor bearing animals were treated with Ad-TK/Ad-Flt3L gene therapy or saline. GCV was administered intraperitoneally one day later for 7 days. One day after the last dose of GCV was administered animals were euthanized and brains were harvested and processed for histology as detailed above. Hematoxylin and eosin (H&E) staining was performed to assess gross histopathological features (16). Immunohistochemistry staining for glial fibrillary acidic protein (GFAP) to mark

astrocytes, myelin basic protein (MBP) to mark myelin sheaths and oligodendrocytes, and Iba1 to mark microglial cells.

Hematoxylin and eosin (H&E):

Liver tissue sections (5 μm thick) from tumor bearing animals treated with saline, radiation, gene therapy, and gene therapy and radiation were stained with H&E (16).

Statistical analysis

All data were analyzed using GraphPad Prism version 8, or R (version 3.1.3). All animal studies were carried out with at least 3 animals per group (specified in each experiment). The statistical test used is indicated in each figure. A $p \leq 0.05$ was considered significant.

Results

Mutant ACVR1 NS release DAMPs in vitro

Due to the invasive nature of brainstem gliomas and their refractive response to current therapies we wanted to assess the efficacy of immune stimulatory TK/Flt3L gene therapy. The release of DAMPs is crucial for the success of TK/Flt3L mediated therapy, therefore, we first assessed whether mACVR1 NS released DAMPs *in vitro* after treatment with GCV alone, TK alone, or GCV+TK, with, or without 3 Gray (Gy) of irradiation (IR). We found that mACVR1 NS treated with GCV+TK released increased levels of calreticulin ($p<0.0001$; **Fig. 3.1**), high mobility group box 1 protein (HMGB1) ($p<0.0001$; **Fig. 3.1**), and adenosine triphosphate (ATP) ($p = 0.0071$; **Fig. 3.1**). We also observed that the combination of GCV+TK with IR further increased the levels of calreticulin ($p<0.0001$; **Fig. 3.1**), HMGB1 ($p=0.0375$; **Fig. 3.1**), and the release of ATP ($p = 0.0158$; **Fig. 3.1**) by the mACVR1 NS.

Pre-clinical testing of immune stimulatory gene therapy

Having established that mACVR1 NS release calreticulin, HMGB1, and ATP *in vitro* following treatment with either IR or TK+GCV, we next tested the efficacy of this treatment paradigm *in vivo*. Five days' post intracranial tumor implantation into the pons (**Fig. 3.2A**), mice were assigned to four treatment groups as indicated in Figure 3.2. Our results demonstrate that Ad-TK/Ad-Flt3L therapy was more effective in prolonging the median survival (MS) of mACVR1 brainstem glioma bearing mice compared to animals receiving IR,(MS=36 days post implantation (dpi) for TK/Flt3L group vs. 23 dpi for IR group; p = 0.0014, Mantel-Cox test), or . animals receiving saline control treatment (MS=18dpi; p = 0.0015, Mantel-Cox test) (**Fig. 3.2B**). Combining standard of care with gene therapy led to an improved median survival (MS=37 dpi), but did not significantly affect the efficacy of Ad-TK/Ad-Flt3L therapy (**Fig. 3.2B**).

Assessment of anti-brainstem glioma specific T cells

We next aimed to investigate whether Ad-TK/Ad-Flt3L treatment recruits anti-brainstem glioma specific T cells into the tumor immune microenvironment (TME). To do this, we used the surrogate tumor antigen ovoalbumin (OVA)(13,17) expressing mACVR1 cells (mACVR1-OVA NS). We were able to quantify tumor specific CD8 T cells in the TME through the use of the SIINFEKL-H2Kb tetramer (**Fig. 3.3A**). We observed a 3.8-fold increase in the frequency of tumor specific CD8 T cells in the TME after treatment with Ad-TK/Ad-Flt3L gene therapy (p = 0.0007; ***, **Fig. 3.3B**). To test the impact of Ad-TK/Ad-Flt3L gene therapy on the activation status of CD8 T cells in the TME, we stained effector T cells for the expression of IFNγ after re-stimulating CD8 T cells isolated from the TME with mACVR1-OVA NS-lysate for 24 hrs. Our data show that IFNγ is increased 3.8 fold (p = 0.0038; **, **Fig. 3.3C**) in CD8 T cells from Ad-TK/Ad-Flt3L gene therapy treated mice compared to saline controls. To test if Ad-TK/Ad-Flt3L

gene therapy affected antigen-specific T cell proliferation we labeled splenocytes with 5-(and 6)-carboxyfluorescein diacetate succinimidyl ester (CFSE), and stimulated them with the OVA cognate SIINFEKL peptide. As a positive control we also stimulated splenic T cells from OT-1 mice that have their TCR engineered to recognize the SIINKEKL peptide. Our results show that the percentage of T cells that proliferated in response to the SIINKEKL peptide was greater (1.7 fold, $p < 0.0001$, **Fig. 3.3D**) in mice treated with Ad-TK/Ad-Flt3L gene therapy compared to the saline treated control group. Additionally, the cytotoxicity of T cells isolated from the spleen of animals treated with Ad-TK/Ad-Flt3L gene therapy was observed to be significantly higher (1.95 fold, $p = 0.004$ at 20:1 ratio, **Fig. 3.3E**) when compared with the saline treated group indicating that gene therapy significantly enhanced the cytotoxic activity of splenic T cells.

Histopathological analysis

To evaluate any potential adverse effects of delivering gene therapy into the brainstem we performed a detailed histopathological analysis of brains from non-tumor bearing animals. After the animals were treated intracranially with Ad-TK/Ad-Flt3L, GCV was administered intraperitoneally one day after adenoviral injection for seven days. Brains were harvested for neuropathology analysis 24 hours after the last dose of GCV was administered. Architectural integrity was assessed by H&E staining and by immunohistochemistry using GFAP (astrocytes), MBP (myelin sheaths, oligodendrocytes) and Iba1 (microglia). No gross tissue abnormalities were observed in response to TK/Flt3L therapy compared to the saline controls (**Fig. 3.4**). There was also no change in GFAP or MBP expression in response to TK/Flt3L therapy indicating that the brain architecture was unaffected (**Fig. 3.4**). There was no increase in Iba1 expression in the animals treated with TK/Flt3L therapy indicating that gene therapy does not induce inflammation in normal brain tissue 8 days' post treatment. (**Fig. 3.4**).

Assessment of systemic toxicity

To assess potential systemic toxicity due to TK/Flt3L or IR treatment, we performed H&E staining on liver sections and complete hematological and serum biochemical analysis in tumor bearing animals from the saline, TK/Flt3L, and TK/Flt3L + IR treatment groups. The liver sections from all treatment groups had normal hepatocyte architecture and did not show signs of inflammation or necrosis (**Fig. 3.5**). The white blood cell counts were within normal range for the saline, TK/Flt3L, and TK/Flt3L + IR groups, but significantly decreased in the IR group in comparison to the saline treated group ($p < 0.0001$, **Fig. 3.6**). This is consistent with a study that found that whole brain radiation significantly decreased total white blood cell counts (18). Red blood cell, hemoglobin, hematocrit, platelet, lymphocyte, neutrophil, and monocyte counts were not significantly affected by TK/Flt3L or IR therapy (**Fig. 3.6**). We did not find any significant changes in important enzymes involved in liver (ALT, AST) and kidney (BUN) function as a result of TK /Flt3L or IR therapies (**Fig. 3.6**).

Discussion

DIPG remains an incurable tumor with a poor prognosis (19). The tumors originate in the pons and infiltrate into sensitive regions of the brainstem precluding surgical resection (20). Currently, the treatment option for children with DIPG is limited to radiation to provide palliative care (21). Although radiation can temporarily provide symptomatic relief and extend survival by a few months, it can cause detrimental effects on the developing brain (4,5). Therefore, there is a dire need for new therapeutic interventions. DIPG studies involving the development and implementation of novel therapies have utilized patient derived xenograft models, where human DIPG cells are implanted into the brain of immune deficient mice or rats

to establish intracranial tumors (22,23). One limitation with those models is that immune suppressed animals cannot be used to test immunotherapies or perform immune-related mechanistic studies. We developed an immune competent transplantable mouse model of DIPG harboring the ACVR1 G328V mutation (mACVR1), and this study focuses on the response of mACVR1 brainstem glioma tumors to immunotherapies.

There has been significant progress in the field of cancer immunotherapy leading to improvements in overall survival in many types of solid tumors (6-8,24,25). Advances in immunotherapies include the development of immune therapies targeting immune checkpoints, vaccine approaches against tumor antigens or dendritic cell vaccines designed to stimulate the adaptive immune response, adoptive cell therapy, oncolytic viral therapy, and immune stimulatory gene therapy (25-27). This has led to a growing number of clinical trials testing immunotherapies in DIPG (27).

In recent years, it has been established that activated immune cells are able to migrate and enter into the brain parenchyma, and that the brain has a functional lymphatic system that allows for transport of CNS-antigens to the draining lymph nodes (28,29). Thus, the brain is capable of mounting T cell-mediated adaptive immune responses, but, since there are very low numbers of local professional antigen presenting cells within the normal brain, endogenous immune responses fail to trigger potent immune response against tumor antigens localized in the brain parenchyma (30,31).

In adult glioblastoma (GBM) there is evidence of immune cell infiltration, but an immunosuppressive environment precludes effective anti-tumor immunity (26,32,33). GBM tumors establish an immunosuppressive environment by the release of immunosuppressive

cytokines, such as TGF-β and IL-10, by the recruitment or induction of immunosuppressive cells, such as regulatory T cells, myeloid-derived suppressor cells, or tumor associated macrophages, and by the expression of immune checkpoint receptor ligands (32-38). In comparison to adult GBM, initial studies of the tumor microenvironment in DIPG have found that there is a low number of immune infiltrates in human DIPG tumors and that they do not express inflammatory cytokines and chemokines (39,40). These data provide support for the use of an immune modulatory therapeutic strategy to enhance the recruitment of immune cells into the tumor, with the aim of mounting an effective anti-DIPG immune response.

We have previously demonstrated that combined immune stimulatory gene therapy mediated through the delivery of adenoviruses encoding herpes simplex virus type 1 thymidine kinase (TK) and fms-like tyrosine kinase 3 ligand (Flt3L) leads to tumor regression and long term survival in several rodent models of glioblastoma (GBM) (10,11,41-43). This therapy is based on inducing tumor cell death though expression of suicide gene TK (44,45). Tumor antigens and damage-associated molecular pattern molecules (DAMPs), such as calreticulin, high mobility group box1 (HMGB1), and ATP, are released by dying tumor cells (12,46). The effectiveness of this combination therapy also relies on Flt3L to recruit dendritic cells into the tumor microenvironment, while the release of HMGB1 stimulates TLR2-dependent activation of dendritic cells (10,45,47). Activated dendritic cells can then transport antigens to the draining lymph nodes and induce tumor specific T cell responses (10,45). Initial results from the first in human Phase 1 clinical trial of combined adenoviral delivery of TK and Flt3L for the treatment of adult GBM are promising and report that the therapy was well tolerated (48). However, it has been established that the biology of DIPG and GBM is different (49). Therefore, it is necessary to assess the safety and efficacy of TK/Flt3L therapy in pre-clinical models of brainstem glioma.

Herein, we demonstrate that treatment with TK/Flt3L gene therapy in mice bearing mACVR1 brainstem gliomas stimulates a strong anti-tumor cytotoxic immune response leading to a significant increase in survival (**Fig. 3.2B**). Treatment with TK/Flt3L increased the frequency of tumor-specific CD8 T cells (**Fig. 3.3B**) in the tumor microenvironment and increased toxicity as demonstrated by enhanced IFNγ production (**Fig. 3.3C**).

Additionally, delivery of TK/Flt3L into the normal brainstem did not induce any local or systemic cytotoxicity. Hematoxylin and eosin staining and immunostaining for GFAP (astrocytes), MBP (myelin sheaths, oligodendrocytes), and Iba1 (activated macrophages and microglia) was used to assess local toxicity, and we observed no architectural abnormalities or overt inflammation as a result of TK/Flt3L therapy. Histological examination of hematoxylin and eosin stained liver tissue did not show signs of inflammation, necrosis, or alterations in normal hepatocyte structure. Hematological toxicity, assessed by complete blood count and serum chemistry analysis, indicated that TK/Flt3L therapy did not induce any toxicity as values from a TK/Flt3L treated group were not significantly altered when compared to saline treated animals. Our results are consistent with other pre-clinical studies that report the brainstem can tolerate adenoviral mediated immunotherapy (50,51). Results from a clinical trial (NCT03178032) utilizing adenoviral vector delivery of an oncolytic virus into the pons of DIPG patients will also shed light on the feasibility and toxicity of intratumoral adenoviral delivery into the brainstem (52).

In conclusion, we provide compelling evidence that warrants further development of conditionally cytotoxic immune stimulatory gene therapy for the treatment of DIPG. We anticipate that in the clinic, this approach could also be used in combination with immune

checkpoint blockade to further enhance the therapeutic efficacy of the TK/Flt3L-mediated anti-brain stem glioma immune response.

Figures

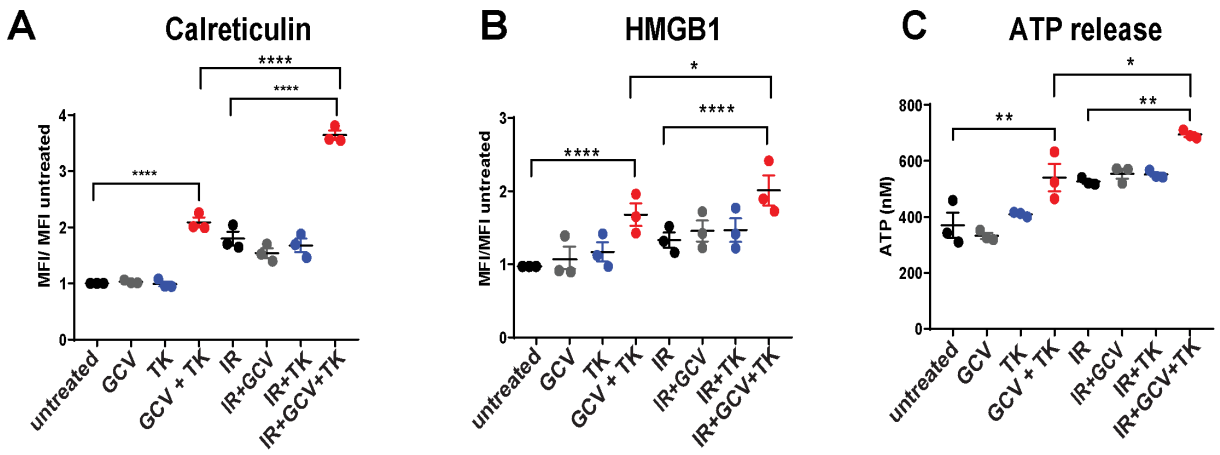

Figure 3.1 TK+GCV and radiation induce release DAMPs by mACVR1 NS

mACVR1 NS were treated with TK (500 MOI) and/ or 3 Gray (Gy) ionizing radiation (IR), followed by GCV (25 µM) 24 hours later. Following a 48-hour incubation, levels of calreticulin and HMGB1 were assessed by flow cytometry, while levels of ATP release were assessed using a colorimetric assay. MFI = mean fluorescence intensity; * $p < 0.05$; **** $p < 0.0001$; two-way ANOVA, followed by Turkey's multiple comparisons.

A Experimental design

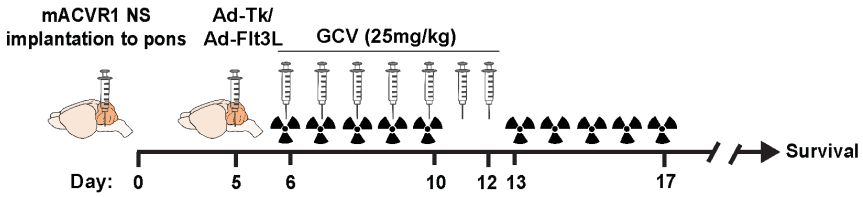

B Kaplan Meier Survival curves of mACVR1 brainstem glioma bearing mice treated with TK/Flt3L +/- radiation

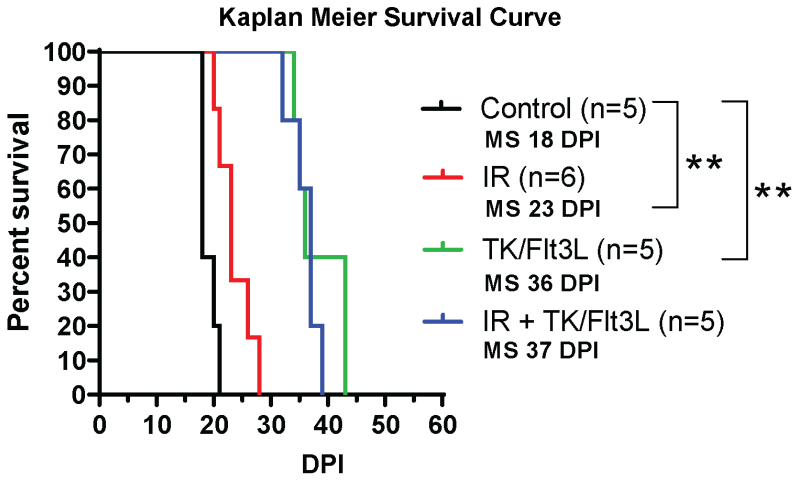

Group	% increased surival	p value
IR vs. saline	27.7	0.0086
TK/Flt3L vs. saline	100	0.0015
TK/Flt3L+ IR vs. saline	105.5	0.0031

Figure 3.2 Efficacy of Immune-Stimulatory Gene Therapy

(**A**) Experimental design showing mice bearing mACVR1 brainstem gliomas treated with saline or TK/FLT3L gene therapy on day 5 post tumor implantation, followed by intraperitoneal administration of GCV (25 mg/kg) on day 6-12. Radiation was administered at a dose of 2Gy/Day for 5d for two weeks 5 days' post tumor implantation; mice were monitored for survival. (**B**) Kaplan-Meier survival analysis for mice bearing mACVR1 tumors treated with saline (n = 5), IR (n = 6), TK+ GCV (n=5), or IR+TK+GCV (n=5). Data were analyzed using log-rank (Mantel-Cox) test; ** $p < 0.005$

Figure 6

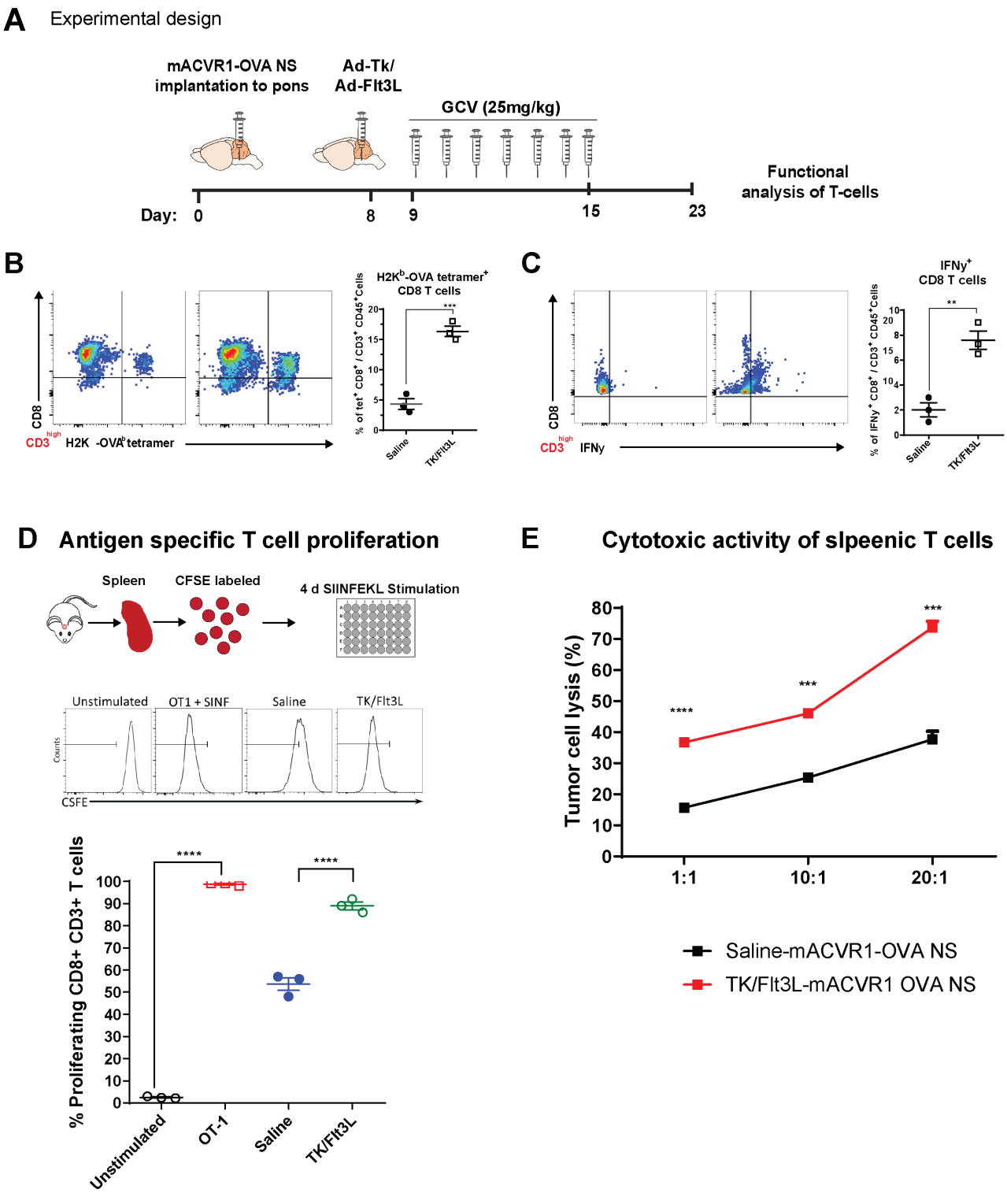
A
Experimental design
mACVR1-OVA NS implantation to pons
Ad-Tk/ Ad-Flt3L
GCV (25mg/kg)
Day: 0 8 9 15 23
Functional analysis of T-cells
B
CD8
CD3high H2K -OVAb tetramer
H2Kb-OVA tetramer+ CD8 T cells
% of tet+ CD8+ / CD3+ CD45+Cells
Saline
TK/Flt3L
C
CD8
CD3high IFNy
IFNy+ CD8 T cells
% of IFNy + CD8+ / CD3+ CD45+Cells
Saline
TK/Flt3L
D
Antigen specific T cell proliferation
Spleen
CFSE labeled
4 d SIINFEKL Stimulation
Unstimulated
OT1 + SINF
Saline
TK/Flt3L
Counts
CSFE
% Proliferating CD8+ CD3+ T cells
Unstimulated
OT-1
Saline
TK/Flt3L
E
Cytotoxic activity of slpeenic T cells
Tumor cell lysis (%)
1:1
10:1
20:1
Saline-mACVR1-OVA NS
TK/Flt3L-mACVR1 OVA NS

Figure 3.3 Immune stimulatory gene therapy induces tumor specific T-cell infiltration

(**A**)Experimental design showing mice bearing mACVR1-OVA brainstem gliomas treated with saline or TK/FLT3L gene therapy on day 8 post implantation, followed by intraperitoneal administration of GCV (25 mg/kg) on day 9-15. (**B**) Tumor specific CD8 T cells within the TME of mACVR1-OVA tumors were analyzed by staining for SIINFEKL-Kb tetramer. (**C**) Activation status of CD8 T cells within the TME was analyzed by staining for IFNγ after stimulation with tumor lysate. Representative flow plots for each group are displayed; *** $p < 0.001$, ** $p < 0.01$; unpaired t test. Bars represent mean ± SEM (n = 3 biological replicates, where resected tumors from 3 animals were pooled for the control group and 5 animals were pooled for the gene therapy group). (**D**) Experimental design showing splenocytes from saline or TK/FLT3L treated mACVR1-OVA tumor bearing mice labeled with CFSE and then stimulated with 100 nM of SIINFEEKL peptide for four days in culture to assess CD8+ T cell proliferation. Histograms show representative CFSE staining from unstimulated splenocytes (negative control), OT-1 splenocytes undergoing rapid proliferation in response to SIINFEKL (positive control), and the effect of SIINFEKL-induced T cell proliferation on splenocytes from saline or TK/Flt3L treated mACVR1-OVA tumor bearing mice. Quantification of splenocytes undergoing T cell proliferation; **** $p < 0.0001$; oneway ANOVA followed by followed by Turkey's multiple comparisons. Bars represent mean ± SEM (n = 3 biological replicates). (**E**) Splenocytes from saline or TK/Flt3L treated mice were incubated with mACVR1-OVA NS, for 24 hours at the indicated ratios. Lysis of tumor cells was assessed by using Annexin-V. mACVR1 NS undergoing apoptosis were identified as Annexin-V+/$CD45^-$ cells. Data were compared using unpaired t test; **** $p < 0.0001$; *** <0.001. Bars represent mean ± SEM (n = 3 biological replicates).

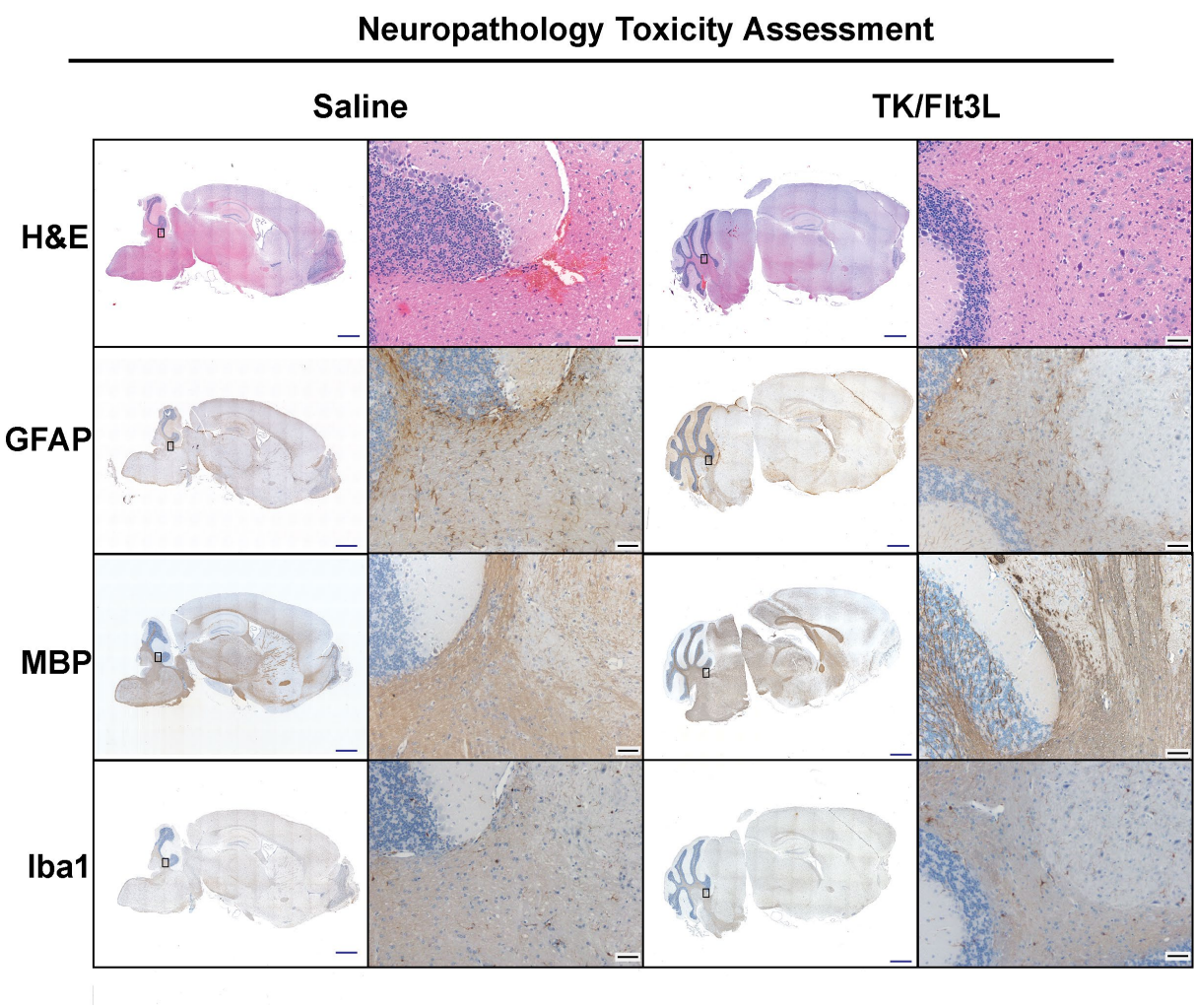

Figure 3.4 Neuropathology Toxcicity Assessment

Assessment of local toxicity of adenoviral delivery of TK/Flt3L into normal brainstem. Mice were injected in the pons with Ad-TK and Ad-Flt3L, or saline. GCV was administered intraperitoneally 24 h post vector delivery for 7 days. 24 h after the last dose of GCV was administered neuropathological analysis of the brain was assessed by H&E staining and immunostaining for GFAP (astrocytes), MBP (myelin sheaths, oligodendrocytes), and Iba1 (microglia). Black box represents magnified area. Blue scale bar = 1 mm. Black scale bar = 50 µm.

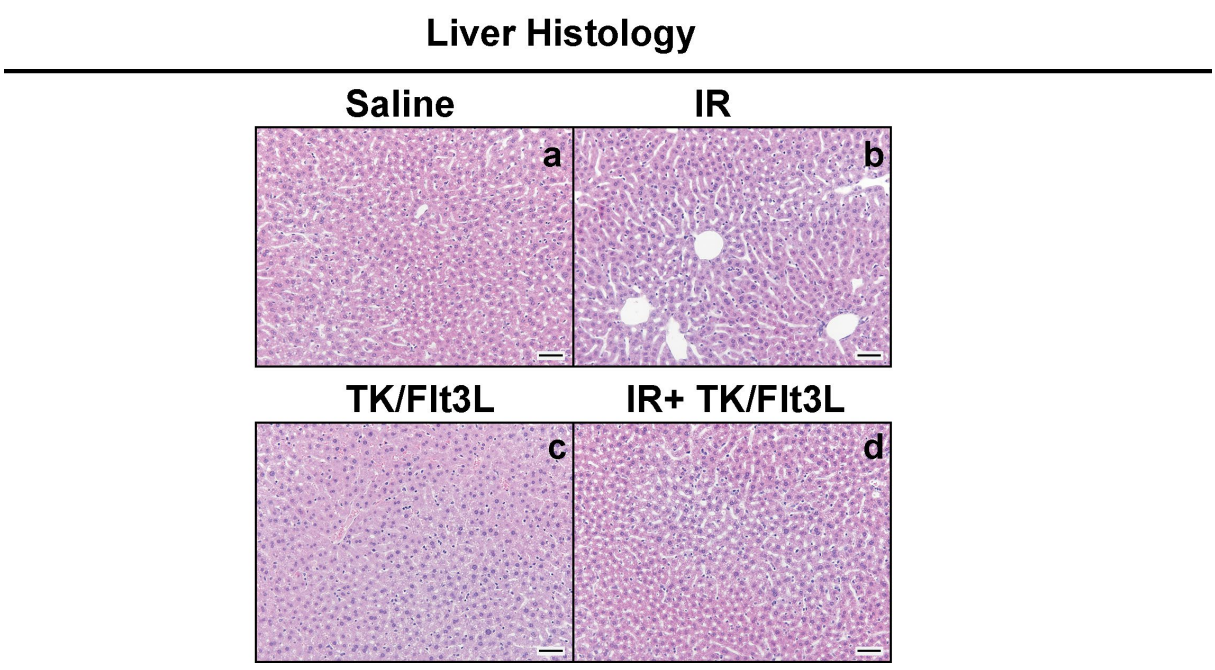

Figure 3.5 Liver Histology

Mice bearing mACVR1 brainstem gliomas were treated with saline or TK/ FLT3L gene therapy on day 5 post tumor implantation, followed by intraperitoneal administration of GCV (25 mg/kg) on days 6-12. Radiation was administered at a dose of 2 Gy/Day for 5d for two weeks 5 days' post tumor implantation. Livers were processed for histology on day 23. Bright field images of paraffin embedded liver sections stained with H&E of animals that were treated with (a) saline, (b) IR, (c) Tk/Flt3L + GCV or (d) Tk/Flt3L + GCV+ IR. Scale bar = 50 μm.

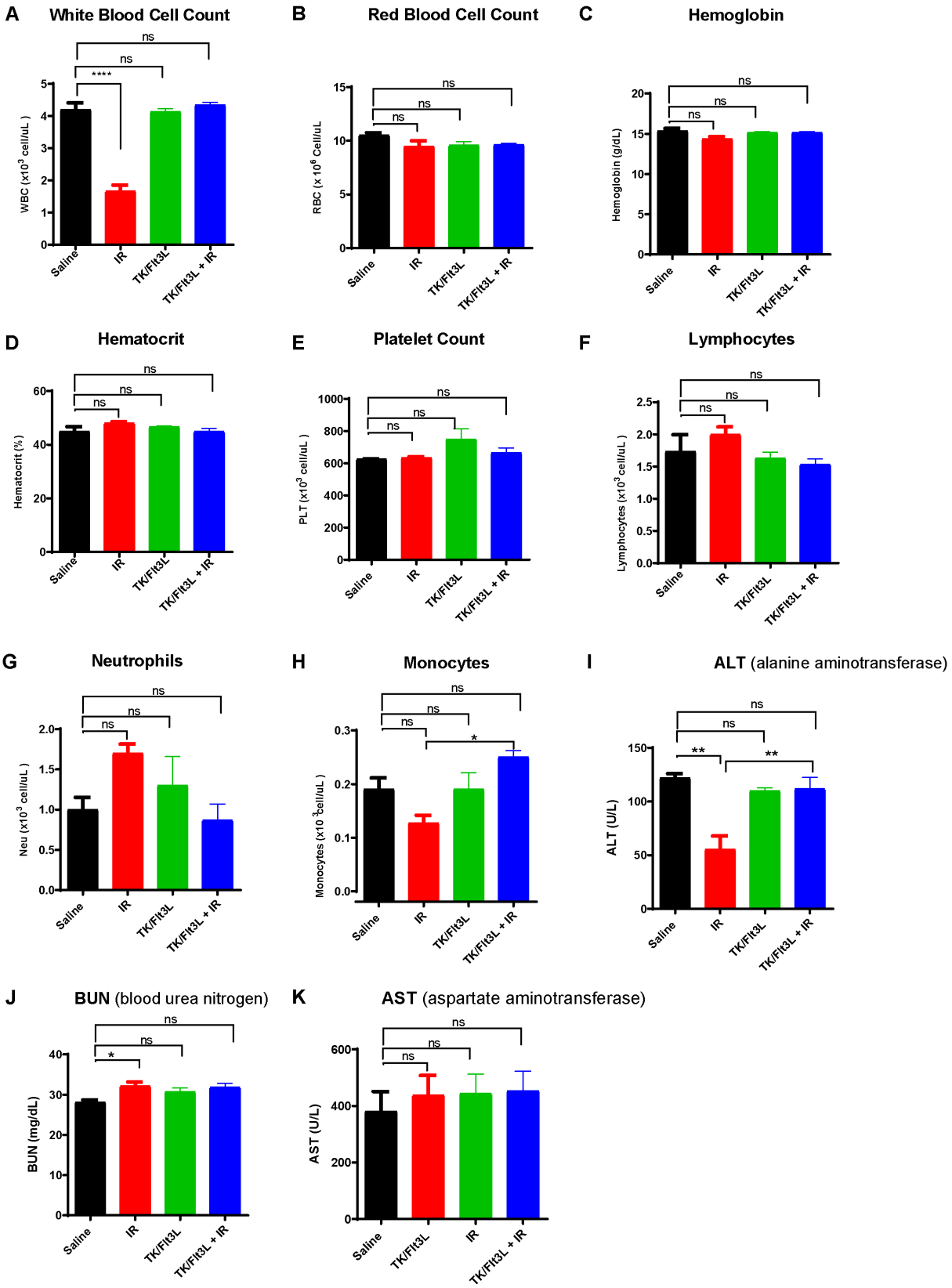
A
White Blood Cell Count
WBC (x10³ cell/uL)
B
Red Blood Cell Count
RBC (x 10⁶ Cell/uL
C
Hemoglobin
Hemoglobin (g/dL)
D
Hematocrit
Hematocrit (%)
E
Platelet Count
PLT (x10³ cell/uL)
F
Lymphocytes
Lymphocytes (x10³ cell/uL)
G
Neutrophils
Neu (x10³ cell/uL)
H
Monocytes
Monocytes (x10 ³cell/uL)
I
ALT (alanine aminotransferase)
ALT (U/L)
J
BUN (blood urea nitrogen)
BUN (mg/dL)
K
AST (aspartate aminotransferase)
AST (U/L)
ns
****
*
**
Saline
IR
TK/Flt3L
TK/Flt3L + IR

Figure 3.6 Hematology and serum chemistry

Mice bearing mACVR1 brainstem gliomas were treated with saline or TK/FLT3L gene therapy on day 5 post tumor implantation, followed by intraperitoneal administration of GCV (25 mg/kg) on days 6-12. Radiation was administered at a dose of 2 Gy/Day for 5d for two weeks 5 days' post tumor implantation. Blood and serum samples were drawn on day 23 to assess clinical parameters. (A) White blood cell (WBC), (B) red blood cell (RBC), (C) hemoglobin, (D) hematocrit, (E) Platelet (PLT), (F) Lymphocytes, (G) Neurotrophils (Neu), (H) Monocytes, (I) alanine aminotransferase (ALT), (J) blood urea nitrogen (BUN), (K) aspartate aminotransferase (AST).

References

1. Ostrom QT, de Blank PM, Kruchko C, Petersen CM, Liao P, Finlay JL*, et al.* Alex's Lemonade Stand Foundation Infant and Childhood Primary Brain and Central Nervous System Tumors Diagnosed in the United States in 2007-2011. Neuro Oncol **2015**;16 Suppl 10:x1-x36 doi 10.1093/neuonc/nou327.
2. Ostrom QT, Gittleman H, Truitt G, Boscia A, Kruchko C, Barnholtz-Sloan JS. CBTRUS Statistical Report: Primary Brain and Other Central Nervous System Tumors Diagnosed in the United States in 2011-2015. Neuro Oncol **2018**;20(suppl_4):iv1-iv86 doi 10.1093/neuonc/noy131.
3. Rashed WM, Maher E, Adel M, Saber O, Zaghloul MS. Pediatric diffuse intrinsic pontine glioma: where do we stand? Cancer Metastasis Rev **2019** doi 10.1007/s10555-019-09824-2.
4. Jackson S, Patay Z, Howarth R, Pai Panandiker AS, Onar-Thomas A, Gajjar A*, et al.* Clinico-radiologic characteristics of long-term survivors of diffuse intrinsic pontine glioma. J Neurooncol **2013**;114(3):339-44 doi 10.1007/s11060-013-1189-0.
5. Bledsoe JC. Effects of Cranial Radiation on Structural and Functional Brain Development in Pediatric Brain Tumors. Journal of Pediatric Neuropsychology **2015**;2(1-2):3-13 doi 10.1007/s40817-015-0008-2.
6. Hodi FS, O'Day SJ, McDermott DF, Weber RW, Sosman JA, Haanen JB*, et al.* Improved survival with ipilimumab in patients with metastatic melanoma. N Engl J Med **2010**;363(8):711-23 doi 10.1056/NEJMoa1003466.
7. Reck M, Rodriguez-Abreu D, Robinson AG, Hui R, Csoszi T, Fulop A*, et al.* Pembrolizumab versus Chemotherapy for PD-L1-Positive Non-Small-Cell Lung Cancer. N Engl J Med **2016**;375(19):1823-33 doi 10.1056/NEJMoa1606774.
8. Motzer RJ, Escudier B, McDermott DF, George S, Hammers HJ, Srinivas S*, et al.* Nivolumab versus Everolimus in Advanced Renal-Cell Carcinoma. N Engl J Med **2015**;373(19):1803-13 doi 10.1056/NEJMoa1510665.
9. Kantoff PW, Higano CS, Shore ND, Berger ER, Small EJ, Penson DF*, et al.* Sipuleucel-T immunotherapy for castration-resistant prostate cancer. N Engl J Med **2010**;363(5):411-22 doi 10.1056/NEJMoa1001294.
10. Curtin JF, Liu N, Candolfi M, Xiong W, Assi H, Yagiz K*, et al.* HMGB1 mediates endogenous TLR2 activation and brain tumor regression. PLoS Med **2009**;6(1):e10 doi 10.1371/journal.pmed.1000010.
11. Candolfi M, Yagiz K, Foulad D, Alzadeh GE, Tesarfreund M, Muhammad AK*, et al.* Release of HMGB1 in response to proapoptotic glioma killing strategies: efficacy and neurotoxicity. Clin Cancer Res **2009**;15(13):4401-14 doi 10.1158/1078-0432.CCR-09-0155.
12. Krysko DV, Garg AD, Kaczmarek A, Krysko O, Agostinis P, Vandenabeele P. Immunogenic cell death and DAMPs in cancer therapy. Nat Rev Cancer **2012**;12(12):860-75 doi 10.1038/nrc3380.
13. Kamran N, Kadiyala P, Saxena M, Candolfi M, Li Y, Moreno-Ayala MA*, et al.* Immunosuppressive Myeloid Cells' Blockade in the Glioma Microenvironment Enhances the Efficacy of Immune-Stimulatory Gene Therapy. Mol Ther **2017**;25(1):232-48 doi 10.1016/j.ymthe.2016.10.003.

14. Mineharu Y, Kamran N, Lowenstein PR, Castro MG. Blockade of mTOR signaling via rapamycin combined with immunotherapy augments antiglioma cytotoxic and memory T-cell functions. Mol Cancer Ther **2014**;13(12):3024-36 doi 10.1158/1535-7163.MCT-14-0400.
15. Goldberg JE, Sherwood SW, Clayberger C. A novel method for measuring CTL and NK cell-mediated cytotoxicity using annexin V and two-color flow cytometry. J Immunol Methods **1999**;224(1-2):1-9 doi 10.1016/s0022-1759(98)00038-6.
16. Candolfi M, Curtin JF, Nichols WS, Muhammad AG, King GD, Pluhar GE*, et al.* Intracranial glioblastoma models in preclinical neuro-oncology: neuropathological characterization and tumor progression. J Neurooncol **2007**;85(2):133-48 doi 10.1007/s11060-007-9400-9.
17. Yang J, Sanderson NS, Wawrowsky K, Puntel M, Castro MG, Lowenstein PR. Kupfer-type immunological synapse characteristics do not predict anti-brain tumor cytolytic T-cell function in vivo. Proc Natl Acad Sci U S A **2010**;107(10):4716-21 doi 10.1073/pnas.0911587107.
18. Alexander TC, Butcher H, Krager K, Kiffer F, Groves T, Wang J*, et al.* Behavioral Effects of Focal Irradiation in a Juvenile Murine Model. Radiat Res **2018**;189(6):605-17 doi 10.1667/RR14847.1.
19. Veldhuijzen van Zanten SEM, Baugh J, Chaney B, De Jongh D, Sanchez Aliaga E, Barkhof F*, et al.* Development of the SIOPE DIPG network, registry and imaging repository: a collaborative effort to optimize research into a rare and lethal disease. J Neurooncol **2017**;132(2):255-66 doi 10.1007/s11060-016-2363-y.
20. Louis DN, Perry A, Reifenberger G, von Deimling A, Figarella-Branger D, Cavenee WK*, et al.* The 2016 World Health Organization Classification of Tumors of the Central Nervous System: a summary. Acta Neuropathol **2016**;131(6):803-20 doi 10.1007/s00401-016-1545-1.
21. Cohen KJ, Jabado N, Grill J. Diffuse intrinsic pontine gliomas-current management and new biologic insights. Is there a glimmer of hope? Neuro Oncol **2017**;19(8):1025-34 doi 10.1093/neuonc/nox021.
22. Hashizume R, Smirnov I, Liu S, Phillips JJ, Hyer J, McKnight TR*, et al.* Characterization of a diffuse intrinsic pontine glioma cell line: implications for future investigations and treatment. J Neurooncol **2012**;110(3):305-13 doi 10.1007/s11060-012-0973-6.
23. Caretti V, Sewing AC, Lagerweij T, Schellen P, Bugiani M, Jansen MH*, et al.* Human pontine glioma cells can induce murine tumors. Acta Neuropathol **2014**;127(6):897-909 doi 10.1007/s00401-014-1272-4.
24. Wolchok JD, Chiarion-Sileni V, Gonzalez R, Rutkowski P, Grob JJ, Cowey CL*, et al.* Overall Survival with Combined Nivolumab and Ipilimumab in Advanced Melanoma. N Engl J Med **2017**;377(14):1345-56 doi 10.1056/NEJMoa1709684.
25. Wang SS, Bandopadhayay P, Jenkins MR. Towards Immunotherapy for Pediatric Brain Tumors. Trends Immunol **2019**;40(8):748-61 doi 10.1016/j.it.2019.05.009.
26. Kamran N, Alghamri MS, Nunez FJ, Shah D, Asad AS, Candolfi M*, et al.* Current state and future prospects of immunotherapy for glioma. Immunotherapy **2018**;10(4):317-39 doi 10.2217/imt-2017-0122.
27. Foster JB, Madsen PJ, Hegde M, Ahmed N, Cole KA, Maris JM*, et al.* Immunotherapy for pediatric brain tumors: past and present. Neuro Oncol **2019**;21(10):1226-38 doi 10.1093/neuonc/noz077.

28. Wilson EH, Weninger W, Hunter CA. Trafficking of immune cells in the central nervous system. J Clin Invest **2010**;120(5):1368-79 doi 10.1172/JCI41911.
29. Louveau A, Smirnov I, Keyes TJ, Eccles JD, Rouhani SJ, Peske JD*, et al.* Structural and functional features of central nervous system lymphatic vessels. Nature **2015**;523(7560):337-41 doi 10.1038/nature14432.
30. Perry VH. A revised view of the central nervous system microenvironment and major histocompatibility complex class II antigen presentation. J Neuroimmunol **1998**;90(2):113-21 doi 10.1016/s0165-5728(98)00145-3.
31. Matyszak MK, Perry VH. The potential role of dendritic cells in immune-mediated inflammatory diseases in the central nervous system. Neuroscience **1996**;74(2):599-608 doi 10.1016/0306-4522(96)00160-1.
32. Rutledge WC, Kong J, Gao J, Gutman DA, Cooper LA, Appin C*, et al.* Tumor-infiltrating lymphocytes in glioblastoma are associated with specific genomic alterations and related to transcriptional class. Clin Cancer Res **2013**;19(18):4951-60 doi 10.1158/1078-0432.CCR-13-0551.
33. Lohr J, Ratliff T, Huppertz A, Ge Y, Dictus C, Ahmadi R*, et al.* Effector T-cell infiltration positively impacts survival of glioblastoma patients and is impaired by tumor-derived TGF-beta. Clin Cancer Res **2011**;17(13):4296-308 doi 10.1158/1078-0432.CCR-10-2557.
34. Dutoit V, Migliorini D, Dietrich PY, Walker PR. Immunotherapy of Malignant Tumors in the Brain: How Different from Other Sites? Front Oncol **2016**;6:256 doi 10.3389/fonc.2016.00256.
35. Bloch O, Crane CA, Kaur R, Safaee M, Rutkowski MJ, Parsa AT. Gliomas promote immunosuppression through induction of B7-H1 expression in tumor-associated macrophages. Clin Cancer Res **2013**;19(12):3165-75 doi 10.1158/1078-0432.CCR-12-3314.
36. Raychaudhuri B, Rayman P, Huang P, Grabowski M, Hambardzumyan D, Finke JH*, et al.* Myeloid derived suppressor cell infiltration of murine and human gliomas is associated with reduction of tumor infiltrating lymphocytes. J Neurooncol **2015**;122(2):293-301 doi 10.1007/s11060-015-1720-6.
37. Wu A, Wei J, Kong LY, Wang Y, Priebe W, Qiao W*, et al.* Glioma cancer stem cells induce immunosuppressive macrophages/microglia. Neuro Oncol **2010**;12(11):1113-25 doi 10.1093/neuonc/noq082.
38. Berghoff AS, Kiesel B, Widhalm G, Rajky O, Ricken G, Wohrer A*, et al.* Programmed death ligand 1 expression and tumor-infiltrating lymphocytes in glioblastoma. Neuro Oncol **2015**;17(8):1064-75 doi 10.1093/neuonc/nou307.
39. Lin GL, Nagaraja S, Filbin MG, Suva ML, Vogel H, Monje M. Non-inflammatory tumor microenvironment of diffuse intrinsic pontine glioma. Acta Neuropathol Commun **2018**;6(1):51 doi 10.1186/s40478-018-0553-x.
40. Lieberman NAP, DeGolier K, Kovar HM, Davis A, Hoglund V, Stevens J*, et al.* Characterization of the immune microenvironment of diffuse intrinsic pontine glioma: implications for development of immunotherapy. Neuro Oncol **2019**;21(1):83-94 doi 10.1093/neuonc/noy145.
41. Ali S, King GD, Curtin JF, Candolfi M, Xiong W, Liu C*, et al.* Combined immunostimulation and conditional cytotoxic gene therapy provide long-term survival in

a large glioma model. Cancer Res **2005**;65(16):7194-204 doi 10.1158/0008-5472.CAN-04-3434.
42. King GD, Muhammad AK, Curtin JF, Barcia C, Puntel M, Liu C*, et al.* Flt3L and TK gene therapy eradicate multifocal glioma in a syngeneic glioblastoma model. Neuro Oncol **2008**;10(1):19-31 doi 10.1215/15228517-2007-045.
43. Ghulam Muhammad AK, Candolfi M, King GD, Yagiz K, Foulad D, Mineharu Y*, et al.* Antiglioma immunological memory in response to conditional cytotoxic/immune-stimulatory gene therapy: humoral and cellular immunity lead to tumor regression. Clin Cancer Res **2009**;15(19):6113-27 doi 10.1158/1078-0432.CCR-09-1087.
44. Moolten FL. Tumor chemosensitivity conferred by inserted herpes thymidine kinase genes: paradigm for a prospective cancer control strategy. Cancer Res **1986**;46(10):5276-81.
45. Castro MG, Candolfi M, Wilson TJ, Calinescu A, Paran C, Kamran N*, et al.* Adenoviral vector-mediated gene therapy for gliomas: coming of age. Expert Opin Biol Ther **2014**;14(9):1241-57 doi 10.1517/14712598.2014.915307.
46. Tang D, Kang R, Coyne CB, Zeh HJ, Lotze MT. PAMPs and DAMPs: signal 0s that spur autophagy and immunity. Immunol Rev **2012**;249(1):158-75 doi 10.1111/j.1600-065X.2012.01146.x.
47. Curtin JF, King GD, Barcia C, Liu C, Hubert FX, Guillonneau C*, et al.* Fms-like tyrosine kinase 3 ligand recruits plasmacytoid dendritic cells to the brain. J Immunol **2006**;176(6):3566-77 doi 10.4049/jimmunol.176.6.3566.
48. Lowenstein PR, Orringer DA, Sagher O, Heth J, Hervey-Jumper SL, Mammoser AG*, et al.* First-in-human phase I trial of the combination of two adenoviral vectors expressing HSV1-TK and FLT3L for the treatment of newly diagnosed resectable malignant glioma: Initial results from the therapeutic reprogramming of the brain immune system. **2019**;37(15_suppl):2019- doi 10.1200/JCO.2019.37.15_suppl.2019.
49. Schroeder KM, Hoeman CM, Becher OJ. Children are not just little adults: recent advances in understanding of diffuse intrinsic pontine glioma biology. Pediatr Res **2014**;75(1-2):205-9 doi 10.1038/pr.2013.194.
50. Martinez-Velez N, Garcia-Moure M, Marigil M, Gonzalez-Huarriz M, Puigdelloses M, Gallego Perez-Larraya J*, et al.* The oncolytic virus Delta-24-RGD elicits an antitumor effect in pediatric glioma and DIPG mouse models. Nat Commun **2019**;10(1):2235 doi 10.1038/s41467-019-10043-0.
51. Schuelke MR, Wongthida P, Thompson J, Kottke T, Driscoll CB, Huff AL*, et al.* Diverse immunotherapies can effectively treat syngeneic brainstem tumors in the absence of overt toxicity. J Immunother Cancer **2019**;7(1):188 doi 10.1186/s40425-019-0673-2.
52. Tejada S, Diez-Valle R, Dominguez PD, Patino-Garcia A, Gonzalez-Huarriz M, Fueyo J*, et al.* DNX-2401, an Oncolytic Virus, for the Treatment of Newly Diagnosed Diffuse Intrinsic Pontine Gliomas: A Case Report. Front Oncol **2018**;8:61 doi 10.3389/fonc.2018.00061.

Chapter 4: Summary and Conclusions

Summary

The work presented in this dissertation demonstrates the feasibility of generating mouse models which recapitulate the histopathological features of diffuse intrinsic pontine glioma (DIPG) using the Sleeping Beauty (SB) transposon system. The SB system enabled us to generate mouse models of brainstem glioma harboring ACVR1 G328V and H3.1 K27M, two prevalent DIPG mutations, in order to investigate their role in DIPG tumorigenesis. We also developed a transplantable model in the adult pons by implantation of tumor neurospheres expressing ACVR1 G328V. The development of this syngeneic model with an intact immune system allowed us to investigate the use of Thymidine Kinase (TK)/Fms-like tyrosine kinase 3 ligand (Flt3L) immune stimulatory therapy for DIPG. Here, I summarize the main conclusions of my thesis work and discuss their translational relevance.

Challenges in the treatment of DIPG

Diffuse intrinsic pontine glioma (DIPG) is a pediatric brainstem tumor with poor survival. Surgical removal is not possible due to the sensitive location and diffusive nature of DIPG. Biopsies are not necessary for diagnosis, so they are not routinely performed. This has hampered the ability to study the biology of this tumor and develop effective therapies. Within

the past decade, collaborations between scientists, clinicians, and clinician scientists within the pediatric neuro-oncology community have led to the discovery of unique mutations driving DIPG, reviewed in chapter one of this thesis (1). This was followed by the development of cell lines and in vivo xenograft models derived from tissue acquired at time of autopsy or biopsy material of DIPG patients (2). Xenograft models are valuable because they have standardized growth rates, times of death, and tumor localization, however, studies must be performed in immunocompromised mice which limits the ability to study the efficacy of immunotherapies (3). To overcome this limitation, we developed a genetically engineered animal model of brainstem glioma expressing DIPG mutations, as described in chapter two of this thesis. This enabled us to assess the role of individual mutations in DIPG pathogenesis. Despite an increased understanding of the biology of the tumor there are still no effective therapies for the treatment of DIPG. Conventional chemotherapeutics and radiation have not shown an effective response therefore we investigated the efficacy of an immune stimulatory gene therapy, described in chapter 3 of this thesis.

Using the Sleeping Beauty Transposase system to generate models of DIPG

In 2014, a DIPG molecular subgroup co-expressing a mutation in activin receptor type I, (ACVR1), a bone morphogenetic (BMP) receptor, and the histone H3.1 K27M mutation (4,5) was identified. ACVR1 mutations and H3.1 K27M mutations are largely restricted to pontine gliomas, and DIPG patients harboring these mutations are characterized as having an earlier age of onset and longer overall survival, further highlighting the unique biology of this subgroup (4). The ACVR1 mutation activates the BMP-Smad1/5 signaling pathway while the H3.1 K27M mutation results in H3K27me3 hypomethylation. During development BMPs promote

astrogliogenesis while inhibiting oligodendrogliogenesis (6-8). BMP signaling is also implicated in supporting the maturation of oligodendrocytes (9). In adult glioblastoma, BMP-Smad1/5/8 signaling induces differentiation of glioblastoma tumor initiating cells and decreases the in vivo tumor initiating ability of GBM cells (10). However, BMP-Smad1/5 signaling has also been shown to promote proliferation and migration in transformed astrocytes (11). Thus, it is unclear what role elevated Smad1/5 signaling plays in DIPG pathogenesis. To address this gap, we developed an animal model expressing the ACVR1 G328V and H3.1 K27M mutations using the Sleeping Beauty (SB) system (12).

We first used the SB system to deliver plasmids encoding DIPG mutations into neural stem cells lining the lateral ventricles, a site where we had previously demonstrated that we could generate high grade gliomas. We demonstrated that mutant ACVR1 tumors had increased levels of phosphorylated Smad1/5/8 indicating upregulation of the BMP pathway. This was confirmed by RNA-seq analysis. We also identified a link between mutant ACVR1 and the regulation of stemness and increased tumor initiating potential. Further, we confirmed that H3.1 K27M mutant tumors exhibited global loss of H3K27me3. Our survival studies revealed that ACVR1 G328V increased median survival, while H31 K27M only enhanced median survival in the presence of the ACVR1 G328V, suggesting a potential cooperation.

Once we had established a working model, we sought to improve it by initiating the tumors in the brainstem since DIPG arises from this anatomical location. We demonstrated that we could successfully induce tumors in the brainstem with histological features of DIPG through delivery of plasmid DNA into the fourth ventricle. The brainstem tumors were diffusive, spread into the cerebellum, and express markers of glioma cells. Although, BMPs play an important role in mediating the differentiation of neural and glioma stem cells, we did not observe any

differences in the expression levels of Nestin or Olig2 in mutant or wt-ACVR1 tumors, indicating that mutant ACVR1 did not affect their differentiation state. Mutant ACVR1 enhanced median survival in our mouse model of brainstem glioma, reproducing the result we had observed in the lateral ventricle tumors. One caveat of this model is that at the time that animals begin to decline in health and present with neurological symptoms the tumors were very small and consequently there was a limited amount of tumor tissue.

A limitation of the SB models of DIPG presented here is the requirement of NRAS as a tumorigenic driver since ACVR1 G328V and H3.1 K27M and were not sufficient to develop tumors when delivered into the postnatal pons. To date, no other genetically engineered models of DIPG have been generated postnatally that don't require additional tumorigenic drivers. However, recently Pathania M. and colleagues demonstrated that the combination of H3.3 K27M and p53 knockdown could transform neural stem cells in the brainstem by delivery of PiggyBac DNA transposon plasmids at embryonic day 12.5, but it took 6-8 months for tumors to develop (13). Another group using in utero electroporation to transfect neural stem cells using PiggyBac DNA transposon plasmids was unable to generate tumors using H3.3 K27M and p53 knockdown at embryonic day 13.5 suggesting that the developmental window is more susceptible to transformation at embryonic day 12.5 (14). It would be interesting to see if at this developmental time point activating ACVR1 G328V and H3.1K27M mutations could be sufficient to transform neural stem cells in the brainstem.

Immune stimulatory gene therapy is effective in a mouse model of DIPG

The lack of immune competent mouse models of DIPG has limited the ability to study the efficacy of immunotherapeutic strategies for the treatment of DIPG. Therefore, one of the

aims of this dissertation was to test the efficacy of a therapeutic strategy developed by our laboratory that modulates the immune system to induce an anti-cancer response in our mouse model of DIPG (15-19). The immune mediated gene therapy approach relies on thymidine kinase (TK)-mediated killing of tumor cells where tumor cell death results in the release of antigens and damage associated molecular pathogen patterns, such as HMGB1, calreticulin, and ATP into the tumor microenvironment (15,20). Previously, our lab has demonstrated that dying glioblastoma tumor cells release HMGB1 and activate dendritic cells recruited to the tumor microenvironment by adenoviral delivery of the adjuvant Flt3L(15). Activated dendritic cells then travel to the draining lymph nodes to initiate an anti-tumor T cell response. This therapeutic strategy has recently completed phase I clinical trial in patients with GBM with promising results (21). Like glioblastoma tumors, DIPGs are also characterized by low immune cell infiltration (22,23). Therefore, we hypothesized that TK/Flt3L therapy would also be effective for the treatment of DIPG.

In chapter 3 of this thesis, we show that intratumoral administration of TK/Flt3L therapy in mice bearing mACVR1 brainstem gliomas triggers a robust anti-tumor immune response that leads to enhanced median survival. We also established brainstem tumors expressing the surrogate tumor antigen ovalbumin and labeled antigen specific anti-brainstem glioma T cells using specific tetramers. Using these brainstem tumors, we demonstrated that TK/Flt3L therapy resulted in the recruitment of anti-brainstem glioma specific CD8 T cells into the tumor immune microenvironment. Treatment with gene therapy also resulted in an increase in the frequency of tumor infiltrating CD8 T cells that release IFNγ, a cytokine released by activated CD8 T cells, was increased when exposed to specific tumor antigens. Additionally, TK/Flt3L therapy also resulted in an increase in splenic CD8 T cell expansion and enhanced their cytotoxic activity.

Neurological examination post treatment with TK/Flt3L and GCV in a normal brain did not reveal any signs of treatment related neuro-toxicity, or overt inflammation. We also did not observe any systemic toxicity as a result of TK/Flt3L therapy and GCV. Overall, our results demonstrate that treatment with TK/Flt3L gene therapy achieves a robust anti-tumor efficacy and can be safely administered in the brainstem. I think future studies could investigate how different DIPG mutations impact the efficacy of immunotherapy. There is speculation, for example, that tumor cells with the H3.1 K27M mutation may have distinct effects on immune cell function compared with tumor cells with the H3.3 K27M mutation (22). Since the K27M mutation affects 80% of DIPGs it will be important to understand the effects of this mutation on the efficacy of TK/Flt3L gene therapy (24-26).

Translational Impact

The work presented in this thesis has significant translational impact because radiation, the current standard of care for DIPG, does not improve the survival of DIPG patients and only provides palliative care. The dismal prognosis dictates the development of novel and safe approaches. In this thesis, I describe the development of a DIPG model bearing mutated ACVR1 or H3.1 K27M, two mutations frequent in DIPG, using the SB transposon system in neonate mice. We also demonstrated that TK/Flt3L therapy can be safely delivered to the brainstem in a transplantable model of DIPG and can generate an anti-tumor therapeutic immune response and extend the survival of mice bearing mACVR1 brainstem tumors. The development of immunocompetent mouse models was invaluable for the analysis of the immune stimulatory effect of TK/Flt3L therapy. The safety studies we performed indicate that TK/Flt3L gene therapy does not elicit immune-mediated toxicity or inflammation which is important because

inflammation in the brainstem could be life threatening. Overall, my thesis work provides support for continued clinical investigation into TK/Flt3L immune stimulatory gene therapy for DIPG.

References

1. Schroeder KM, Hoeman CM, Becher OJ. Children are not just little adults: recent advances in understanding of diffuse intrinsic pontine glioma biology. Pediatr Res **2014**;75(1-2):205-9 doi 10.1038/pr.2013.194.
2. Misuraca KL, Cordero FJ, Becher OJ. Pre-Clinical Models of Diffuse Intrinsic Pontine Glioma. Frontiers in Oncology **2015**;5 doi 10.3389/fonc.2015.00172.
3. Calinescu AA, Nunez FJ, Koschmann C, Kolb BL, Lowenstein PR, Castro MG. Transposon mediated integration of plasmid DNA into the subventricular zone of neonatal mice to generate novel models of glioblastoma. J Vis Exp **2015**(96) doi 10.3791/52443.
4. Taylor KR, Mackay A, Truffaux N, Butterfield Y, Morozova O, Philippe C*, et al.* Recurrent activating ACVR1 mutations in diffuse intrinsic pontine glioma. Nat Genet **2014**;46(5):457-61 doi 10.1038/ng.2925.
5. Buczkowicz P, Hoeman C, Rakopoulos P, Pajovic S, Letourneau L, Dzamba M*, et al.* Genomic analysis of diffuse intrinsic pontine gliomas identifies three molecular subgroups and recurrent activating ACVR1 mutations. Nat Genet **2014**;46(5):451-6 doi 10.1038/ng.2936.
6. Grinspan JB, Edell E, Carpio DF, Beesley JS, Lavy L, Pleasure D*, et al.* Stage-specific effects of bone morphogenetic proteins on the oligodendrocyte lineage. J Neurobiol **2000**;43(1):1-17.
7. Mabie PC, Mehler MF, Kessler JA. Multiple roles of bone morphogenetic protein signaling in the regulation of cortical cell number and phenotype. J Neurosci **1999**;19(16):7077-88.
8. Gomes WA, Mehler MF, Kessler JA. Transgenic overexpression of BMP4 increases astroglial and decreases oligodendroglial lineage commitment. Dev Biol **2003**;255(1):164-77 doi 10.1016/s0012-1606(02)00037-4.
9. See J, Mamontov P, Ahn K, Wine-Lee L, Crenshaw EB, 3rd, Grinspan JB. BMP signaling mutant mice exhibit glial cell maturation defects. Mol Cell Neurosci **2007**;35(1):171-82 doi 10.1016/j.mcn.2007.02.012.
10. Piccirillo SG, Reynolds BA, Zanetti N, Lamorte G, Binda E, Broggi G*, et al.* Bone morphogenetic proteins inhibit the tumorigenic potential of human brain tumour-initiating cells. Nature **2006**;444(7120):761-5 doi 10.1038/nature05349.
11. Hover LD, Owens P, Munden AL, Wang J, Chambless LB, Hopkins CR*, et al.* Bone morphogenetic protein signaling promotes tumorigenesis in a murine model of high-grade glioma. Neuro Oncol **2016**;18(7):928-38 doi 10.1093/neuonc/nov310.

12. Izsvak Z, Ivics Z. Sleeping beauty transposition: biology and applications for molecular therapy. Mol Ther **2004**;9(2):147-56 doi 10.1016/j.ymthe.2003.11.009.
13. Pathania M, De Jay N, Maestro N, Harutyunyan AS, Nitarska J, Pahlavan P*, et al.* H3.3(K27M) Cooperates with Trp53 Loss and PDGFRA Gain in Mouse Embryonic Neural Progenitor Cells to Induce Invasive High-Grade Gliomas. Cancer Cell **2017**;32(5):684-700 e9 doi 10.1016/j.ccell.2017.09.014.
14. Patel SK, Hartley RM, Wei X, Furnish R, Escobar-Riquelme F, Bear H*, et al.* Generation of diffuse intrinsic pontine glioma mouse models by brainstem targeted in utero electroporation. Neuro Oncol **2019** doi 10.1093/neuonc/noz197.
15. Curtin JF, Liu N, Candolfi M, Xiong W, Assi H, Yagiz K*, et al.* HMGB1 mediates endogenous TLR2 activation and brain tumor regression. PLoS Med **2009**;6(1):e10 doi 10.1371/journal.pmed.1000010.
16. Candolfi M, Yagiz K, Foulad D, Alzadeh GE, Tesarfreund M, Muhammad AK*, et al.* Release of HMGB1 in response to proapoptotic glioma killing strategies: efficacy and neurotoxicity. Clin Cancer Res **2009**;15(13):4401-14 doi 10.1158/1078-0432.CCR-09-0155.
17. Ali S, King GD, Curtin JF, Candolfi M, Xiong W, Liu C*, et al.* Combined immunostimulation and conditional cytotoxic gene therapy provide long-term survival in a large glioma model. Cancer Res **2005**;65(16):7194-204 doi 10.1158/0008-5472.CAN-04-3434.
18. King GD, Muhammad AK, Curtin JF, Barcia C, Puntel M, Liu C*, et al.* Flt3L and TK gene therapy eradicate multifocal glioma in a syngeneic glioblastoma model. Neuro Oncol **2008**;10(1):19-31 doi 10.1215/15228517-2007-045.
19. Ghulam Muhammad AK, Candolfi M, King GD, Yagiz K, Foulad D, Mineharu Y*, et al.* Antiglioma immunological memory in response to conditional cytotoxic/immune-stimulatory gene therapy: humoral and cellular immunity lead to tumor regression. Clin Cancer Res **2009**;15(19):6113-27 doi 10.1158/1078-0432.CCR-09-1087.
20. Tang D, Kang R, Coyne CB, Zeh HJ, Lotze MT. PAMPs and DAMPs: signal 0s that spur autophagy and immunity. Immunol Rev **2012**;249(1):158-75 doi 10.1111/j.1600-065X.2012.01146.x.
21. Lowenstein PR, Orringer DA, Sagher O, Heth J, Hervey-Jumper SL, Mammoser AG*, et al.* First-in-human phase I trial of the combination of two adenoviral vectors expressing HSV1-TK and FLT3L for the treatment of newly diagnosed resectable malignant glioma: Initial results from the therapeutic reprogramming of the brain immune system. **2019**;37(15_suppl):2019- doi 10.1200/JCO.2019.37.15_suppl.2019.
22. Lieberman NAP, DeGolier K, Kovar HM, Davis A, Hoglund V, Stevens J*, et al.* Characterization of the immune microenvironment of diffuse intrinsic pontine glioma: implications for development of immunotherapy. Neuro Oncol **2019**;21(1):83-94 doi 10.1093/neuonc/noy145.
23. Lin GL, Nagaraja S, Filbin MG, Suva ML, Vogel H, Monje M. Non-inflammatory tumor microenvironment of diffuse intrinsic pontine glioma. Acta Neuropathol Commun **2018**;6(1):51 doi 10.1186/s40478-018-0553-x.
24. Schwartzentruber J, Korshunov A, Liu XY, Jones DT, Pfaff E, Jacob K*, et al.* Driver mutations in histone H3.3 and chromatin remodelling genes in paediatric glioblastoma. Nature **2012**;482(7384):226-31 doi 10.1038/nature10833.

25. Wu G, Broniscer A, McEachron TA, Lu C, Paugh BS, Becksfort J*, et al.* Somatic histone H3 alterations in pediatric diffuse intrinsic pontine gliomas and non-brainstem glioblastomas. Nat Genet **2012**;44(3):251-3 doi 10.1038/ng.1102.
26. Khuong-Quang DA, Buczkowicz P, Rakopoulos P, Liu XY, Fontebasso AM, Bouffet E*, et al.* K27M mutation in histone H3.3 defines clinically and biologically distinct subgroups of pediatric diffuse intrinsic pontine gliomas. Acta Neuropathol **2012**;124(3):439-47 doi 10.1007/s00401-012-0998-0.

Appendices

A-1: Antibodies

Analysis	Antibody	Company	Catalog number	Dilution
IHC-DAB	Rabbit polyclonal anti-OLIG2	Millipore Sigma	AB9610	1:200
IHC-DAB	Rabbit polyclonal anti-GFAP	Millipore Sigma	AB5804	1:1000
IHC-DAB	Chicken polyclonal nestin	Novus Biologicals	NB100-1604	1:100
IHC-DAB	Rabbit polyclonal anti-SOX2	Abcam	ab97959	1:500
IHC-DAB	Rabbit Anti-Ki67	Abcam	ab15580	1:100
IHC-DAB	Rabbit monoclonal anti-p-ERK1/2	Cell Signaling	4370	1:100
IHC-DAB	Rabbit polyclonal anti p-MEK-1/2	Santa Cruz Biotechnology	sc-7995-R	1:100
WB	Rabbit anti phospho Smad1/Smad5/Smad8 (Ser463/465)	Millipore Sigma	AB3848-I	1:500
IHC Fluorescence	Rabbit anti-phospho Smad1/Smad5/Smad8 (Ser463/465)	Millipore Sigma	AB3848-I	1:50
IHC DAB	Rabbit Monoclonal Anti-Mouse Id1 antibody	Biocheck	BCH-1/37-2	1:100
WB	Rabbit Monoclonal Anti-Mouse Id1 antibody	Biocheck	BCH-1/37-2	1:500
WB	Rabbit Monocolonal Anti-Id2	Calbioreagents	9-2-8	1:500
WB	Mouse monoclonal anti-β-actin	Millipore Sigma	A1978	1:10,000
WB	Rabbit polyclonal anti-Smad1	Abcam	ab63356	1:500
WB	Goat anti-rabbit	Dako	P0448	1:4000
WB	rabbit anti-mouse	Dako	P0260	1:20,000
Flow cytometry	Mouse monoclonal anti CD16/32	Biolegend	101335	1:200
Flow cytometry	Mouse monoclonal anti CD45	Biolegend	103125	1:200
Flow cytometry	Mouse monoclonal anti CD8	Biolgened	100711	1:200
Flow cytometry	Mouse monoclonal anti CD3	Biolegend	100333	1:200
Flow cytometry	SIINFEKL-H2Kb-tetramer-PE	MBL International	TB-5001-1	1:200
Flow cytometry	IFNγ	Biolegend	113603	1:200
Flow cytometry	CD133	Biolegend	141203	1:200

Flow cytometry	CD44	Biolegend	103005	1:200
Flow cytometry	Aldh1	R&D Systems	AAF5869-SP	1:200
IHC-DAB	Vimentin	Abcam	ab92547	1:500
IHC-DAB	IBA1	Abcam	ab178846	1:1000
IHC-DAB	CD8	Cederlane	361003(SY)	1:2000